# UC Davis

**Title**

Aging of Atmospheric Brown Carbon Aerosol

**Authors**

Hems, Rachel F
Schnitzler, Elijah G
Liu-Kang, Carolyn
et al.

**Supplemental Material**

https://escholarship.org/uc/item/6tn249p1#supplemental

Peer reviewed

# Aging of atmospheric brown carbon aerosol

Rachel F. Hems[†*], Elijah G. Schnitzler[‡*], Carolyn Liu-Kang[†], Christopher D. Cappa[∥], Jonathan P.D. Abbatt[†]

[†]Department of Chemistry, University of Toronto, 80 St. George Street, M5S 3H6, Toronto, ON, Canada

[‡]Department of Chemistry, Oklahoma State University, 107 Physical Sciences, Stillwater, OK, USA, 74078.

[∥]Department of Civil and Environmental Engineering, University of California, Davis, CA, USA

*Corresponding authors

## Abstract

Emitted by numerous primary sources and formed by secondary sources, atmospheric brown carbon (BrC) aerosol is chemically complex. As BrC aerosol ages in the atmosphere via a variety of chemical and physical processes, its chemical composition and optical properties change significantly, altering its impacts on climate. Research in the past decade has considerably expanded our understanding of BrC reactions in both the gas and condensed phases. We review these recent advances in BrC aging chemistry with a focus on gas phase reactions leading to BrC formation, aqueous and in-cloud processes, and aerosol particle reactions. Connections are made between single component BrC proxies and more complex chemical mixtures, as well as between laboratory and field measurements of BrC chemistry. General conclusions are that chemical change can darken the BrC aerosol particles over short timescales of hours close to source and that considerable photobleaching and oxidative whitening will occur when BrC is a day or more removed from its source.

# 1   Introduction

## 1.1   Atmospheric BrC and Its Environmental Impacts

Carbonaceous aerosol particles referred to as black carbon (BC) and brown carbon (BrC) absorb light across the visible and near ultraviolet parts of the solar spectrum. BC refers to particles primarily composed of elemental carbon and characterized by broad absorbance across ultraviolet to infrared wavelengths.[1,2] BrC refers to the light absorbing components of organic aerosol.[2] The direct absorption of light by these types of aerosol particles impacts the earth's climate by producing a positive radiative forcing, which refers to a perturbation to earth's radiative equilibrium since pre-industrial times. The dependence of BrC absorbance on wavelength is more pronounced than that of BC, with absorbance increasing steeply at lower wavelengths.[2] The direct radiative forcing of BC has been estimated as the second largest anthropogenic climate forcing agents.[3] Recent studies have shown that BrC can also significantly contribute to positive radiative direct forcing with up to 20 % of total aerosol absorption.[4–6]

Light absorbing aerosol particles, like all particles, may also influence radiative forcing by acting as cloud condensation nuclei (CCN), referred to as the aerosol indirect effect. In particular, cloud droplets also absorb and scatter light in the visible and infrared range of the spectrum. The radiative forcing due to clouds is impacted by the number and size of droplets that form (i.e., related to the number of CCN available), the altitude, and the lifetime of the cloud. Carbonaceous aerosol from biomass burning is thought to contribute significantly to the global indirect radiative forcing.[7] Finally, light absorbing aerosol particles can impact radiative forcing via a variety of aerosol-cloud interactions. These light-absorbing aerosol particles can increase the local temperature, resulting in a decrease of the relative humidity (RH), cloud droplet

evaporation, and altered cloud optical properties.[3] Absorbing particles aloft can also increase atmospheric stability, suppressing vertical uplift required for cloud formation.[8,9] These effects are likely important in areas with high aerosol concentration, for example during biomass burning season,[10,11] and are much more uncertain than the other aerosol climate impacts.

Beyond climate effects, it is evident that inhalation of aerosol particles contributes to adverse health outcomes in humans, including increased mortality.[12–14] Although the toxicities of different aerosol components is uncertain, some particle types have been identified to be particularly harmful, for example those generated from combustion sources.[15–18] Additionally, light absorption by atmospheric particles, such as BC and BrC, can also reduce the amount of sunlight reaching ground-level, impacting the photochemical processes that give rise to smog.[19] Indeed, high concentrations of BrC have been observed to impact atmospheric photochemistry, leading to decreases in ground-level ozone and radicals.[20]

While general understanding of the impacts of BrC on climate and air quality exist, as elucidated above, there remain substantial uncertainties associated with understanding the chemical processes that lead to formation and transformations of atmospheric BrC. As described in more detail in Section 1.4, the aims of this review are to assess the state of the science and highlight recent advancements in the understanding of BrC chemistry.

## 1.2 Sources and Composition of Atmospheric BrC

BrC refers to the subset of organic carbon in aerosol particles that absorbs light at ultraviolet and visible wavelengths, giving it a characteristic brown colour. This colour arises from an ensemble of species with varying abilities to absorb light, from highly to weakly absorbing. BrC has been observed in aerosol particles and cloud water around the world and at all altitudes

throughout the troposphere.[5,21–27] The sources of BrC to the atmosphere have been extensively reviewed by Laskin *et al.* and Yan *et al.* and will be described only briefly here.[2,28]

A dominant source of BrC to the atmosphere is burning of biomass materials.[29–33] Biomass burning emissions arise from uncontrolled sources, such as in wildfires,[34,35] and through more controlled cookstove emissions and domestic wood burning.[24,36,37] BrC emissions from biomass burning may become even more important in the future with increased number and spatial extent of wildfires.[38] Major chemical constituents in biomass burning plumes arise from pyrolysis of lignin and cellulose,[39] such as phenolic compounds and organic acids.[39–41] Lignin pyrolysis products, which have aromatic functionalities that absorb visible light, likely contribute to BrC. However, a large portion (up to 40 %) of the colored BrC compounds remain unidentified.[30,42]

A class of molecules commonly attributed to biomass burning BrC is nitroaromatics,[25,30,37,43–45] specifically nitrophenols (e.g., nitrocatechol, **Figure 1**), which are present in the gas phase, aerosol particles, and cloud and fog water.[37,46–49] Nitrophenols can be directly emitted from combustion processes or can arise via nitration of aromatic compounds that occurs by reaction with $NO_x$ ($NO + NO_2$) or $NO_3$.[46,50,51] Flaming combustion has been associated with higher nitroaromatic concentrations, compared to smoldering combustion, due to the higher $NO_x$ concentration.[46,52] Nitrophenol compounds absorb light at UV and visible wavelengths, but their absorption profile is pH dependent because of the acidity of the phenolic proton; ionized nitrophenolates absorb more strongly at visible wavelengths than the neutral nitrophenol.[53–56] Secondary aerosol particles, which generally have a pH of 3 or lower will primarily have the neutral nitrophenol present, while cloud and fog droplets with higher pH values around 6 can have the nitrophenolate ion present as well.[57] Therefore, BrC absorption by nitrophenol compounds will likely be stronger in cloud and fog water at more neutral pH conditions.
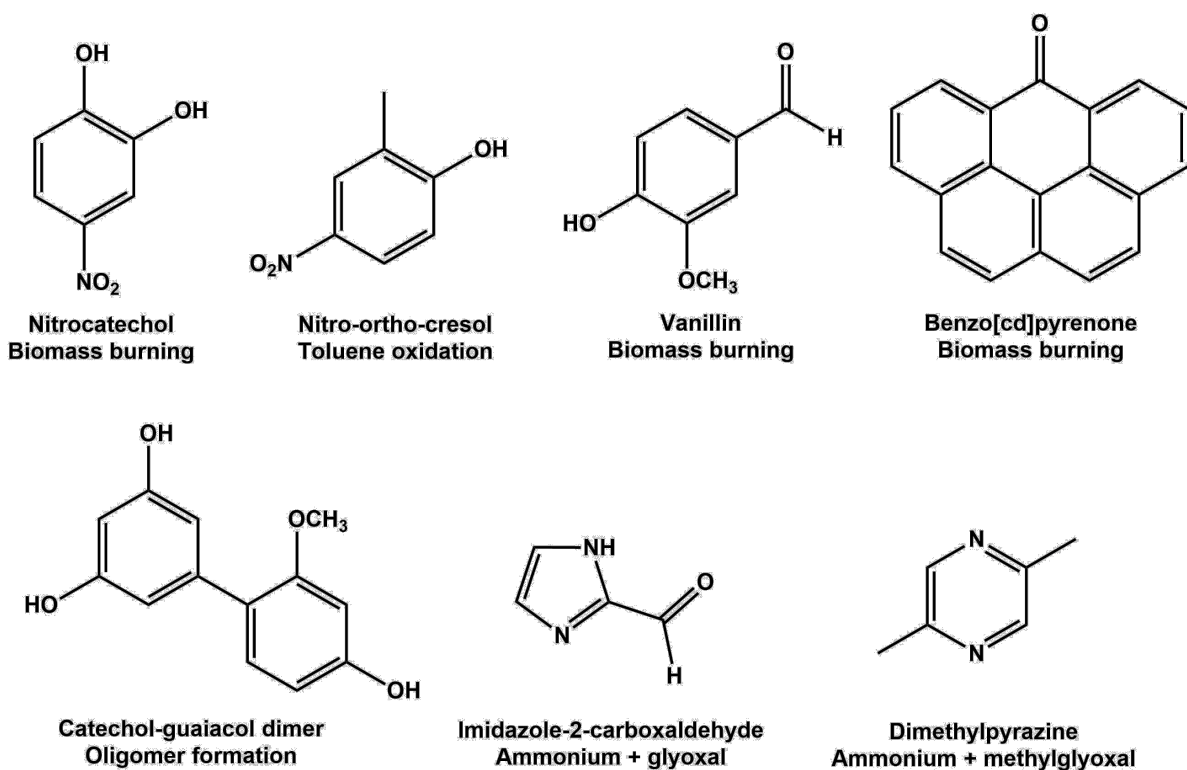
**Figure 1** Representative BrC molecules from a variety of sources. The name of the molecule and its dominant source are included below each structure.

Other aromatic compounds formed during combustion without nitrogen in the structure can also contribute to BrC, such as vanillin (**Figure 1**) and similar lignin-derived carbonyls, and polycyclic aromatic hydrocarbons (e.g., benzo[cd]pyrenone, **Figure 1**).[31,36,58] BrC absorption has also been attributed to high molecular weight compounds, with unknown structures, from biomass burning sources.[59–61]

The composition of carbonaceous aerosols emitted from biomass burning sources depends on the combustion process. At lower temperatures, incomplete combustion will generate BrC-dominated particles, whereas higher temperature flaming combustion conditions generate BC particles more efficiently. The efficiency of the combustion is characterized by the CO-to-

$CO_2$ ratio of the emission and is often parametrized using the modified combustion efficiency (MCE),[62] defined as:

$$MCE = \frac{\Delta CO_2}{\Delta CO_2 + \Delta CO} \qquad (1)$$

where $\Delta CO_2$ and $\Delta CO$ are the concentrations of these species in excess of background values. An MCE value near 1 signifies almost pure flaming and a value near 0.8 signifies predominately smoldering. The utility of the above definition of the MCE relies on $CO_2$ and CO together comprising the vast majority (95 %) of all carbon emissions, with greater CO emissions indicative of incomplete combustion processes.[63] Beyond the MCE values, environmental conditions in the biomass burning plume strongly affect the nature of BrC particles.

Industrial sources also emit precursor compounds that react to form BrC. For example, when oxidized under high $NO_x$ conditions, aromatic compounds such as benzene, toluene, and isomers of xylene, can form absorbing, low-volatility nitroaromatic compounds (e.g., nitro-ortho-cresol, **Figure 1**).[64–69] Nitroaromatic compounds can make up to 10 % of the total aerosol mass in secondary organic aerosol (SOA) generated from these predominately anthropogenic aromatic compounds under high $NO_x$ conditions,[51] and can arise from biomass burning as well.[70] Nitroaromatic compounds identified in this SOA contributed up to 50 % of the total light absorption at 365 nm, indicating their importance as BrC chromophores.[51] Nitration also occurs through heterogeneous reaction of some organic species by $NO_3$ radicals and aqueous-phase reaction with the $NO_2^-$ anion. More details on nitration reactions will be described in Sections 3.1 and Section 4.5.

Oligomeric organic compounds that contribute to BrC light absorption have been identified in SOA material derived from reaction of aromatic compounds, including phenol,

catechol, guaiacol and many more (e.g., catechol-guaiacol dimer, **Figure 1**).[41,71–74] These

oligomers may contribute to the high molecular weight compounds that have been identified as

BrC components from biomass burning. Reactions leading to the formation of light absorbing

aromatic oligomers are described in Section 3.2. Recent measurements of cloud water at

Whiteface Mountain (USA) identified nitroaromatic compounds and aromatic oligomer

compounds associated with biomass burning emissions,[26] reinforcing the relevance of these

compounds.

Another important class of secondary BrC forms from processing in the condensed phase

between reduced nitrogen species and specific components of SOA, known as imine BrC

(**Figure 1**), which is discussed in more detail in Section 3.3.

## 1.3  Characterization of BrC Optical Properties

A few key terms are commonly used to describe the optical properties of carbonaceous

and BrC particles. At the most fundamental level, the complex index of refraction (*m*) of a

material characterizes how the speed of light is affected as it passes through a material along

with the extent of attenuation. It is inherently a property of the material, whether composed of a

single component or many components. The complex index of refraction is used in Mie theory to

calculate a spherical particle's optical properties, which vary with particle size.[75] It has a real

component (*n*) and an imaginary component (*k*), both of which depend on wavelength:

$$m(\lambda) = n(\lambda) + ik(\lambda) \qquad\qquad (2)$$

Strongly dependent on composition, the imaginary component primarily represents the ability of

the material to absorb light. The real component of the refractive index, while not fully

independent of the imaginary component, primarily represents its ability to scatter, depending on

particle phase but with a weaker dependence on composition. Values of $n$ and $k$ for laboratory and ambient particles are often derived from inversion of measured absorption coefficients under an assumption of well-mixed spherical particles.[65,76–80] Therefore, for non-spherical particles or spherical particles containing inclusions, or in cases where the particle shape is not known, the derived $n$ and $k$ values should best be considered effective values that characterize the observed absorption, rather than intrinsic to the particle composition.

The mass absorption coefficient (MAC) is a measure of the absorption capability that considers the mass of the material; the units are $m^2\ kg^{-1}$ or $cm^2\ g^{-1}$. The MAC can be determined for both solution extracts of dissolved aerosol particles and particles suspended in air, which are described below. This distinction is important because experimental methods that look at dissolved BrC typically filter out non-dissolved particles but may remove less soluble species as well. MAC for solution extracts is calculated from bulk absorption with the following equation[2]:

$$MAC(\lambda) = \frac{A(\lambda)\cdot ln(10)}{l\cdot C} \quad\quad (3)$$

where $A(\lambda)$ is absorption at a given wavelength, l is the optical path length and C is the mass concentration of the solution. The solution-phase MAC inherently characterizes only soluble components.

For suspended particles, the MAC is expressed in terms of the absorption cross section normalized by the mass of the component of interest e.g. BC or organic aerosol (OA). The observable MAC depends on the size of the particles of a given composition (i.e., have a constant $n$ and $k$), shown in **Figure 2A**.[81,82] This results from atmospheric particles having diameters similar to the wavelength of solar and terrestrial radiation.[83] For weakly to moderately absorbing particles, typically characteristic of BrC, the MAC generally increases with size until

the size parameter ($x = (\pi D_p)/\lambda$) is approximately 2. Above $x = 2$ the MAC exhibits weak

oscillations with size and eventually starts to decrease as the particles become sufficiently large.

The MAC decrease at large $x$ results from the particles being, at that point, sufficiently thick that

light is not absorbed throughout the entire particle. In the case of highly absorbing particles,

characteristic of BC or, perhaps, BrC at sufficiently small wavelengths, the oscillations are

damped and the turnover point (from increasing to decreasing MAC with size) shifts towards $x =$

1. The implications of this size dependent behavior is that the atmospheric impact of light

absorption by particles of a given composition is intrinsically dependent on the size distribution

of those particles and how this evolves in space and time.[84] The size-dependent behavior

complicates the comparison of MAC values observed for BrC-containing solutions versus

suspended particles. The approximate relationship between these is obtained by considering the

MAC normalized to the value at the small particle limit (**Figure 2B**). For weakly to moderately

absorbing systems, and given typical atmospheric size distributions, the approximate scaling

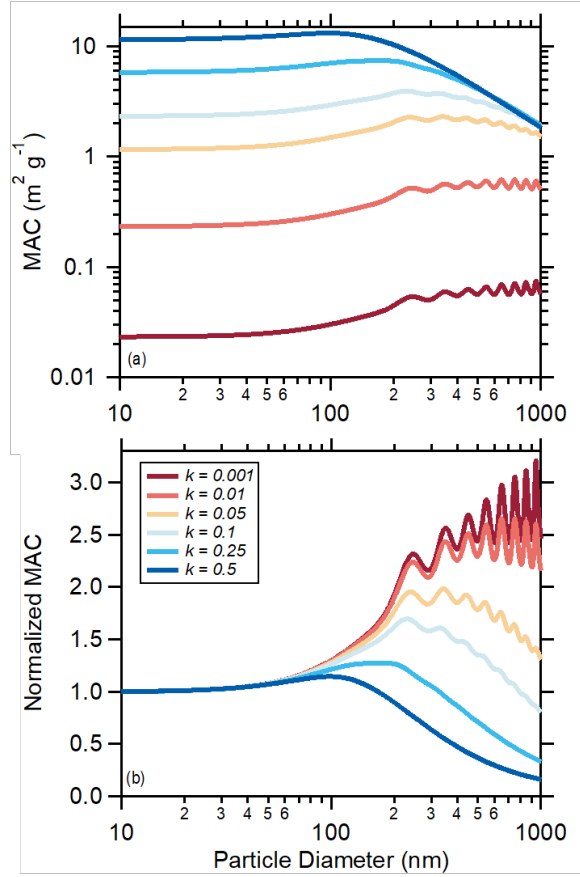factor required to relate the solution-phase MAC to the suspended-aerosol MAC is about 2.[84]

**Figure 2** Mie theory calculation of the (a) absolute MAC and (b) the MAC normalized to the small particle limit, for particles having a density of 1 g cm$^{-3}$ and $n$ = 1.5 at 405 nm. Different values of the imaginary refractive index ($k$) are assumed.

The wavelength dependence of the MAC is related to the absorption Angström exponent (AAE) and is described by the following equation[85]:

$$AAE = -\frac{\ln(MAC_{\lambda 1}/MAC_{\lambda 2})}{\ln(\lambda_1/\lambda_2)} \qquad (4)$$

where $MAC_\lambda$ is the mass absorption coefficient at a specific wavelength, and $\lambda$ is the wavelength. AAE is a measure of the variation of aerosol absorption with wavelength. It is widely used as a quantitative method to differentiate BC from BrC. AAE values for BC are generally accepted as

being close to unity (1), whereas a value substantially greater than 1 is associated with BrC due to the pronounced increase in the absorption coefficient at shorter wavelengths.

Single scattering albedo (SSA) is another wavelength-dependent property used to describe the absorption of aerosol particles. It is defined as the ratio of scattering coefficient over extinction, corresponding to the sum of the absorption and scattering cross sections ($\sigma_{abs}$ and $\sigma_{scat}$, respectively):

$$SSA(\lambda) = \frac{\sigma_{scat}(\lambda)}{\sigma_{abs}(\lambda) + \sigma_{scat}(\lambda)} \qquad (5)$$

An SSA value close to 1 indicates mainly scattering particles, whereas SSA values below 1 arise from aerosol absorption.

## 1.4  Aging of Atmospheric BrC: Goals of this Review

It is now well known that numerous aging processes proceed during the day-to-week timescales that prevail for carbonaceous aerosol before they undergo wet or dry deposition from the atmosphere.[86–90] Direct and indirect photoreactions can occur either in the aerosol particles or when they are incorporated into cloud droplets. Whereas direct photolysis refers to the action of a photon on a BrC molecule, indirect photoreactions occur when sunlight produces a reactive species (such as OH or $^1O_2$) which then reacts with the BrC compound. Heterogeneous oxidation can occur, in which a gas-phase oxidant (such as OH, $NO_3$, or $O_3$) undergoes a collision with an aerosol particle, leading to chemical modification of the particle. Beyond radical-induced oxidation processes, a wide range of closed-shell, condensed-phase reactions also occur in both aerosol particles and cloud droplets, leading to the formation of chemically complex molecules.

Through these studies, it is now apparent that carbonaceous aerosol components can also be oxidized on an atmospherically-relevant timescale into smaller, more volatile molecules that arise from fragmentation reactions.[91] The probability of fragmentation increases with the degree of oxygenation of the organic constituents. On the other hand, reactions between either stable molecules or radicals in the condensed phase can lead to the formation of oligomeric species[92] that are substantially less volatile and may enhance BrC absorption.

The goal of this review article is to assess the state of the science associated with the chemical aging of atmospheric BrC. In particular, unlike BC, which is more chemically inert, OA is chemically reactive and its optical properties can change throughout its lifetime in the atmosphere. Many characteristics of molecules that make them absorptive in the near ultra-violet and visible regions of the spectrum – such as the presence of extended conjugation or nitrogen-containing functional groups – also make them chemically reactive. The degree to which BrC changes its optical properties via atmospheric chemical aging will affect its direct radiative forcing. Although chemical processing may also drive changes in the hygroscopicity of BrC-containing carbonaceous aerosol, the review does not assess how this may affect indirect radiative forcing.  After this introductory section, the article begins with consideration of gas-phase reactions that lead to the formation of secondary BrC (Section 2). This is followed by Section 3 that addresses in-cloud and aqueous reactions, and Section 4 that describes aerosol particle processes, i.e., out-of-cloud. The majority of work in this field has been conducted in the laboratory, but connections will be made to atmospheric behavior and field studies that have identified changes in aerosol optical properties via atmospheric aging (Section 5). The review concludes with comments on general behavior in the atmosphere and suggestions for future study (Section 6).

As noted above, this article builds upon prior reviews on atmospheric BrC and aerosol optical properties, that have in part addressed the aging issue.[2,28,93–96] For that reason, this article focusses primarily on chemical advances of this rapidly moving field that have occurred in the past decade or so.

## 2  Gas Phase Reactions Leading to BrC

The chemical generation of absorbing molecules in the gas phase, which condense to form SOA can contribute to the formation one form of secondary BrC. There are indications that this can occur with primary emitted precursors, both in polluted settings[97] and within biomass burning plumes.[98] However, the extent of secondary BrC influence is still poorly defined with one study[97] reporting up to 30 % of total BrC formation in the Los Angeles area, whereas another[99] showing minor impacts. Biogenic gas-phase precursors are unlikely as important as those arising from incomplete combustion, in particular aromatic compounds.[100] The formation of light-absorbing SOA onto aerosol particles most likely occurs close to the BrC source, whereas the oxidative and photochemical aging processes described in more detail in Sections 3 and 4 will occur as the particles move away from the source regions.

As particles age in the atmosphere, they often also undergo dilution. This can lead to enhanced loss of higher volatility aerosol components and may be particularly important for the evolution of primary biomass burning particles that are emitted with high concentrations. Various studies have suggested that higher volatility components are less absorbing than lower volatility components.[95,101–103] As such, dilution-driven evaporative loss can lead to particles having a greater absorptivity over time. However, we note that in the absence of concurrent chemical formation of new or more absorbing aerosol components the total absolute absorption by the aerosols will be largely unaffected.

Understanding of secondary BrC formation derives from both laboratory experiments involving SOA formation from reaction of individual precursors or mixtures of precursors and from field observations. In general, the absorptivity of the SOA formed depends on the chemical identity of the precursor, the reaction conditions, and the extent of aging. A common finding across studies is that nitroaromatic compounds (NACs)[40,53,104] are important components of secondary BrC. For example, higher MAC values for laboratory[100,104] and field[69] observations of SOA are associated with formation of NACs.

For an individual SOA precursor, the absorptivity of the SOA formed generally increases as the relative $NO_x$ concentration increases. While this is true for many precursors, including anthropogenic aromatic and biogenic compounds,[100,105] the MAC values are highest when NACs are formed. For aromatic precursors, the increase in absorptivity is likely associated with enhanced formation of NACs at higher relative $NO_x$. In particular, early photo-oxidation experiments demonstrated the formation of NACs when $NO_x$ was present.[106] Oxidation of toluene in high-$NO_x$ conditions formed over 15 different absorbing molecules, with NACs accounting for 60 % of the absorbance from 300 - 400 nm.[100] In the case of $NO_x$-free conditions, the majority of the products formed were non-aromatic compounds with high degrees of saturation.[100] Field observations of NACs from an area with high $NO_x$ also display an increase with $NO_x$ concentrations until a saturation point, where organic products stabilize with a shift towards formation of inorganic nitrate.[69]

Consideration of the reaction mechanisms associated with oxidation of aromatic species aids in understanding the $NO_x$ concentration effects on the formation of NACs. For example, catechol is a VOC emitted from biomass burning that has high gas-phase reactivity.[50,107] The reaction of catechol with either OH or $NO_3$ radicals both formed SOA.[50] The dominant product via reaction

with NO₃, 4-nitrocatechol (4NC), was also present in significant amounts after reaction with OH, indicating similar reaction pathways for both radicals. The proposed mechanism for this reaction includes hydrogen abstraction of a phenolic hydrogen by either OH or NO₃ radicals, forming a β-hydroxyphenoxy radical, which subsequently reacts with NO₂ to form 4NC (**Figure 3**).[50] Similar reactions mechanisms have been observed for other biomass burning VOCs such as phenol, resorcinol, eugenol, guaiacol, and syringol.[108–111] This mechanism was also observed with the precursor trimethylbenzene (TMB), which did not produce as many NACs as toluene because the addition of NO₂ to the phenoxy radical formed is inhibited.[100] This reaction pathway contributed to formation of nitrophenols.[69]
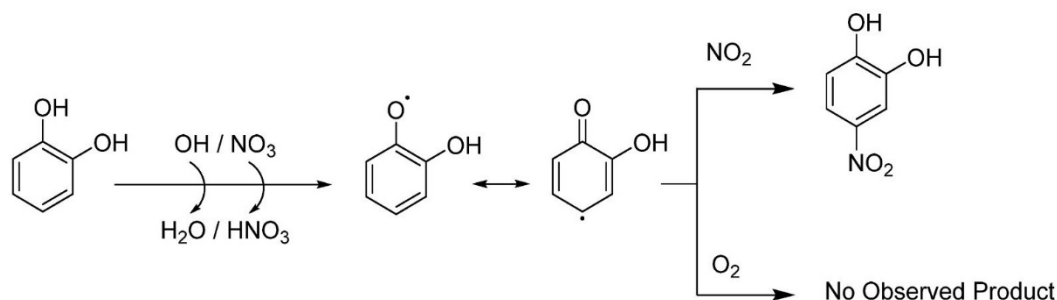


**Figure 3** Proposed reaction mechanism for the formation of 4NC from catechol in the presence of NO$_x$ [Reprinted with permission from Finewax *et al.*[50] Copyright 2018 American Chemical Society]

While SOA formed from biogenic compounds, such as isoprene and monoterpenes, tends to be less absorbing than that formed from aromatic compounds, a weak NO$_x$ dependence to the SOA absorptivity has also been observed for some biogenic SOA precursors.[100,112] Nonetheless, most studies indicate that biogenic precursors contribute little to BrC.[113–115] However, it is important to keep in mind that many studies often look at the total absorptivity of the OA, not distinguishing between individual molecules or even OA types. Consequently, formation of non-

or weakly absorbing SOA can still impact the observed overall OA absorptivity ($MAC$ or $k$) through addition of non-absorbing OA mass even if the absolute absorption remains unchanged. For this reason, it is important to distinguish between the measurement of absolute absorption versus absorptivity, especially for studies of ambient particles.

To complement fundamental studies on individual precursors, there are a number of recent experiments that have considered the behavior that results when whole smoke samples, i.e. primary organic particles plus accompanying VOCs, are chemically aged.[52,70,116–124] The chemical and physical processes involved in these experiments are complex and have not all been decoupled, and there are challenges in distinguishing between absorption by the primary OA and the secondary OA. Nonetheless, most laboratory studies show that for relatively short aging times, with equivalent atmospheric aging times of a day or less, dilution-corrected organic aerosol mass increases due to SOA formation. (We note that the extent of SOA formation varies substantially between different studies. Some of this variability likely results from the use of different biomass fuels. However, some of this derives from the lack of clarity regarding the extent to which the POA evaporates in these laboratory experiments, versus in the ambient environment.[35,95,123,125,126]) Experiments conducted with environmental chambers demonstrate that the total BrC absorption can increase (after correction for dilution) at low photochemical ages due to formation of absorbing SOA material, which adds to the POA absorption.[120–123] Some studies have attempted to apportion the observed total absorption into contributions from SOA and POA. These studies have generally found that the SOA is somewhat absorbing, however with an absorptivity that is lower than for POA although this depends importantly on the chemical identity of the SOA precursors and reaction conditions.[70,118,123]

Given both the generally stronger absorptivity of BC and primary OA compared to SOA, variability in the extent of SOA formation, and the need to make assumptions regarding how the mixing state of BC affects the total absorptivity, uncertainties associated with SOA from these complex mixtures are substantial. Some studies indicate that the SOA absorptivity may vary substantially between different biomass fuels.[121,127] In contrast, it was recently determined that the use of common properties for the SOA absorptivity describe the observed behavior across a wide range of different fuels and burns.[123] Some variability is to be expected, as the particular gas-phase precursors depend on fuel type and burn conditions,[128–130] although it is possible that the chemical nature of the SOA formed is not overly sensitive to moderate variations in the initial VOC mixture.[70,131,132] These studies also indicate that the SOA has a fairly strong wavelength dependence to absorption, with AAE values on the order of five. This is substantially larger than the AAE for BC. AAE values for SOA formed from oxidation of biomass burning smoke can be either larger than or smaller than those for POA, dependent on the fuel type and burn conditions.[101,121,123,127]

At longer equivalent atmospheric aging times there can be a decrease in the dilution-corrected amount of organic aerosol present.[52,117,119] This indicates the occurrence of fragmentation of highly oxidized organics, both within the gas and the particle phases, leading to reduced SOA formation as well as evaporation of particle-phase constituents, and corresponds to the now-well-understood transition from functionalization to fragmentation as aging proceeds.[88,91] Additionally, at long photochemical ages the precursor compound has reacted entirely away, thus there is no longer primary gas phase material present to form SOA. The lack of formation of new absorbing SOA, coupled with the loss of more absorbing POA, leads to a decrease in the total absorption over time. In addition, both chemical bleaching and photobleaching can contribute further to the decrease in dilution-corrected absorption over time,

and even to a decrease in the BrC absorptivity, discussed further in Sections 3 and 4. Indeed, the degree of absorption can change, at times with a corresponding decrease in the AAE.[52,116] These intense aging experiments are typically conducted in oxidation flow tube reactors, where complex chemistry can occur with the very high gas phase radical concentrations present. The individual results are strongly dependent on the type of fuel burned (e.g. peat vs wood), flaming vs. smoldering combustion, and whether the polar or non-polar components of the BrC aerosol particles are analyzed.

# 3   Aqueous and In-Cloud Reactions of BrC

Liquid water in the atmosphere is an important medium in which reactions take place, changing the chemical composition and physical properties, such as absorbance. Atmospheric liquid water also impacts the overall fate of aerosol particles and water-soluble gases. Aerosol particles can take up water at elevated RH and can have liquid water concentrations ranging up to 0.01 g m$^{-3}$ when deliquesced.[90] Aerosol particles act as CCN, forming cloud or fog droplets when water vapour is sufficiently supersaturated (i.e., above 100 % RH). Cloud and fog droplets can contain up to 300 times as much liquid water as deliquesced aerosol particles, with mass concentrations ranging from 0.05 – 3 g m$^{-3}$ and 0.1 – 0.3 g m$^{-3}$, for cloud and fog droplets respectively.[90,133] Cloud droplets range in size from approximately 10 – 20 μm in diameter and have lifetimes in the atmosphere ranging from minutes to hours.[90,133,134] The majority of cloud and fog droplets do not reach a size that can precipitate, instead evaporating and releasing their chemical constituents as particles and gases.[133] Cloud and fog cycling, with formation and evaporation and the aqueous-phase chemical reactions in between, results in a large potential for aqueous processing of atmospheric compounds.

Sunlight drives many reactions in the aqueous phase both through direct absorption of light by organic species and through the generation of radical oxidants (e.g., OH). As in the gas phase, the OH radical is one of the most important oxidants in the aqueous phase, with an uncertain and variable concentration. Sources of OH radicals in aqueous aerosol particles, cloud, and fog droplets vary, both spatially and temporally, thereby altering the production rate of aqueous OH radical. Additionally, the loss processes for OH radical can vary, which also affect its concentration. The few studies that have assessed aqueous OH radical concentrations show it can span several orders of magnitude, from $1\times10^{-16}$ to $1\times10^{-13}$ M.[135–138]

Aqueous oxidation reactions can occur rapidly, such that chemical lifetimes of organic compounds with respect to aqueous-phase OH oxidation can be similar to those in the gas phase.[139] For example, the gas phase lifetime of phenol with respect to OH radical reaction ($k_{phenol(g)} = 2.8 \times 10^{-11}$ cm$^3$ molec$^{-1}$ s$^{-1}$, $[OH]_{(g)} = 1 \times 10^6$ molec cm$^{-3}$) is 10 hours; the aqueous phase lifetime of phenol with respect to OH radical reaction ($k_{phenol(aq)} = 8.4 \times 10^9$ M$^{-1}$ s$^{-1}$, $[OH]_{(aq)} = 1 \times 10^{-16}$ M to $1\times10^{-13}$ M)[135] ranges between 0.33 to 330 hours within the likely range of $[OH]_{aq}$.[139] Reactions that cannot occur in the gas phase, such as those catalyzed by dissolved metals, are observed in aqueous aerosol particles and cloud and fog droplets.[140] Additionally, reactions which may be limited by diffusion in viscous aerosol particles can occur more rapidly with higher liquid water content and faster mixing timescales.[141] However, important reactions in the gas phase involving $O_3$ and $NO_x$ are less likely to occur in the aqueous phase due to the low water-solubility of these molecules.

Excitation of organic chromophores (i.e. BrC) can produce oxidants (other than OH radical) in the aqueous phase. This phenomenon has been extensively studied in natural waters, initiated by excitation of chromophoric dissolved organic matter.[142,143] The absorption of sunlight by

organic chromophores can promote them to an excited triplet state ($^3$C*). The triplet excited state can react with organic compounds or can produce reactive photooxidants including singlet molecular oxygen ($^1$O$_2$). Photo-excitation to generate triplet excited organic compounds has also been observed in the atmospheric condensed phase.[41,71–73,144–151] Reaction of either the triplet excited organic compounds or singlet oxygen can result in significant oxidation of organic compounds in the aqueous phase. Photosensitized chemistry may also be important in formation of SOA mass, either through aqueous reactions[41,71–73] or heterogeneous uptake of reactive gases.[145–148,152] Measurements of collected ambient fog water and aqueous extracts of aerosol particles show that photosensitized reactions occur when chromophoric organic compounds, or BrC, are present.[149,150] Aerosol particles, which have much lower liquid water concentrations, were observed to have more than 30 times the concentration of triplet organic compounds compared to fog droplets.[150] The concentration of triplet organic compounds that form increased with increasing particle mass to water mass ratios,[150] indicating that this reaction mechanism could be enhanced in highly polluted cloud or fog water and lower liquid water containing aerosol particles.

Aqueous aging of BrC can lead to the loss of absorption or to the formation of new chromophores, which contribute to secondary BrC. How BrC changes with aqueous oxidation will depend on both the type of BrC, as well as the dominant reactions that take place (e.g., photoreaction, OH oxidation). In the remainder of this section, we discuss recent studies on the aqueous reactions of biomass burning and nitroaromatic, oligomeric BrC, and imine-derived species and describe advances in our understanding of the complex processes arising when water droplets become highly concentrated upon evaporation. The majority of these aqueous aging measurements have been carried out on bulk aqueous solutions, rather than on droplets or aqueous aerosol particles, unless otherwise noted.

## 3.1  Aqueous Reactions of Biomass Burning and Nitroaromatic BrC

In addition to forming in the gas phase (Section 2), highly functionalized nitroaromatic compounds are sufficiently soluble to significantly partition to the aqueous phase. Aqueous photonitration of, for example, phenol, guaiacol, methylcatechol and vanillin, can occur via exposure to UV light in the presence of dissolved nitrite to form nitrophenol compounds.[153–156] These nitrated products absorb light more strongly in the visible region of the spectrum than the precursor compounds.[153] Nitration also occurs without the presence of light, for example, by reaction of aromatic compounds with nitrous acid/nitrite.[157,158] These nitration reactions may have a greater contribution to BrC formation during the night or in other low-light conditions.

Aqueous aging of biomass burning BrC and isolated nitroaromatic compounds has shown both formation and loss of chromophores within the same exposures. First, increases in absorption that result from formation of chromophoric compounds have been observed in laboratory studies of UV light exposure of aqueous wood smoke BrC (generated from pyrolysis of cherry wood)[61,159] ambient biomass burning BrC (collected in Crete, Greece),[61] and nitrophenol compounds (including 4-nitrophenol, 5-nitroguaiacol and 4-nitrocatechol).[160] This increase in absorption is attributed to the formation of oxygenated and larger molecular weight products which absorb light more strongly at visible wavelengths. The majority of the absorption increase in wood smoke BrC during UV light exposure has been attributed to formation of molecules > 400 Da (**Figure 4**).[61,159] While absorption was also observed for molecules < 400 Da, the relative contribution to absorption during photoreaction was less than 50 %.[61,159] However, with continued UV light exposure of this wood smoke BrC (generated from pyrolysis of cherry wood), the absorptivity decreases slowly owing to the occurrence of photobleaching.[61,159] Photosensitized triplet excited state reactions from aromatic precursors can

lead to chromophore formation through the generation of aromatic dimer and oligomer compounds with much higher molecular weight (further discussion in Section 3.2).[71–73] These triplet excited state reactions can be fast enough to compete with other reactions in the aqueous phase.[41] For example, photosensitized reactions between dimethoxybenzaldehyde and biomass burning derived phenols (phenol, guaiacol, and syringol) were observed to have large kinetic rate constants.[41] Second, an initial increase in absorption is not universally observed across studies, with different chemical systems exhibiting differing behavior. For example, in another study looking at biomass burning BrC (from the whole smoke of four biofuels: sawgrass, peat, ponderosa pine, and black spruce)[58] or nitrophenol-containing BrC (derived from benzene, toluene, p-xylene, and naphthalene precursors),[56] the absorption decreased continuously with UV light exposure. This variability in absorption change and how the absorption responds to UV light exposure likely indicates the relative importance of photolysis, or breakdown of chromophores, compared to formation of chromophores that take place in each BrC sample. In a majority of these studies, even with significant photobleaching, the absorption is not completely lost and at least ~20 % of the absorbing material (in the near-UV and visible range) is recalcitrant against decay.[56,58,61,159]

In addition to aqueous reactions initiated by UV light, laboratory studies have been carried out to investigate the effect of OH oxidation on BrC absorption. The change in absorbance during OH oxidation generally mirrors the trend for product formation during oxidation of organic compounds, which moves from functionalization to fragmentation reactions.[91] Initial increases in absorption are linked to reaction products dominated by functionalization of chromophores, where there is an addition of oxygenated functional groups. This reaction mechanism is expected to generate unique products from those produced by UV light exposure and photosensitized reactions (discussed above). This is followed by a loss of

absorption and an increase in products formed by fragmentation where there is cleavage of C-C bonds. For example, the aqueous OH oxidation of individual nitrophenol compounds (4-nitrophenol, 5-nitroguaiacol 4-nitrocatechol, and 2,4-dinitrophenol) resulted in an initial enhancement in absorption and formation of oxygenated products, followed by loss of absorption and formation of fragmented products from cleavage of the aromatic ring with continued OH oxidation.[160,161] For example, an initial increase in absorption with OH oxidation was also observed in aqueous extracts of wood smoke BrC and was driven by an increase in absorption by high molecular weight compounds (>400 Da), which appear to be less easily broken down compared to lower molecular weight compounds (**Figure 4**).[61] OH oxidation without the presence of light, initiated by Fenton chemistry, did not lead to an increase in absorption for biomass burning BrC at early times, and absorption across the UV-visible spectrum only decreased with OH oxidation.[162] This result possibly indicates that the strong absorption enhancement requires both OH oxidation and photoreactions to occur, although it should be noted that the wood source and burning conditions differed between these two studies.[61,162] Atmospheric equivalent lifetimes for photobleaching in aqueous-solutions from UV light and OH reactions have been estimated to vary between a few hours to more than a day.[58,61,159–161]
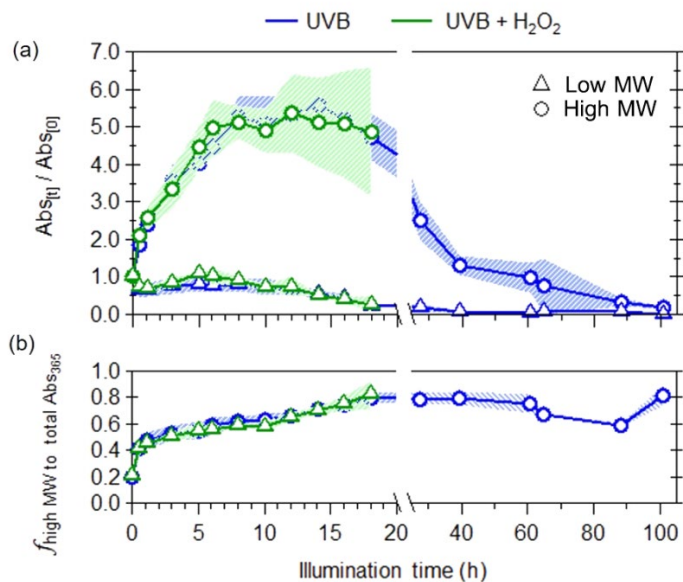
**Figure 4** (A) Change in light absorption at 365 nm for low- and high-molecular weight (MW) water-soluble wood smoke BrC fractions upon exposure to UVB light alone or upon exposure to UVB with $H_2O_2$ present, leading to generation of OH radicals in the aqueous phase. (B) Contribution of high-MW fraction to total light absorbance at 365 nm in water-soluble wood smoke BrC. The shaded areas represent the variability ($\pm 1\sigma$) in multiple experiments (n = 3). [Reprinted with permission from Wong *et al.*[61] Copyright 2019].

There is much to be learned by comparing the absorbance aging behaviour of BrC proxies that are single molecules to the behavior of more chemically complex samples, such as the BrC from biomass burning discussed above. An example is shown in **Figure 5**, which compares the MAC values as a function of OH exposure for nitrocatechol at 420 nm[161] and wood smoke BrC samples in aqueous solutions at 400 nm.[163] The maximum absorbance for a single precursor molecule, such as nitrocatechol, occurs at a much lower OH exposure than was observed for the more complex wood (pine and red oak) smoke BrC precursors. Moreover, the wood smoke BrC maintains the increased absorbance to much higher OH exposure. These

differences in absorbance with photochemical aging indicate that single precursor compounds may not capture the absorbance of complex mixtures likely to be found in the atmosphere. While similar types of chemistry were identified in the oxidation of these two cases (e.g., addition of oxygen-containing functional groups to aromatic molecules),[161,163] it appears that there are additional processes occurring or molecules present in the chemically complex samples (i.e., wood smoke) that must not be overlooked. A difference in single component lifetime compared with total BrC absorbance was also observed for aerosol (i.e. out-of-cloud) photoreactions of biomass burning smoke BrC[164] (discussed in Section 4.1).
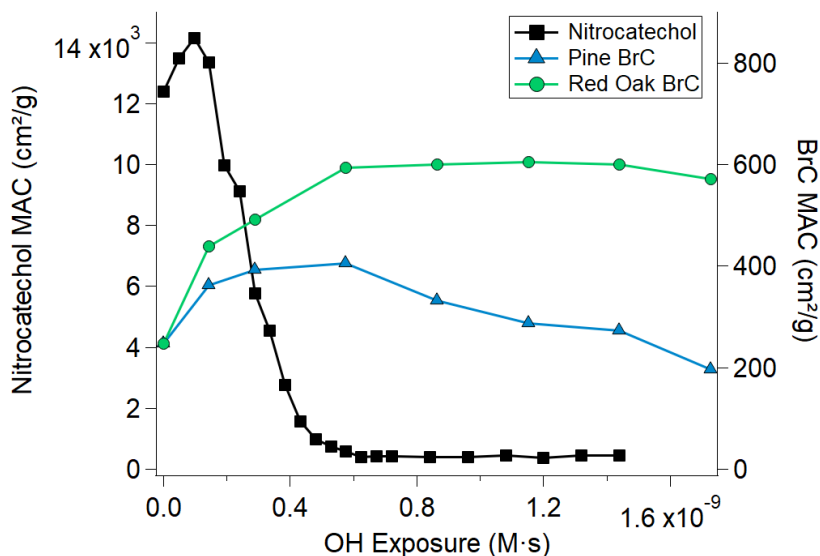


**Figure 5** MAC as a function of OH exposure for nitrocatechol (@ 420 nm, left axis)[161] and wood smoke BrC (@ 400 nm, right axis) precursors[163].

## 3.2  Formation of Oligomeric BrC Molecules in the Aqueous Phase

As mentioned in Section 1.2, condensed phase reactions of aromatic compounds can lead to the formation of absorbing oligomers that contribute to BrC. Aromatic oligomer compounds can absorb light at longer wavelengths than the individual monomer compounds due to the

extended π-conjugation.[165] These oligomers form from reactions of aromatic monomer

compounds, such as phenol, guaiacol, syringol, vanillin and other phenolic carbonyls during

aqueous photoreaction and OH oxidation.[72–74] The mechanism of formation of oligomer

compounds is through radical coupling reactions, either through an oxygen atom (from a

hydroxyl functional group) or a carbon atom in the aromatic ring (**Figure 6**).[72] Through this

mechanism, radical coupling may continue with more than 2 monomers. Oligomers as large as
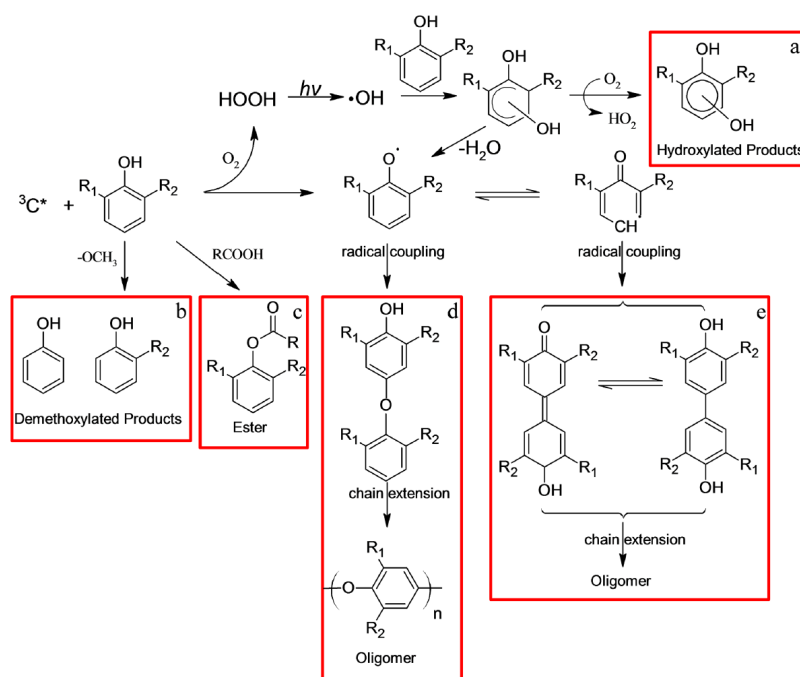
the hexamer have been identified with nano-DESI MS.[72]



**Figure 6** Schematic of the formation mechanism of hydroxylated species, dimers and higher

oligomers, esters, and demethoxylated products from aqueous photooxidation of phenolic

compounds. [Reprinted with permission from Yu *et al.*[72] Copyright 2014]

Dark iron-catalysed reactions of phenolic compounds can also lead to the formation of

aromatic oligomers.[166–168] Although formed through a different mechanism, the resulting

oligomers are expected to be similar to those formed through photoreactions (**Figure 6**).[166,168] In

addition, oligomeric products form through reactions of iron with two common aromatic

oxidation products, fumaric acid and muconic acid.[167–169] While iron is present in dust particles

and is emitted from anthropogenic sources such as fly ash,[170] the importance and prevalence of

these iron reactions with phenolic compounds has yet to be demonstrated. In the specific case of

syringol, oligomeric compounds may also form through dark reactions in the presence of

chloride salts.[171] It remains to be seen whether this may also occur for other aromatic molecules.

## 3.3  Aging of Imine BrC in the Aqueous Phase

Condensed phase and heterogeneous reactions (discussed in Sections 4.4 and 4.5) of

reduced nitrogen and organic compounds can form BrC species with imine-type functional

groups. For example, imine BrC compounds form through secondary reaction in the condensed

phase between ammonia or particulate ammonium and components from limonene SOA.[54,172–175]

The compounds in these samples that contribute to their visible light absorption are imines and

N-heterocycles such as imidazoles and pyrroles.[173] These imines and N-heterocycles have also

been observed to form through aqueous phase reactions of glyoxal and methylglyoxal, with

ammonium or amines (e.g., imidazole-2-carboxaldehyde, **Figure 1**) in both bulk aqueous

solutions[176–183] and aqueous aerosol.[184] Numerous combinations of atmospherically relevant

aldehydes and ammonia or amines have been observed to participate in this chemistry, including

aldehydes such as methylglyoxal, glyoxal, glycolaldehyde and amines such as glycine and

alkylamines.[180,182,185–195] More recently, pyrazine compounds have also been observed as

products from the reaction of methylglyoxal and ammonium (e.g., dimethylpyrazine, **Figure

1**).[185,196] While these small aldehydes have high volatilities, they are water-soluble and partition

to the aqueous phase. Their reactions in the aqueous phase can result in irreversible uptake.

Imine BrC reactions investigated in the laboratory tend to need high concentrations of reactants

and long reaction times (e.g. on the order of days). However, cloud and fog droplet evaporation can accelerate the formation of these light absorbing compounds (see Section 3.4).[197–200] As with nitrophenol compounds, the compounds in imine BrC have pH dependent light absorption. For example, the absorption of imidazole-2-carboxaldehyde (**Figure 1**), a commonly observed product from imine BrC, shifts to lower wavelengths at lower pH as it moves to its hydrated form.[201] Therefore, the contribution of these chromophores to BrC may also be lower under more acidic conditions.

While dark aqueous reactions can lead to the formation of imine BrC, exposure to sunlight and oxidation by OH radicals rapidly degrade it. Loss of absorption from imine BrC has been investigated in laboratory studies using a variety of precursors to form imine BrC.[159,160,192,194,202–205] The lifetime of methylglyoxal and ammonium derived imine BrC with respect to UV light exposure occurred over minutes, primarily due to the loss of imidazole-2-carboxaldehyde + methylglyoxal oligomers and other nitrogen containing compounds (**Figure 7**).[160,192,206] OH oxidation in the aqueous phase also proceeds rapidly, with similar lifetimes on the order of minutes to hours.[160,203] Rapid photobleaching by exposure to UV light was observed to occur through loss of compounds across the full molecular weight range, although photolysis was more rapid for lower molecular weight compounds.[159] Lifetimes with respect to UV light exposure were hours for other aldehyde-amine mixtures which form imine BrC,[188,192,193,207] indicating that this class of secondary BrC is not photochemically stable and will not be long lived in the presence of sunlight. Absorption due to this imine BrC may only be significant near to sources or if the source production is large and/or sustained over time.
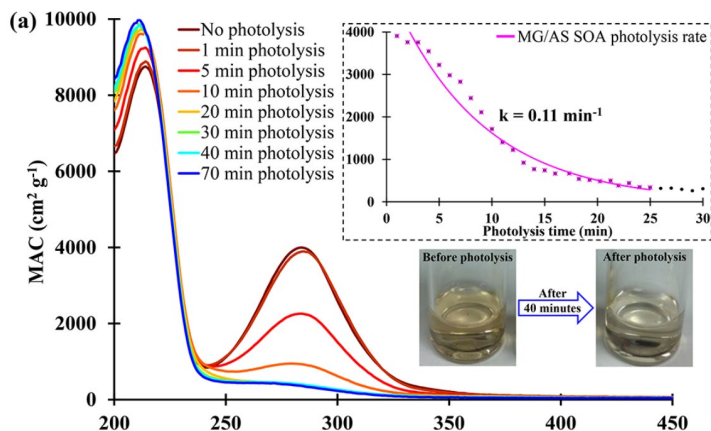
**Figure 7** Wavelength-dependent MAC of methylglyoxal (MG)/ammonium sulfate (AS) BrC during aqueous photoreaction. The inset shows the time dependence of MAC for MG/AS BrC at 280 nm. The photos illustrate the visible change in the MG/AS BrC sample color from brown to colorless during photoreaction. [Reprinted with permission from Aiona *et al*.[206] Copyright 2017 American Chemical Society]

## 3.4  Cloud and Fog Droplet Evaporation Processes Leading to BrC

Briefly discussed for imine BrC above (Section 3.3), atmospheric processing by evaporation of cloud or fog droplets, or aqueous aerosol (near 100 % RH) can enhance the rate at which BrC forms. The evaporation process from bulk solution[185] or from aqueous aerosol[186,197,200] can decrease the timescale of reactions from hours or days to seconds in the cases of the reactions of glyoxal or methylglyoxal with ammonium sulfate and other aldehyde-amine mixtures. The driving factor is principally concentration of reactants, where the concentrations of solutes in evaporated droplets can be orders of magnitude larger than the bulk solution used to generate the droplets. Compounds that exhibit "salting-in" effects, where their Henry's law constants increase with increasing salt concentration, could be especially important in the chemistry during the evaporation processes.[186,197] It should be noted that evaporation does not lead to the

concentration of all compounds; for example, upon evaporation of droplets, glycoladehyde partitioned into the gas phase (i.e., evaporated) before reaction could take place.[186] Other factors leading to increased BrC formation during evaporation are the presence of water elimination steps in forming chromophores[185] and the increase in surface reactions as the surface area to volume ratio increases.[200] A recent study demonstrated that the BrC formation process from evaporating aqueous aerosol particles occurs most efficiently at intermediate relative humidity values of roughly 60%.[208]

Recent work has expanded the investigation of BrC formation by evaporation processes of aqueous mixtures of SOA in the presence of sulfuric acid.[209] For SOA made from high concentrations of α-pinene, β-pinene, limonene, and isoprene oxidation that was collected and extracted into water and adjusted to pH 2 with sulfuric acid, evaporation led to increases in absorption at ultra-violet and visible wavelengths, with the largest increases observed for limonene SOA (**Figure 8**).[209] The most abundant chromophores in the evaporated limonene SOA were attributed to organosulfate compounds that form through acid-catalysed reactions.[209] These results indicate that evaporation-driven BrC formation can be important in organic mixtures other than the imine BrC system. BrC formation through aqueous reactions of glyoxal and sulfite leading to organosulfates compounds has also been observed recently[210] and may indicate that these types of reactions can be important even without evaporation.
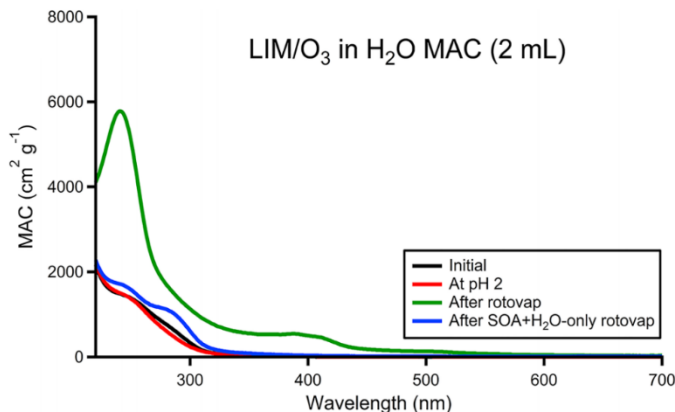
**Figure 8** MAC values of limonene (LIM)/O₃ secondary organic material dissolved in 2 mL of water (black). Also shown are MAC values after the addition of $H_2SO_4$ to pH 2 in 2 mL of water and further dilution to 4 and 20 mL (red), after the evaporation of the solutions (green), and after the evaporation with LIM/O₃ secondary organic material and water only with no pH adjustment (blue). [Reprinted with permission from Fleming *et al.*[209] Copyright 2019 American Chemical Society]

While many laboratory studies have identified the formation of BrC upon droplet or bulk solution evaporation, confirmation of this process has yet to be observed in ambient cloud droplets and aerosol particles. Recently, evaporation of ambient aerosol particles collected during the summer in Maryland down to a RH below 41 % led to no increase in absorbance.[211] However, this study did not investigate cloud processing, where the extent of water loss is far greater than associated with drying of an aerosol particle. In addition, organic precursors, such as glyoxal and methylglyoxal, were not expected to be in sufficiently high concentration in the ambient particles to result in an observable increase in absorbance.[211] Further ambient observations of evaporation of cloud droplets and aerosol particles are needed.

# 4 Particulate Phase Reactions of BrC

Downstream of sources, such as biomass burning, primary and secondary BrC aerosol is susceptible to aging with respect to direct or indirect photolysis, other photoreactions, reactive uptake, or heterogeneous oxidation.[212–214] Irradiation can break apart chromophores, produce oxidants in situ, or facilitate photosensitized reactions.[144,164,212,215] Reactive uptake of ammonia or amines to dicarbonyl-containing organic aerosol, or conversely of dicarbonyl compounds to ammonium-containing aerosol, can lead to the formation of imine and nitrogen-containing BrC.[213,216–218] Heterogeneous reactions with gaseous ozone and OH and $NO_3$ radicals can lead to oxidative aging, resulting in changes in both composition and absorptivity.[116,168,214,219,220] These reactions can be limited by diffusion for (semi-)solid BrC particles, which will be more important at low RH as particle viscosity increases with decreasing RH.[221–226] Moreover, SOA including secondary BrC can be internally mixed with aggregates of BC, leading to drastic changes in morphology, absorption efficiency, and hygroscopicity of BC,[99,121,131,227] though less pronounced than those induced by secondary inorganic species.[228–230]

Several aspects specific to the atmospheric processing of particulate BrC compared to aqueous BrC require introduction. First, we consider particulate effects on photoreactions within particles, including photolysis and photosensitized reactions. In contrast to droplets, submicron aerosol particles have diameters on the same order as the wavelengths of visible light. Assuming the particles are well-mixed and spherical, their absorption and scattering cross sections can be calculated from Mie theory. In the submicron regime, for particles having constant composition, the absorption and scattering efficiencies vary with particle size at a given wavelength. Accounting for this size dependent behavior is important to consider when interpreting observations.[231,232] Due to this size dependency, the AAE observed for bulk samples of aqueous

BrC using liquid waveguide capillaries, for example, is not necessarily the same as that observed for suspended particles using photo-acoustic spectrometers and other in situ methods.[233,234] Moreover, MAC values obtained for bulk samples may differ from those observed for suspended particles having the same composition owing to these particulate effects.[235,236] In addition to influencing the optical properties of aerosol populations, particulate effects influence the spatial distribution of light within individual irradiated particles. For example, for 500 nm particles, incident light with a wavelength of 445 nm is predicted to be concentrated at the opposite hemisphere of the particle, and this effect could play a role in enhancing photochemical reactions at the surface of submicron particles.[237]

Furthermore, particulate effects influence heterogeneous reactions, on the basis of the viscosity of the particles.[221] SOA viscosity and its dependence on RH has been measured for both biogenic (e.g., isoprene[222] and α-pinene[223]) and anthropogenic (e.g., toluene[224]) precursors, and highly viscous SOA slows kinetics by limiting diffusion of reactants within particles, since only a small fraction of molecules at or near the surface may be accessible for heterogeneous chemical attack.[225,226] In the context of particulate BrC, kinetic limitations have been explored for SOA from individual surrogate species,[238] including 4-methyl-5-nitrocatechol,[239] as well as complex mixtures of SOA deposited on substrates and exposed to ammonia.[240,241] For toluene SOA, reactive uptake of ammonia leading to browning, described in more detail below (Section 4.2), was limited for up to 24 hr at <20 % RH.[240,241] Recently, direct measurements of the viscosities and diffusion coefficients of limonene SOA constituents after exposure to ammonia have been reported.[242] The average diffusion coefficient of constituent fluorophores in the limonene SOA decreased from $6\times10^{-9}$ cm$^2$ s$^{-1}$ at 90 % RH to $7\times10^{-13}$ cm$^2$ s$^{-1}$ at about 30 % RH, as shown in **Figure 9**, corresponding to a shift in mixing time for 200 nm particles from 0.002 to 14 s, still quite short, suggesting that this material is well mixed under most ambient

conditions.[242] Finally, predictions based on molecular composition data from high-resolution

mass spectrometry indicate that the viscosity of primary particulate BrC may not vary as widely

with RH as SOA from $\alpha$-pinene or toluene,[243] but this has not been measured directly.
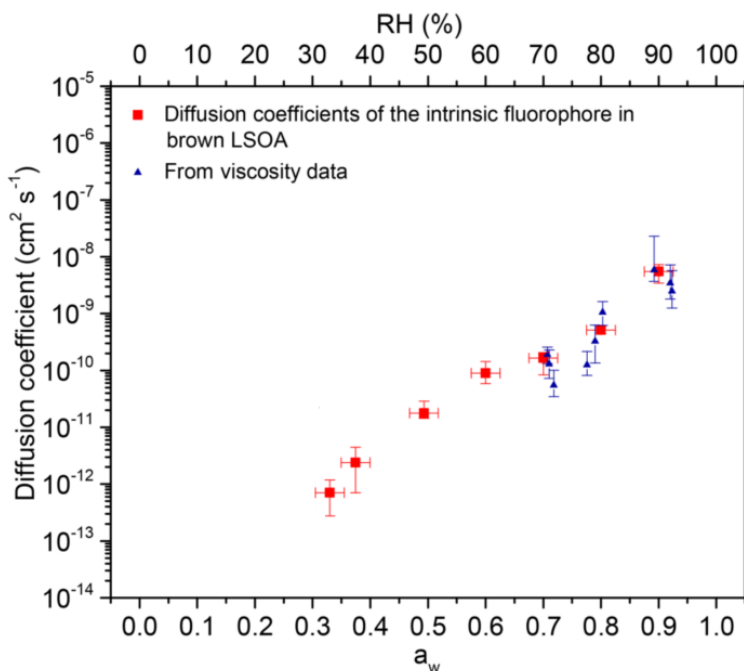


**Figure 9** Diffusion coefficients in secondary BrC derived from ozonolysis of limonene as a

function of the activity of water (or RH). Red squares denote diffusion coefficients measured

directly using fluorescence recovery after photobleaching, and blue triangles denote those

derived indirectly from viscosities measured using the poke-flow method and the Stokes-Einstein

equation. [Adapted with permission from Ullmann *et al*.[242] Copyright 2019]

## 4.1 Photoreactions of Particulate BrC

The role of direct photolysis at ultraviolet wavelengths in the aging of organic aerosol

was demonstrated when it was shown that significant SOA mass could be lost due to the

fragmentation of highly functionalized first-generation particulate products of $\alpha$-pinene when

they were exposed to radiation in the absence of additional oxidant.[244] In a subsequent investigation of $\alpha$-pinene SOA, less oxidized components, including carbonyl-containing compounds, were shown to photolyze most rapidly, such that the composition of the remaining particles shifted to more oxidized components.[245] This rapid carbonyl photolysis is in agreement with earlier observations of limonene SOA deposited on filters and exposed to monochromatic UV radiation, including the detection of resulting CO.[246] More recently, the production of VOCs due to the photolysis of light absorbing $\alpha$-pinene and limonene SOA, deposited on quartz crystal microbalance substrates, has also been quantified, and those VOCs ionizable by proton-transfer comprise about half the lost SOA mass.[247] Interestingly, mass loss due to photolysis of more absorptive guaiacol SOA is less rapid than that of $\alpha$-pinene and limonene SOA.[247] Based on absorption cross sections from the UV into the visible range for SOA derived from a wide range of precursors, photolysis is likely a broadly relevant process in the aging of particulate BrC in the atmosphere.[115]

Photoreactions may also result in changes to mass absorption coefficients, in addition to mass,[248] for particulate BrC. For 2,4-dinitrophenol, a representative BrC aerosol constituent, mixed into deposits of $\alpha$-pinene and limonene SOA generated under a range of conditions including exposure to ammonia to produce strongly absorbing limonene SOA, irradiation from 290-400 nm resulted in excitation to a triplet state followed first by abstraction of hydrogen from another molecule and then an array of products.[212] Concurrently, absorbance spectra exhibited a decrease at UV wavelengths and an increase at short visible wavelengths of 400 - 450 nm. Significantly, the rate constant for photodegradation decreased three-fold when going from 95 % to 5 % RH, due to increased viscosity of the SOA matrices. The strong RH dependence is a consequence of the bimolecular hydrogen abstraction that follows electronic excitation, such that the two reactants must diffuse and collide, so it may not be as critical to unimolecular photolytic

processes.[212] Recently, similar irradiation was applied to wood smoke particles, generated from a variety of fuels and combustion conditions, collected on filters.[164] The light-driven decay of individual chromophores as well as total absorbance was measured. Although some identified compounds decayed within hours, as shown in **Figure 10**, the lifetimes in terms of the total absorbance of the mixed compounds were between about 10 and 40 days, depending on the fuel.[164] These long lifetimes could be due to the conversion between primary and secondary BrC species or the recalcitrance of unidentified BrC species, and they suggest that other aging processes, such as OH oxidation, may generally be more impactful for primary particulate BrC.[164]
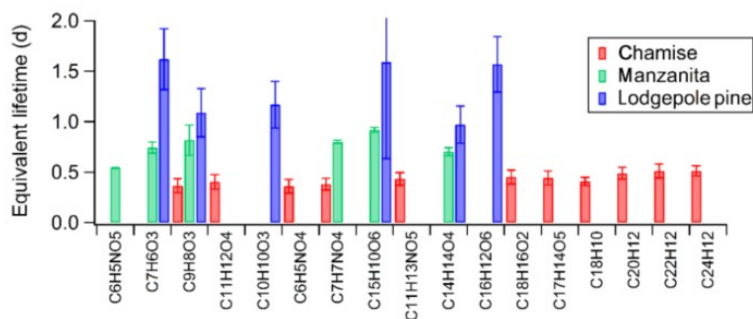


**Figure 10** Equivalent lifetimes with respect to UV irradiation of individual primary BrC constituents emitted from controlled burns of three fuel species. Common constituents include oxygenated aromatic compounds (e.g., $C_9H_8O_3$ attributed to veratraldehyde) and polycyclic aromatic hydrocarbons (e.g., $C_{24}H_{12}$ attributed to coronene), products of lignin decomposition and incomplete combustion, respectively. [Reprinted with permission from Fleming et al.[164] Copyright 2020]

As described previously in Section 3, photosensitized processing, involving a catalytic cycle of electronic excitation of an absorbing species to its triplet state and energy transfer to another otherwise unreactive species, has been shown to occur for particulate BrC.[144,146,215,249]

For surrogate photosensitizers of humic acid and 4-benzoylbenzoic acid in mixed organic and

inorganic matrixes, exposure to UVA light and high concentrations of limonene, roughly 300

ppb, resulted in particle growth, likely due to the production of oxidants at the air-particle

interface after excitation of humic acid, followed by reaction with colliding limonene

molecules.[250] Recently, this mechanism has been investigated for particulate BrC under a broader

range of conditions. Additional surrogate photosensitizers, including imidizole-2-carboxaldehyde

and benzophenone deposited in non-absorbing organic aerosol components, have been probed,

and the release of $HO_2$ from the particles to the gas phase was detected by scavenging with

NO.[251] Humic acid has been investigated further, under different light conditions and VOC

concentrations, and it was shown that this photosensitized processing is likely not competitive

with conventional oxidation pathways for VOCs under lower light intensities and limonene

concentrations, which are more representation of atmospheric conditions.[215] Photosensitized

oxidative uptake of limonene has also been investigated for more atmospherically relevant

secondary particulate BrC, generated in a photo-oxidation chamber, but it was similarly found to

be uncompetitive under typical ambient conditions; nonetheless, as pointed out by others, this

process could play a role in the highly localized leaf boundary layer.[249]

## 4.2  Reactive Uptake of Ammonia Leading to Particulate Imine BrC

Many experimental[213,216,240,252] and modelling[253,254] developments regarding reactive

uptake of ammonia to organic aerosol, which can lead to browning through reactions with

dicarbonyl compounds and the formation of imine and other nitrogen-containing products (see

Section 3.3), have been discussed in detail[255] in the years since the review of Laskin et al.[235]

Here, our focus is on recent results that have not been previously reviewed. Further insights have

been gained on the kinetics and mechanisms of nitrogen-containing compound formation upon

reactive uptake of ammonia to SOA from both biogenic (isoprene[241] and $\alpha$-pinene[256]) and anthropogenic (benzene,[257] toluene,[241,258] $p$-xylene,[259] 1,3,5-trimethylbenzene[260]) precursors in flow-tube and chamber studies. For toluene-derived SOA in the presence of $NH_3$, increasing the concentration of $SO_2$ was found to result in higher yields of organonitrates and other nitrogen-containing compounds;[258] this effect was attributed to increased surface acidity due to $SO_2$, leading to enhanced uptake of $NH_3$ to the SOA particles.[258] On the other hand, uptake of $NH_3$ and a range of aliphatic amines to a homologous series of linear saturated dicarboxylic acids cannot be explained simply by amine basicity and substrate acidity; $NH_3$ exhibits uptake to malonic acid but not larger succinic through glutaric acids, attributed in part to the comparatively open crystal structure of malonic acid, which accommodates neutralization.[261] For the complex mixtures of organics in SOA, uptake of $NH_3$ is constrained by diffusion limitations in highly viscous materials.[240,241] Reactive uptake of $NH_3$ to toluene SOA is slowed at RH conditions below 30 %, but that to isoprene SOA is independent of RH even under dry conditions (RH < 10 %), demonstrating how viscosity and, in turn, reactive uptake changes with not only ambient conditions but also SOA precursor.[241]

New insights have been gained for related but distinct processing of particulate BrC. Recently, the chemistry of ammonia and dicarbonyl compounds in the particle phase has been investigated upon reversing the identity of the gaseous reactant; that is, probing reactive uptake of glyoxal and methylglyoxal to ammonium- and methylaminium-containing inorganic particles,[217,218] building on earlier work on glyoxal reactive uptake.[262,263] In this scenario, decreasing RH accelerates rather than slows the formation of light-absorbing products, such as 2,2'-biimidazole, due to the salting-in effect (Section 3.4) of the dicarbonyl compounds.[217,218] Finally, the BrC forming potential of reactions between ammonia and acrolein, as a representative mono-carbonyl compound, has been explored for both the particle and bulk

aqueous phases; in the aqueous phase of ammonium-containing particles and films, a range of

nitrogen-containing products was detected, including non-volatile oligomeric and pyridinium

compounds and semi-volatile 3-methylpyridine, which was also detected in the gas phase, and a

weak absorption band was observed near 430 nm.[264] These observations indicate that the reactive

uptake of ammonia leading to particulate BrC most often considered in the context of glyoxal

and methylglyoxal may be relevant for a wider range of carbonyl compounds.

## 4.3    Heterogeneous Ozonolysis of Unsaturated BrC Components

Ozone may oxidize compounds that contain unsaturated functional groups, reacting

rapidly with alkenes and more slowly with aromatics, including polycyclic aromatic

hydrocarbons.[265] We begin by discussing heterogeneous ozone oxidation of secondary BrC and

its precursors, for which insights at this molecular level have been reported.[202,219,266–268]

Ozonolysis of particulate products of $(NH_4)_2SO_4$ and methylglyoxal leads to extensive

fragmentation; for example, secondary species formed through aldol condensation breakdown

into formic, acetic, and pyruvic acids.[202] Interestingly, exposure to ozone nonetheless leads to an

increase in absorptivity at visible wavelengths, as the formation of carbonyl groups contributes

enough absorption enhancement to compensate for the bleaching generally expected from the

destruction of unsaturated carbon-carbon bonds.[202] Since this study, additional insights have

been gained through heterogeneous ozone oxidation of individual potential precursors of

secondary BrC in the laboratory, including catechol and other phenolic compounds.[219,266,267] For

example, ozonolysis of thin films of catechol results in both direct oxidation to form first

muconic acid followed by smaller mono- and dicarboxylic acids and indirect oxidation by OH

formed in situ to give polyhydroxylated aromatic compounds, including bi- and terphenyl

oligomers.[266] The latter, highly functionalized products contribute to increased absorptivity at

visible wavelengths[266,269] as well as increased hygroscopicity, due to the presence of many

hydrogen bond donor and acceptor groups.[270] Furthermore, heterogeneous ozone oxidation of

particulate trimethylamine, a precursor of secondary imine BrC, has been shown to lead to a

range of oxygen- and nitrogen-containing products distributed across both the gas and particle

phases, including several with known health effects, like nitromethane.[268] In the atmosphere, this

pathway could compete with the formation of secondary imine BrC but also could itself lead to

changes in the optical properties of particles with amines.

Although exposure of particulate BrC to ozone occurred in several oxidation flow reactor

studies, where ozone is used as a precursor to OH,[116–119,271,272] the evolution of the chemical and

optical properties of BrC derived from biomass burning due to heterogeneous oxidation by ozone

alone has only recently been investigated.[273,274] For primary BrC generated from controlled

smoldering of ponderosa pine needle litter, which was passed through a charcoal denuder to

prevent the formation of SOA, exposure to ozone leads to evolution in both complex refractive

index and composition, measured using an aerosol mass spectrometer (AMS).[273] Specifically, at

30 % RH, oxidation rapidly leads to an appreciable decrease in $C_xH_y^+$ ions, associated with

reduced species, and simultaneous increase in $C_xH_yO_z^+$ ions, associated with more oxidized

species, as shown in **Figure 11A**. Accompanying this chemical evolution are decreases in the

imaginary component, $k$, of the complex refractive indices at 405 and 532 nm. At 405 nm, $k$

decreases from roughly 0.004 to less than 0.003, as shown in **Figure 11B**. Interestingly, because

$k$ decreases more rapidly at 532 nm than 405 nm, the AAE increases with ozone exposure, as

shown in **Figure 11C**. However, these changes cease after the equivalent of less than one hour in

the atmosphere. This later recalcitrance to ozone exposure may indicate that only a fraction of

the primary BrC components are susceptible to ozonolysis or that the viscosity of the aerosol

either near the particle surface or throughout increases significantly during the reaction. It is also

possible that the observed heterogeneous ozone oxidation occurs by the Langmuir-Hinshelwood mechanism, as has been observed for other species of atmospheric interest,[275] including crystalline benzo[a]pyrene.[225,276] Considering the above discussion of diffusion limitations, exploring the effect of RH could potentially help to deconvolute these complex processes. For example, exposure of aged primary BrC particles to higher RH could lead to plasticization and further evolution, although this needs to be explored.[224] In contrast to the uniform bleaching observed for BrC from smoldering pine needle litter, an initial absorption enhancement followed by bleaching upon ozone exposure in a smog chamber was recently observed for BrC internally mixed with BC from a propane-air diffusion burner.[274]
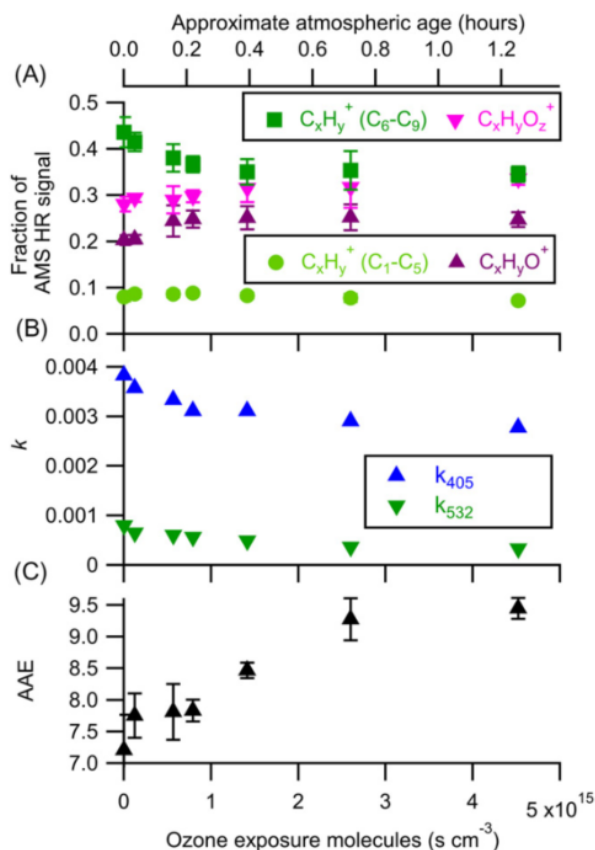


**Figure 11** Evolution of primary BrC (A) composition, (B) imaginary refractive indices at 405 and 532 nm, and (C) AAE during aging with respect to ozone exposure. Panel (a) shows

fragment ions observed using an AMS, as described in the main text. Equivalent atmospheric age, shown on the top axis, assumes an average ozone mixing ratio of 40 ppb. [Reprinted from Browne *et al.*[273] by permission of The American Association for Aerosol Research, www.aaar.org, Copyright 2019]

## 4.4  Heterogeneous OH Oxidation of Particulate BrC

The evolution of the composition and absorptivity of primary BrC due to heterogeneous OH oxidation has been investigated in flow tube[116–119,271–273] and smog chamber[120–122,220] experiments. Here, observations from experiments in which volatile emissions (gas-phase components) of biomass burning have been scavenged are especially of interest, as this allows distinguishing between the coupled effects of heterogeneous oxidation and SOA formation.[220,271,273] In oxidation flow tubes, very high OH concentrations can be generated in the presence of ozone and water, and OH exposure is used to calculate an equivalent age in the atmosphere. Equivalent ages of up to roughly five days have been explored.[271,273] For primary BrC generated from smoldering Alaskan peak, heterogeneous OH oxidation at 20-30 % RH leads to an increase in the O:C due to functionalization, accompanied by appreciable decreases in $k$ at 375 and 405 nm.[271] At 405 nm, $k$ decreases by roughly 25 %, from about 0.010 to 0.0075, after the equivalent of 4.5 days in the atmosphere, and the SSA increases accordingly.[271] For primary BrC generated from smoldering ponderosa pine needles, OH exposure at 30 % RH leads to evolution of components that are recalcitrant with respect to ozone, reflected by further consumption of reduced species (i.e., $C_xH_y^+$ ions measured by AMS).[273] Similarly, at 405 nm, $k$ decreases by about 30 % after five equivalent days in the atmosphere. Furthermore, an effective uptake coefficient (which is the ratio of reactive collisions monitored by either consumption of precursor or formation of product to the total number of collisions), $\gamma_{OH}$, of 0.5 can be derived.[273]

Neglecting shifts in particle size distributions, uniform bleaching is observed for BrC from both sources.[271,273] However, the first day[271] or two[273] of aging of particulate BrC is not captured in these oxidation flow reactor experiments, and this period can be probed using smog chamber experiments, in which the OH concentration is much lower. For nascent primary BrC generated from smoldering pine wood, OH exposure at both 15 and 60 % RH leads to a rapid absorption enhancement within the first 2.5 hr of equivalent age followed by gradual bleaching, such that the aged particles are less absorptive than the starting material after about 10 hr of equivalent age, as shown in **Figure 12**.[220] This sequential enhancement and bleaching suggests that the primary BrC is well-mixed even at 15 % RH, and it closely parallels behaviour observed during aqueous OH oxidation of BrC, as discussed in Section 3.1.[161,163] Enhancement may involve the formation of highly functionalized or oligomeric species from phenolic compounds like catechol,[266] which are prevalent biomass burning emissions.[277] For heated primary BrC generated under the same conditions, no initial enhancement occurs, as shown in **Figure 12**, suggesting that the remaining, lower volatility constituents have less capacity for absorption enhancement.[220]
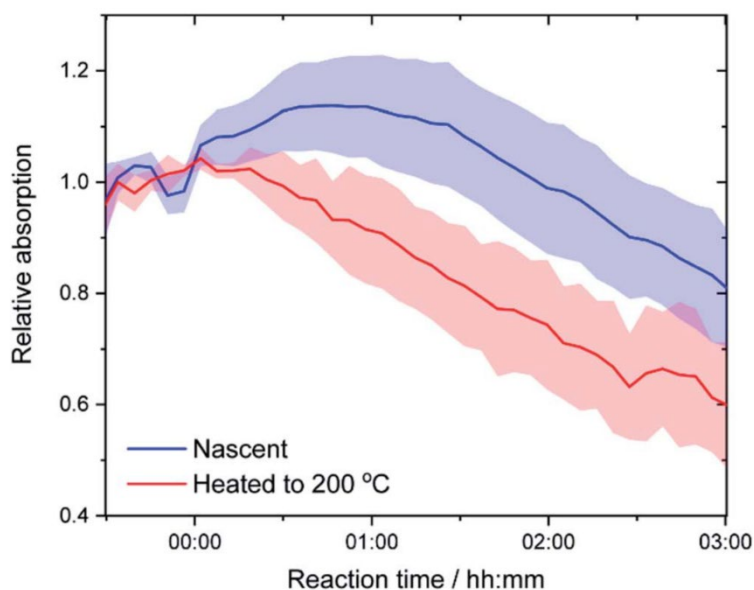
**Figure 12** Evolution of nascent and heated primary BrC from smoldering pine at 405 nm during photochemical aging in a smog chamber at 60% RH. [Reprinted with permission from Schnitzler *et al.*[220] Copyright 2020 The Royal Society of Chemistry]

Heterogeneous OH oxidation of secondary BrC has been investigated in fewer studies, or in the case of absorbing SOA forming from gas-phase precursors, the SOA formation process has not been decoupled from the heterogeneous oxidation process.[202,278] For unsaturated aldol condensation products of $(NH_4)_2SO_4$ and methylglyoxal, OH exposure in a flow tube at 60-70 % RH leads to fragmentation; for example, oxidation of six-carbon constituents results in a range of small acids, likely including pyruvic and oxalic acids.[202] Furthermore, reactants at both *m/z* react efficiently with OH, exhibiting uptake coefficients greater than one. When $\gamma_{OH} > 1$, each collision of OH with a particle results in the formation of more than one product molecule or loss of more than one reactant, suggesting an in-situ source of additional radical species. For low volatility products of aqueous OH oxidation of resorcinol, evolution upon OH exposure in a smog chamber varies with RH.[278] At 60 % RH, rapid absorption enhancement is followed by uniform bleaching, and these significant changes in absorptivity indicate first that the particles are well-mixed and second that OH oxidation is very efficient, with $\gamma_{OH} > 1$ for reaction of both a model precursor and strongly absorbing intermediate. At 15 % RH, little change in absorptivity occurs, as the particles are so viscous that diffusion of the starting material from the bulk of the particle to the surface is limited.[278]

## 4.5  Heterogeneous $NO_3$ Oxidation of Particulate BrC

While recent observations of the formation and evolution of absorbing aerosol particles that are referred to as tar balls,[214,279] characterized by optical properties that are intermediate

between those of BrC and BC,[280] are largely beyond the scope of this review, heterogeneous oxidation by $NO_3$ radical of selected particulate fractions of tar balls can be considered as an example of a potential night-time source of BrC.[234] For all constituents of tar balls, separated into three classes of polarity by extraction, exposure to $NO_3$ radical in a flow tube under dry conditions leads to significant nitration, either by hydrogen abstraction followed by $NO_x$ addition or $NO_3$ addition directly, and an appreciable rise in absorptivity. Specifically, MAC values significantly increase across the visible spectrum after $NO_3$ exposure equivalent to one night in the atmosphere. For non- and moderately polar constituents, which begin as more absorptive than the most polar fraction, absorption enhancement coincides with decay of methoxy monomers and oligomers and formation of a broad range of nitroaromatics. For the polar constituents, the increase in absorption also coincides with a significant decrease in $C_2H_4O_2^+$ ions derived in AMS spectra from levoglucosan and other anhydrous sugars, which do not contribute to the absorptivity of the whole tar balls.[234] Importantly, this night-time source of particulate BrC results in compounds (i.e., nitroaromatics) that do not rapidly decompose at sunrise, unlike representative imine BrC constituents.[159,160,202] Indeed, nitroaromatics are ubiquitous constituents of ambient BrC in both the aqueous and particle phases.[30,281] Still, $NO_3$ initiated processing of primary BrC does increase its susceptibility to photolysis, such that subsequent day-time bleaching is dominated by light-driven processing rather than heterogeneous OH oxidation.[282] Specifically, the lifetimes of $NO_3$ processed BrC in terms of visible light absorption with respect to photolysis and OH oxidation are on the order of 10 hours and 30 days, respectively.[282] Furthermore, photolysis of constituent organonitrates in $NO_3$ processed particulate BrC is a source of gas-phase reactive nitrogen species.[282]

# 5  Connections to the Atmosphere

As described in the Introduction (Section 1), light-absorbing organic aerosol can have a strong impact on radiative forcing through direct absorption of sunlight, but a quantitative assessment of these impacts remains highly uncertain.[94] A theme to this review is that these radiative effects will only be accurately assessed if we understand the relationships between the molecular composition of BrC aerosol and its optical properties as the particles evolve with time in the atmosphere. Some questions of importance include: How does the MAC value change with residence time in the atmosphere? What about the absolute absorption? What is the response to different oxidants and to light? Are the effects similar during the day as during the night?
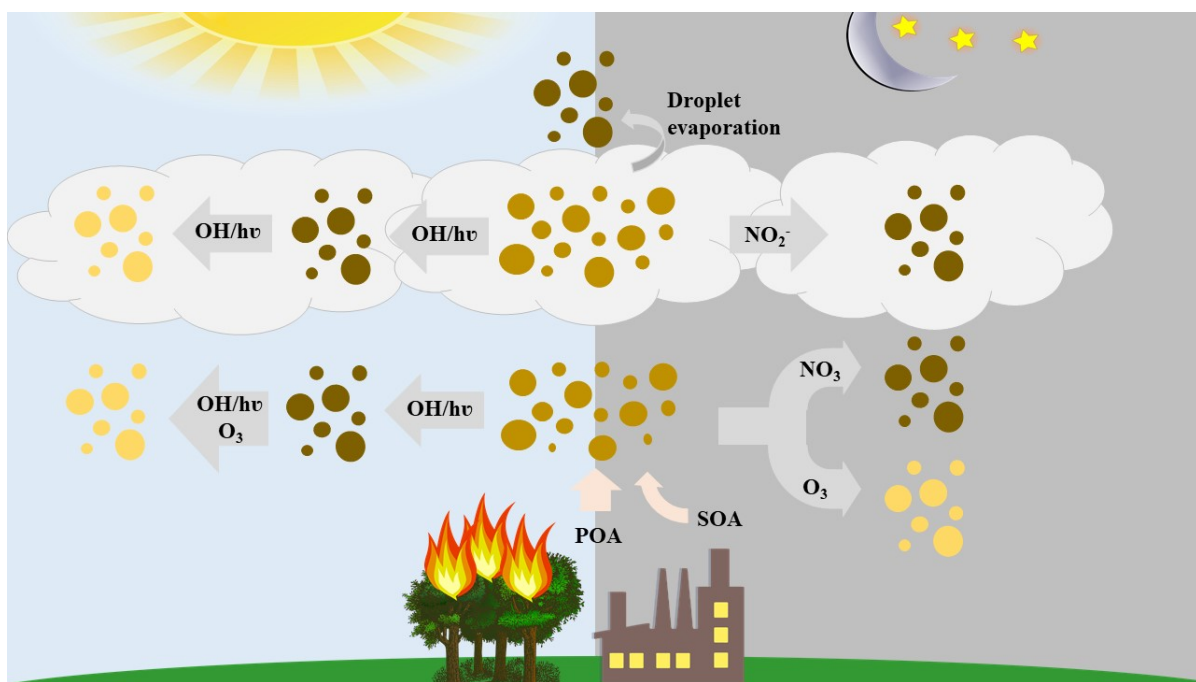


**Figure 13** Conceptual depiction of absorbance change during BrC aging processes in the atmosphere.

The chemistry reviewed above illustrates that multiple processes will change the molecular composition and optical properties of these light-absorbing particles. As shown in **Figure 13**, BrC aging processes include heterogeneous reactions (discussed in Section 4) and in-cloud processes (discussed in Section 3) that are driven by photochemistry (primarily daytime), non-photochemical reactions (daytime and nighttime), and droplet evaporation. Aging mechanisms addressed include photoreactions, nitration, and oxidative processing, both in the aqueous phase and of suspended particles. The darkness in the BrC color depicted in **Figure 13** summarizes general conclusions from the impact of each aging process on absorption. Associated changes in physical and hygroscopic properties will also influence the wet deposition lifetimes of BrC particles and their capacity for long-range transport. For example, increased oxidation related to an increase in N and O atoms in BrC particles is believed to enhance particle viscosity and surface tension, leading to the formation of tarballs.[279] An important point to make concerning **Figure 13** is that multi-day aging will involve sequential daytime and nighttime processes not illustrated in the figure, i.e. aerosol aged during the night will then be aged during the following day, and so on.[282]

While studies of individual aging mechanisms are leading to improved fundamental understanding of their effect on the optical properties of BrC materials, these different processes will all proceed across a full day-night cycle in the atmosphere. To illustrate the potential extent and relative timescales of each aging process, simple parametrizations as a function of atmospheric exposure time were developed from select laboratory experiments that addressed primary biomass burning BrC (**Figure 14**). We emphasize that other important aging processes potentially occurring in the environment are not included here, especially SOA formation close to source. As such, the scenarios presented in **Figure 14** (and **Figure S1**) are most representative of conditions removed from the source. The studies represented in these figures only address

processes which have been the focus of considerable attention with the data presented in a format that could be easily parameterized. Given that different fuels and experimental conditions will affect the predictions, it is currently not possible to put firm bounds on these timescales.

To construct the parameterizations, the exposures employed in the lab experiments were scaled to conditions that will commonly be encountered in the atmosphere (details in Supporting Information). The absorption transformations are presented over a 40-hour exposure timescale for illustrative purposes only, assuming constant exposure conditions, i.e. constant OH or $NO_3$ exposure rarely occurs continuously over a 40-hour period. Consequently, it is best to view the exposure timescale in **Figure 14** as the accumulated time over which the particles will experience such environmental conditions. The purpose of the figure is to illustrate potential atmospheric behavior, which will strongly depend on the specific nature of the BrC substrate and the atmospheric aging conditions. For example, the photo-enhancement in the photolysis studies will likely be strongly dependent on the nature of the UV light source and the specific chromophores.[61,159] To encompass the range of behavior observed in the lab, parameterizations of additional studies are presented in **Figure S1**.

**Figure 14** illustrates that while some processes cause an increase in absorption, others lead to bleaching. For example, both aqueous and heterogeneous OH oxidation promote an initial increase in absorption followed by a subsequent decrease.[61,163,278] The short-term behavior is likely arising from functionalization of the molecules which increases electron density and delocalization. With further oxidation, molecular fragmentation increases with a loss of electron delocalization, and decrease of absorption abilities when the molecules become highly oxygenated.[91] Photoreaction experiments also demonstrate such an initial photo-enhancement followed by photobleaching, likely initiated by photosensitized reactions and/or radical reactions

to form functionalized or oligomeric products.[58,73,150] However, we note that some photodegradation studies have shown the bleaching component to occur at slower rates that those exhibited in the OH oxidation experiments.[61,159,163,164] One issue in all photoreaction experiments is how much of the absorption photo-enhancement is via direct photolysis and how much via indirect photolysis driven by radicals generated by the light absorption. One study has demonstrated that the concentration of OH radicals present in aqueous solution upon exposure to UV-B radiation was only one third higher when 1.5 mM of $H_2O_2$, an OH photolytic precursor, was purposefully added to the solution, compared to UV-B radiation alone.[61]

As shown in **Figure 14**, in contrast to OH, $NO_3$ radical heterogeneous reactions lead to a photo-enhancement effect at a slower rate, probably through formation of nitro-aromatic species.[234] An initial study showed that $O_3$ oxidation leads rapidly to a small amount of bleaching (approximately 20 % loss in absorbance), probably driven by ozonolysis of double bonds in the molecules.[273] There is evidence for recalcitrant absorption within the particles that ozone is not able to remove.[273]
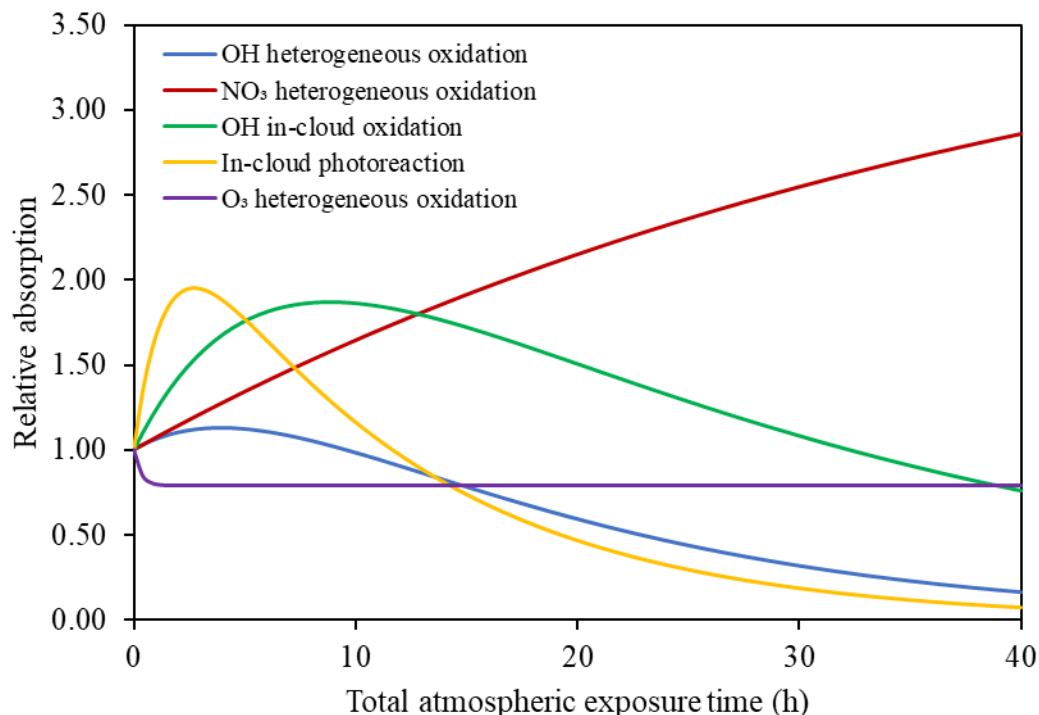
**Figure 14** Relative absorption change for aging of BrC obtained from biomass burning samples in the laboratory.[61,163,273,278,283] The horizontal axis is the total atmospheric exposure time assuming constant exposure conditions, derived in some cases by scaling conditions in the laboratory to those that will be experienced in the ambient atmosphere. As described in the text, the exposure will usually be discontinuous, e.g. direct and indirect photoreactions will only occur with sunlight, while $NO_3$ and $O_3$ reactions may dominate during low light or nighttime conditions. See Supporting Information for full details.

General conclusions can be drawn from **Figure 14**. Notably, changes are occurring on timescales of one-to-two days equivalent exposure time, or less. This timescale is roughly consistent with laboratory experiments where biomass burning aerosol was exposed to natural light.[284] In the case of ozone, the oxidative bleaching is so rapid that it will unlikely be observable immediately downwind of a BrC source, especially if SOA formation is occurring. For light-driven processes – both direct photoreactions and OH oxidation – the long-term effect

after only a few days of daytime exposure will also lead to bleaching. In contrast, nighttime oxidation by $NO_3$ radicals will likely lead to enhanced BrC absorption.[285]  An interesting question is whether the photo-enhancements experienced at night can be maintained during sunlight exposure. Will the more strongly absorbing nitrated compounds rapidly photo-degrade in daylight?

Recognizing that the ambient aerosol optical properties will integrate all these effects, it is valuable to turn to the results from field measurements to see their correspondence to laboratory experiments. Studies of this type are particularly challenging to conduct. For example, air masses monitored by time-resolved measurements at a ground site will be subject to not only changing atmospheric exposures but also changing BrC source conditions. Emissions from an isolated BrC source are ideally followed in a Lagrangian manner with measures of transport age and integrated photochemical age for the sampled air. In that regard, an important aircraft study[35] monitored water-soluble BrC absorption for up to two days residence time within biomass burning plumes which did not experience cloud formation, using CO to normalize for dilution effects (**Figure 15**). This study found the half-life of BrC absorption at 365 nm from two forest fires in the western United States to be 9 to 15 hours. No more than 24 hours of sunlight exposure were required to decrease the BrC absorption by 90 %, with a small amount of absorption remaining at longer transport times. The AAE values dropped from 3.5 - 4.0 to 1, indicating a shift from values characteristic of BrC to a common value for BC. Overall, a conclusion of this study was that the majority of the initial BrC was chemically unstable, with indications of a small ($\approx$ 10 %) absorption signal after a day or two of atmospheric processing. This one-day whitening timescale is consistent with modeling studies of both aircraft and aerosol optical depth data, such as from the IMPROVE network.[286–288]

Comparing **Figures 14 and 15**, this bleaching behavior in BrC emitted from forest fires is most consistent with that demonstrated by heterogeneous OH oxidation and direct photobleaching. However, the photobleaching modeled in **Figure 14** simulates in-cloud conditions, which were not present during the measurements made in **Figure 15**, and direct photobleaching of non-aqueous BrC may not occur as rapidly (discussed in Section 4.1). Note that the data presented in **Figure 15** are at 365 nm whereas those in **Figure 14** are between 400 to 405 nm (except for in-cloud OH oxidation at 365 nm), and the response to bleaching chemistry may be somewhat faster at lower wavelengths.
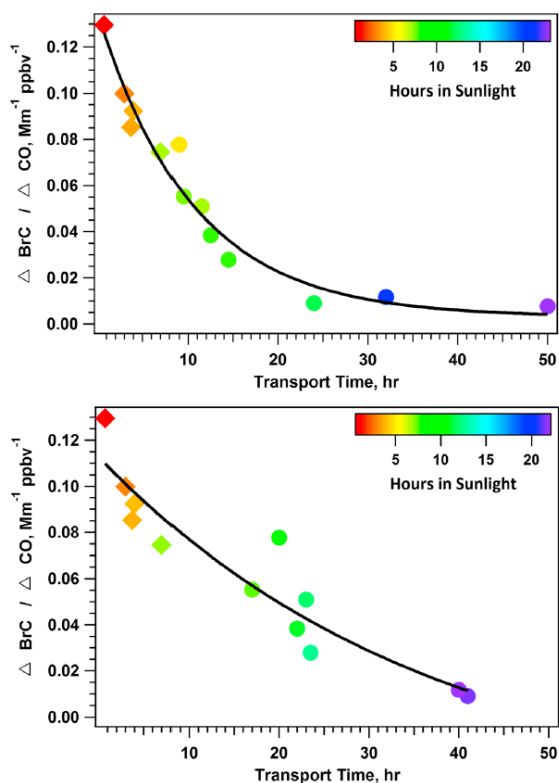


**Figure 15** The decrease of 365 nm absorption of water soluble BrC was measured in two wildfire plumes (top and bottom) in the western United States. Aircraft measurements permitted encounters with the plume at the indicated transport times and photochemical ages. [Reprinted with permission from Forrister *et al.*[35] Copyright 2015 John Wiley and Sons]

Using the same aircraft-mounted experimental methods, the dynamic nature of water soluble BrC has also been measured during convective uplift to the upper troposphere.[5] This study observed that the importance of BrC absorption relative to BC absorption roughly doubled in the upper troposphere (9 – 12 km altitude) compared to the air feeding the convection at lower altitudes (1 – 3 km). As a result, BrC contributes more than 34 % of the radiative forcing from absorbing carbonaceous aerosols at high altitudes, compared to 15 % at lower altitudes.[5] The processes giving rise to this increase are unknown but are unlikely due to faster scavenging of BC aerosol particles which tend to be more hydrophobic than BrC particles.[5] Rather, it is probably arising either from in-cloud formation of BrC or via enhancement of BrC via droplet evaporation processes. An additional aspect of this study was to evaluate the absorption of BrC that is part of the convective outflow. In contrast to the behavior exhibited in **Figure 15** for plumes at lower altitude, the particles in the upper troposphere exhibit no change in absorption with one day of aging.[5] It is interesting to speculate whether the low temperatures of the upper troposphere increase the viscosity of the particles[289] so that heterogeneous aging processes are not as efficient as at ground level. Further evidence for BrC formation or increase with aqueous processing has been observed for fog processing of biomass burning emissions in Bologna, Italy[290] and Kanpur, India[291], as well as during periods of high aerosol liquid water content in wintertime in Xianghe, China.[292]

Some studies have also attempted to explicitly model BrC emissions and aging in global chemical transport models.[286–288,293] While there is still uncertainty in the absorption intensity of different organic aerosol sources and how that absorption changes with atmospheric aging in the model, these studies find that BrC has a measurable impact on both the direct radiative effect and on photochemical ozone production, even with the inclusion of photobleaching.[287,293]

# 6 Future Studies

This is an emerging field of research with many open questions and priorities. From the laboratory perspective, an important variable to consider is the nature of the BrC material. While studies of individual molecules are valuable to decipher mechanisms, the high degree of chemical complexity of atmospheric BrC needs to be confronted. Research has pointed to the important role of higher molecular weight, low volatility molecules that may be more chemically robust with respect to bleaching chemistry than small molecules, such as the monomeric nitrophenol species.[59–61,101,159] What is the chemical nature of these higher molecular weight species? Are they dimeric structures of nitro-phenolic compounds formed as secondary species within the BrC material? Or are they part of the SOA material that forms in the gas phase? Alternatively, are these larger molecules part of a cascade of smaller and smaller products formed from degradation of large biopolymers in lignin or solid fuel components? How important are charge-exchange processes in forming BrC within aerosol?[294–296]

Studies of BrC material in aqueous solutions are crucial to simulate cloud-processing conditions. However, care should be taken to work with realistic concentrations of water-soluble organic carbon. Most laboratory studies use much larger volumes of solvent than are present in cloud water, so that the BrC species that are water-soluble in such conditions are not necessarily soluble under true cloud conditions. Large solvent volumes also affect the partitioning of gas phase species. As well, clouds are highly dynamic environments with very frequent droplet evaporation (and formation) occurring. The potential enhancement of absorption that has been observed to occur upon rapid drying of water solutions containing BrC (Section 3.4) is deserving of more study as a potential processing pathway.

Although in-cloud conditions are important to study, there is a dearth of laboratory studies conducted with suspended BrC particles. Initial studies have focused on heterogeneous oxidation using the OH and NO$_3$ radicals,[271,278,283] but there are very few studies of suspended BrC particles that address photochemical evolution using exposure to environmentally realistic light intensity and wavelengths.[284] As well, although initial studies have been conducted to assess heterogeneous oxidation processes, close to the BrC source there may also be formation of SOA, where molecules that may or may not be light absorbing will be condensing on the particles (Section 2).[70] What is the net effect of photochemistry, heterogeneous oxidation, and secondary condensation processes? Will the heterogeneous oxidation processes occur as rapidly if condensation of SOA material is occurring simultaneously? Related to this, there remain questions regarding the phase and diffusive nature of the particles. As mentioned in Sections 4 and 5, low temperatures may enhance the viscosity of the BrC particles.[289] Most laboratory studies are performed at room temperature. To what degree does that bias our understanding of aging timescales, especially for heterogeneous oxidation that may be restricted to the surfaces of highly viscous particles? From an experimental perspective, caution should be used in interpreting results from oxidation flow reactors that use high radical concentrations, given the potential for radical-radical chemistry to dominate over auto-oxidation in such conditions.[297]

Lastly, the chemical transformations that occur with atmospheric aging need to be studied at the molecular level. With the increasing sophistication of analytical methods that permit such analyses (e.g., EESI-MS,[298,299] HPLC/PDA/HRMS[103,300,301]), there is promise for better connections between laboratory and field studies of BrC aging.

# 7 References

(1) Andreae, M. O.; Gelencsér, A. Black Carbon or Brown Carbon? The Nature of Light-Absorbing Carbonaceous Aerosols. *Atmospheric Chem. Phys.* **2006**, *6* (10), 3131–3148. https://doi.org/10.5194/acp-6-3131-2006.

(2) Laskin, A.; Laskin, J.; Nizkorodov, S. A. Chemistry of Atmospheric Brown Carbon. *Chem. Rev.* **2015**, *115* (10), 4335–4382. https://doi.org/10.1021/cr5006167.

(3) Ramanathan, V.; Carmichael, G. Global and Regional Climate Changes Due to Black Carbon. *Nat. Geosci.* **2008**, *1* (4), 221–227. http://dx.doi.org.proxy.lib.umich.edu/10.1038/ngeo156.

(4) Feng, Y.; Ramanathan, V.; Kotamarthi, V. R. Brown Carbon: A Significant Atmospheric Absorber of Solar Radiation? *Atmospheric Chem. Phys.* **2013**, *13* (17), 8607–8621. https://doi.org/10.5194/acp-13-8607-2013.

(5) Zhang, Y.; Forrister, H.; Liu, J.; Dibb, J.; Anderson, B.; Schwarz, J. P.; Perring, A. E.; Jimenez, J. L.; Campuzano-Jost, P.; Wang, Y.; Nenes, A.; Weber, R. J. Top-of-Atmosphere Radiative Forcing Affected by Brown Carbon in the Upper Troposphere. *Nat. Geosci.* **2017**, *10* (7), 486–489. https://doi.org/10.1038/ngeo2960.

(6) Zeng, L.; Zhang, A.; Wang, Y.; Wagner, N. L.; Katich, J. M.; Schwarz, J. P.; Schill, G. P.; Brock, C.; Froyd, K. D.; Murphy, D. M.; Williamson, C. J.; Kupc, A.; Scheuer, E.; Dibb, J.; Weber, R. J. Global Measurements of Brown Carbon and Estimated Direct Radiative Effects. *Geophys. Res. Lett.* **2020**, *47* (13), e2020GL088747. https://doi.org/10.1029/2020GL088747.

(7) Chuang, C. C.; Penner, J. E.; Prospero, J. M.; Grant, K. E.; Rau, G. H.; Kawamoto, K. Cloud Susceptibility and the First Aerosol Indirect Forcing: Sensitivity to Black Carbon and Aerosol Concentrations. *J. Geophys. Res. Atmospheres* **2002**, *107* (D21), AAC 10-1-AAC 10-23. https://doi.org/10.1029/2000JD000215.

(8) Menon, S.; Hansen, J.; Nazarenko, L.; Luo, Y. Climate Effects of Black Carbon Aerosols in China and India. *Science* **2002**, *297* (5590), 2250–2253. https://doi.org/10.1126/science.1075159.

(9) Ramanathan, V.; Chung, C.; Kim, D.; Bettge, T.; Buja, L.; Kiehl, J. T.; Washington, W. M.; Fu, Q.; Sikka, D. R.; Wild, M. Atmospheric Brown Clouds: Impacts on South Asian Climate and Hydrological Cycle. *Proc. Natl. Acad. Sci.* **2005**, *102* (15), 5326–5333. https://doi.org/10.1073/pnas.0500656102.

(10) Koren, I.; Kaufman, Y. J.; Remer, L. A.; Martins, J. V. Measurement of the Effect of Amazon Smoke on Inhibition of Cloud Formation. *Science* **2004**, *303* (5662), 1342–1345. https://doi.org/10.1126/science.1089424.

(11)     Kaufman, Y. J.; Koren, I. Smoke and Pollution Aerosol Effect on Cloud Cover. *Science* **2006**, *313* (5787), 655–658. https://doi.org/10.1126/science.1126232.

(12)     Dockery, D. W.; Pope, C. A.; Xu, X.; Spengler, J. D.; Ware, J. H.; Fay, M. E.; Ferris, B. G.; Speizer, F. E. An Association between Air Pollution and Mortality in Six U.S. Cities. *N. Engl. J. Med. Boston* **1993**, *329* (24), 1753–1759. https://doi.org/10.1056/NEJM199312093292401.

(13)     Pope, C. A.; Dockery, D. W. Health Effects of Fine Particulate Air Pollution: Lines That Connect. *J. Air Waste Manag. Assoc.* **2006**, *56* (6), 709–742. https://doi.org/10.1080/10473289.2006.10464485.

(14)     Anenberg, S. C.; Achakulwisut, P.; Brauer, M.; Moran, D.; Apte, J. S.; Henze, D. K. Particulate Matter-Attributable Mortality and Relationships with Carbon Dioxide in 250 Urban Areas Worldwide. *Sci. Rep.* **2019**, *9* (1), 1–6. https://doi.org/10.1038/s41598-019-48057-9.

(15)     Rohr, A. C.; Wyzga, R. E. Attributing Health Effects to Individual Particulate Matter Constituents. *Atmos. Environ.* **2012**, *62*, 130–152. https://doi.org/10.1016/j.atmosenv.2012.07.036.

(16)     Kelly, F. J.; Fussell, J. C. Size, Source and Chemical Composition as Determinants of Toxicity Attributable to Ambient Particulate Matter. *Atmos. Environ.* **2012**, *60*, 504–526. https://doi.org/10.1016/j.atmosenv.2012.06.039.

(17)     Park, M.; Joo, H. S.; Lee, K.; Jang, M.; Kim, S. D.; Kim, I.; Borlaza, L. J. S.; Lim, H.; Shin, H.; Chung, K. H.; Choi, Y.-H.; Park, S. G.; Bae, M.-S.; Lee, J.; Song, H.; Park, K. Differential Toxicities of Fine Particulate Matters from Various Sources. *Sci. Rep.* **2018**, *8* (1), 1–11. https://doi.org/10.1038/s41598-018-35398-0.

(18)     Daellenbach, K. R.; Uzu, G.; Jiang, J.; Cassagnes, L.-E.; Leni, Z.; Vlachou, A.; Stefenelli, G.; Canonaco, F.; Weber, S.; Segers, A.; Kuenen, J. J. P.; Schaap, M.; Favez, O.; Albinet, A.; Aksoyoglu, S.; Dommen, J.; Baltensperger, U.; Geiser, M.; El Haddad, I.; Jaffrezo, J.-L.; Prévôt, A. S. H. Sources of Particulate-Matter Air Pollution and Its Oxidative Potential in Europe. *Nature* **2020**, *587* (7834), 414–419. https://doi.org/10.1038/s41586-020-2902-8.

(19)     He, S.; Carmichael, G. R. Sensitivity of Photolysis Rates and Ozone Production in the Troposphere to Aerosol Properties. *J. Geophys. Res. Atmospheres* **1999**, *104* (D21), 26307–26324. https://doi.org/10.1029/1999JD900789.

(20)     Mok, J.; Krotkov, N. A.; Arola, A.; Torres, O.; Jethva, H.; Andrade, M.; Labow, G.; Eck, T. F.; Li, Z.; Dickerson, R. R.; Stenchikov, G. L.; Osipov, S.; Ren, X. Impacts of Brown Carbon from Biomass Burning on Surface UV and Ozone Photochemistry in the Amazon Basin. *Sci. Rep.* **2016**, *6* (1), 1–9. https://doi.org/10.1038/srep36940.

(21)     Liu, J.; Scheuer, E.; Dibb, J.; Diskin, G. S.; Ziemba, L. D.; Thornhill, K. L.; Anderson, B. E.; Wisthaler, A.; Mikoviny, T.; Devi, J. J.; Bergin, M.; Perring, A. E.; Markovic, M. Z.; Schwarz, J. P.; Campuzano-Jost, P.; Day, D. A.; Jimenez, J. L.; Weber, R. J. Brown

Carbon Aerosol in the North American Continental Troposphere: Sources, Abundance, and Radiative Forcing. *Atmospheric Chem. Phys.* **2015**, *15* (14), 7841–7858. https://doi.org/10.5194/acp-15-7841-2015.

(22)  Bikkina, S.; Sarin, M. Brown Carbon in the Continental Outflow to the North Indian Ocean. *Environ. Sci. Process. Impacts* **2019**, *21* (6), 970–987. https://doi.org/10.1039/C9EM00089E.

(23)  Liu, J.; Scheuer, E.; Dibb, J.; Ziemba, L. D.; Thornhill, K. L.; Anderson, B. E.; Wisthaler, A.; Mikoviny, T.; Devi, J. J.; Bergin, M.; Weber, R. J. Brown Carbon in the Continental Troposphere. *Geophys. Res. Lett.* **2014**, *41* (6), 2191–2195. https://doi.org/10.1002/2013GL058976.

(24)  Stockwell, C. E.; Christian, T. J.; Goetz, J. D.; Jayarathne, T.; Bhave, P. V.; Praveen, P. S.; Adhikari, S.; Maharjan, R.; DeCarlo, P. F.; Stone, E. A.; Saikawa, E.; Blake, D. R.; Simpson, I. J.; Yokelson, R. J.; Panday, A. K. Nepal Ambient Monitoring and Source Testing Experiment (NAMaSTE): Emissions of Trace Gases and Light-Absorbing Carbon from Wood and Dung Cooking Fires, Garbage and Crop Residue Burning, Brick Kilns, and Other Sources. *Atmospheric Chem. Phys.* **2016**, *16* (17), 11043–11081. http://dx.doi.org.proxy.lib.umich.edu/10.5194/acp-16-11043-2016.

(25)  Desyaterik, Y.; Sun, Y.; Shen, X.; Lee, T.; Wang, X.; Wang, T.; Collett, J. L. Speciation of "Brown" Carbon in Cloud Water Impacted by Agricultural Biomass Burning in Eastern China. *J. Geophys. Res. Atmospheres* **2013**, *118* (13), 7389–7399. https://doi.org/10.1002/jgrd.50561.

(26)  Cook, R. D.; Lin, Y.-H.; Peng, Z.; Boone, E.; Chu, R. K.; Dukett, J. E.; Gunsch, M. J.; Zhang, W.; Tolic, N.; Laskin, A.; Pratt, K. A. Biogenic, Urban, and Wildfire Influences on the Molecular Composition of Dissolved Organic Compounds in Cloud Water. *Atmospheric Chem. Phys.* **2017**, *17* (24), 15167–15180. http://dx.doi.org.proxy.lib.umich.edu/10.5194/acp-17-15167-2017.

(27)  Chakrabarty, R. K.; Gyawali, M.; Yatavelli, R. L. N.; Pandey, A.; Watts, A. C.; Knue, J.; Chen, L.-W. A.; Pattison, R. R.; Tsibart, A.; Samburova, V.; Moosmüller, H. Brown Carbon Aerosols from Burning of Boreal Peatlands: Microphysical Properties, Emission Factors, and Implications for Direct Radiative Forcing. *Atmospheric Chem. Phys.* **2016**, *16* (5), 3033–3040. https://doi.org/10.5194/acp-16-3033-2016.

(28)  Yan, J.; Wang, X.; Gong, P.; Wang, C.; Cong, Z. Review of Brown Carbon Aerosols: Recent Progress and Perspectives. *Sci. Total Environ.* **2018**, *634*, 1475–1485. https://doi.org/10.1016/j.scitotenv.2018.04.083.

(29)  Washenfelder, R. A.; Attwood, A. R.; Brock, C. A.; Guo, H.; Xu, L.; Weber, R. J.; Ng, N. L.; Allen, H. M.; Ayres, B. R.; Baumann, K.; Cohen, R. C.; Draper, D. C.; Duffey, K. C.; Edgerton, E.; Fry, J. L.; Hu, W. W.; Jimenez, J. L.; Palm, B. B.; Romer, P.; Stone, E. A.; Wooldridge, P. J.; Brown, S. S. Biomass Burning Dominates Brown Carbon Absorption in the Rural Southeastern United States. *Geophys. Res. Lett.* **2015**, *42* (2), 653–664. https://doi.org/10.1002/2014GL062444.

(30)  Lin, P.; Bluvshtein, N.; Rudich, Y.; Nizkorodov, S. A.; Laskin, J.; Laskin, A. Molecular Chemistry of Atmospheric Brown Carbon Inferred from a Nationwide Biomass Burning Event. *Environ. Sci. Technol.* **2017**, *51* (20), 11561–11570. https://doi.org/10.1021/acs.est.7b02276.

(31)  Budisulistiorini, S. H.; Riva, M.; Williams, M.; Chen, J.; Itoh, M.; Surratt, J. D.; Kuwata, M. Light-Absorbing Brown Carbon Aerosol Constituents from Combustion of Indonesian Peat and Biomass. *Environ. Sci. Technol.* **2017**, *51* (8), 4415–4423. https://doi.org/10.1021/acs.est.7b00397.

(32)  Hecobian, A.; Zhang, X.; Zheng, M.; Frank, N.; Edgerton, E. S.; Weber, R. J. Water-Soluble Organic Aerosol Material and the Light-Absorption Characteristics of Aqueous Extracts Measured over the Southeastern United States. *Atmospheric Chem. Phys.* **2010**, *10* (13), 5965. https://doi.org/10.5194/acp-10-5965-2010.

(33)  Baduel, C.; Voisin, D.; Jaffrezo, J.-L. Seasonal Variations of Concentrations and Optical Properties of Water Soluble HULIS Collected in Urban Environments. *Atmospheric Chem. Phys.* **2010**, *10* (9), 4085–4095. https://doi.org/10.5194/acp-10-4085-2010.

(34)  Selimovic, V.; Yokelson, R. J.; McMeeking, G. R.; Coefield, S. In Situ Measurements of Trace Gases, PM, and Aerosol Optical Properties during the 2017 NW US Wildfire Smoke Event. *Atmospheric Chem. Phys.* **2019**, *19* (6), 3905–3926. https://doi.org/10.5194/acp-19-3905-2019.

(35)  Forrister, H.; Liu, J.; Scheuer, E.; Dibb, J.; Ziemba, L.; Thornhill, K. L.; Anderson, B.; Diskin, G.; Perring, A. E.; Schwarz, J. P.; Campuzano-Jost, P.; Day, D. A.; Palm, B. B.; Jimenez, J. L.; Nenes, A.; Weber, R. J. Evolution of Brown Carbon in Wildfire Plumes. *Geophys. Res. Lett.* **2015**, *42* (11), 4623–4630. https://doi.org/10.1002/2015GL063897.

(36)  Fleming, L. T.; Lin, P.; Laskin, A.; Laskin, J.; Weltman, R.; Edwards, R. D.; Arora, N. K.; Yadav, A.; Meinardi, S.; Blake, D. R.; Pillarisetti, A.; Smith, K. R.; Nizkorodov, S. A. Molecular Composition of Particulate Matter Emissions from Dung and Brushwood Burning Household Cookstoves in Haryana, India. *Atmospheric Chem. Phys.* **2018**, *18* (4), 2461–2480. https://doi.org/10.5194/acp-18-2461-2018.

(37)  Mohr, C.; Lopez-Hilfiker, F. D.; Zotter, P.; Prévôt, A. S. H.; Xu, L.; Ng, N. L.; Herndon, S. C.; Williams, L. R.; Franklin, J. P.; Zahniser, M. S.; Worsnop, D. R.; Knighton, W. B.; Aiken, A. C.; Gorkowski, K. J.; Dubey, M. K.; Allan, J. D.; Thornton, J. A. Contribution of Nitrated Phenols to Wood Burning Brown Carbon Light Absorption in Detling, United Kingdom during Winter Time. *Environ. Sci. Technol.* **2013**, *47* (12), 6316–6324. https://doi.org/10.1021/es400683v.

(38)  Flannigan, M. D.; Krawchuk, M. A.; Groot, W. J. de; Wotton, B. M.; Gowman, L. M. Implications of Changing Climate for Global Wildland Fire. *Int. J. Wildland Fire* **2009**, *18* (5), 483–507. https://doi.org/10.1071/WF08187.

(39)  Simoneit, B. R. T. Biomass Burning — a Review of Organic Tracers for Smoke from Incomplete Combustion. *Appl. Geochem.* **2002**, *17* (3), 129–162. https://doi.org/10.1016/S0883-2927(01)00061-0.

(40)  Xie, M.; Chen, X.; Hays, M. D.; Holder, A. L. Composition and Light Absorption of N-Containing Aromatic Compounds in Organic Aerosols from Laboratory Biomass Burning. *Atmospheric Chem. Phys.* **2019**, *19* (5), 2899–2915. https://doi.org/10.5194/acp-19-2899-2019.

(41)  Smith, J. D.; Sio, V.; Yu, L.; Zhang, Q.; Anastasio, C. Secondary Organic Aerosol Production from Aqueous Reactions of Atmospheric Phenols with an Organic Triplet Excited State. *Environ. Sci. Technol.* **2014**, *48* (2), 1049–1057. https://doi.org/10.1021/es4045715.

(42)  Bluvshtein, N.; Lin, P.; Flores, J. M.; Segev, L.; Mazar, Y.; Tas, E.; Snider, G.; Weagle, C.; Brown, S. S.; Laskin, A.; Rudich, Y. Broadband Optical Properties of Biomass-Burning Aerosol and Identification of Brown Carbon Chromophores. *J. Geophys. Res. Atmospheres* **2017**, *122* (10), 5441–5456. https://doi.org/10.1002/2016JD026230.

(43)  Claeys, M.; Vermeylen, R.; Yasmeen, F.; Gómez-González, Y.; Chi, X.; Maenhaut, W.; Mészáros, T.; Salma, I. Chemical Characterisation of Humic-like Substances from Urban, Rural and Tropical Biomass Burning Environments Using Liquid Chromatography with UV/Vis Photodiode Array Detection and Electrospray Ionisation Mass Spectrometry. *Environ. Chem.* **2012**, *9* (3), 273–284. https://doi.org/10.1071/EN11163.

(44)  Iinuma, Y.; Böge, O.; Gräfe, R.; Herrmann, H. Methyl-Nitrocatechols: Atmospheric Tracer Compounds for Biomass Burning Secondary Organic Aerosols. *Environ. Sci. Technol.* **2010**, *44* (22), 8453–8459. https://doi.org/10.1021/es102938a.

(45)  Chow, K. S.; Huang, X. H. H.; Yu, J. Z. Quantification of Nitroaromatic Compounds in Atmospheric Fine Particulate Matter in Hong Kong over 3 Years: Field Measurement Evidence for Secondary Formation Derived from Biomass Burning Emissions. *Environ. Chem.* **2016**, *13* (4), 665–673. http://dx.doi.org/10.1071/EN15174.

(46)  Harrison, M. A. J.; Barra, S.; Borghesi, D.; Vione, D.; Arsene, C.; Iulian Olariu, R. Nitrated Phenols in the Atmosphere: A Review. *Atmos. Environ.* **2005**, *39* (2), 231–248. https://doi.org/10.1016/j.atmosenv.2004.09.044.

(47)  Lüttke, J.; Levsen, K.; Acker, K.; Wieprecht, W.; Möller, D. Phenols and Nitrated Phenols in Clouds at Mount Brocken. *Int. J. Environ. Anal. Chem.* **1999**, *74* (1–4), 69–89. https://doi.org/10.1080/03067319908031417.

(48)  Lüttke, J.; Scheer, V.; Levsen, K.; Wünsch, G.; Neil Cape, J.; Hargreaves, K. J.; Storeton-West, R. L.; Acker, K.; Wieprecht, W.; Jones, B. Occurrence and Formation of Nitrated Phenols in and out of Cloud. *Atmos. Environ.* **1997**, *31* (16), 2637–2648. https://doi.org/10.1016/S1352-2310(96)00229-4.

(49)  Bianco, A.; Riva, M.; Baray, J.-L.; Ribeiro, M.; Chaumerliac, N.; George, C.; Bridoux, M.; Deguillaume, L. Chemical Characterization of Cloudwater Collected at Puy de Dôme by FT-ICR MS Reveals the Presence of SOA Components. *ACS Earth Space Chem.* **2019**, *3* (10), 2076–2087. https://doi.org/10.1021/acsearthspacechem.9b00153.

(50) Finewax, Z.; de Gouw, J. A.; Ziemann, P. J. Identification and Quantification of 4-Nitrocatechol Formed from OH and $NO_3$ Radical-Initiated Reactions of Catechol in Air in the Presence of $NO_x$: Implications for Secondary Organic Aerosol Formation from Biomass Burning. *Environ. Sci. Technol.* **2018**, *52* (4), 1981–1989. https://doi.org/10.1021/acs.est.7b05864.

(51) Xie, M.; Chen, X.; Hays, M. D.; Lewandowski, M.; Offenberg, J.; Kleindienst, T. E.; Holder, A. L. Light Absorption of Secondary Organic Aerosol: Composition and Contribution of Nitroaromatic Compounds. *Environ. Sci. Technol.* **2017**, *51* (20), 11607–11616. https://doi.org/10.1021/acs.est.7b03263.

(52) Sengupta, D.; Samburova, V.; Bhattarai, C.; Kirillova, E.; Mazzoleni, L.; Iaukea-Lum, M.; Watts, A.; Moosmüller, H.; Khlystov, A. Light Absorption by Polar and Non-Polar Aerosol Compounds from Laboratory Biomass Combustion. *Atmospheric Chem. Phys.* **2018**, *18* (15), 10849–10867. https://doi.org/10.5194/acp-18-10849-2018.

(53) Jacobson, M. Z. Isolating Nitrated and Aromatic Aerosols and Nitrated Aromatic Gases as Sources of Ultraviolet Light Absorption. *J. Geophys. Res. Atmospheres* **1999**, *104* (D3), 3527–3542. https://doi.org/10.1029/1998JD100054.

(54) Lee, H. J. (Julie); Aiona, P. K.; Laskin, A.; Laskin, J.; Nizkorodov, S. A. Effect of Solar Radiation on the Optical Properties and Molecular Composition of Laboratory Proxies of Atmospheric Brown Carbon. *Environ. Sci. Technol.* **2014**, *48* (17), 10217–10226. https://doi.org/10.1021/es502515r.

(55) Hinrichs, R. Z.; Buczek, P.; Trivedi, J. J. Solar Absorption by Aerosol-Bound Nitrophenols Compared to Aqueous and Gaseous Nitrophenols. *Environ. Sci. Technol.* **2016**, *50* (11), 5661–5667. https://doi.org/10.1021/acs.est.6b00302.

(56) Aiona, P. K.; Luek, J. L.; Timko, S. A.; Powers, L. C.; Gonsior, M.; Nizkorodov, S. A. Effect of Photolysis on Absorption and Fluorescence Spectra of Light-Absorbing Secondary Organic Aerosols. *ACS Earth Space Chem.* **2018**, *2* (3), 235–245. https://doi.org/10.1021/acsearthspacechem.7b00153.

(57) Pye, H. O. T.; Nenes, A.; Alexander, B.; Ault, A. P.; Barth, M. C.; Clegg, S. L.; Collett Jr., J. L.; Fahey, K. M.; Hennigan, C. J.; Herrmann, H.; Kanakidou, M.; Kelly, J. T.; Ku, I.-T.; McNeill, V. F.; Riemer, N.; Schaefer, T.; Shi, G.; Tilgner, A.; Walker, J. T.; Wang, T.; Weber, R.; Xing, J.; Zaveri, R. A.; Zuend, A. The Acidity of Atmospheric Particles and Clouds. *Atmospheric Chem. Phys.* **2020**, *20* (8), 4809–4888. https://doi.org/10.5194/acp-20-4809-2020.

(58) Lin, P.; Aiona, P. K.; Li, Y.; Shiraiwa, M.; Laskin, J.; Nizkorodov, S. A.; Laskin, A. Molecular Characterization of Brown Carbon in Biomass Burning Aerosol Particles. *Environ. Sci. Technol.* **2016**, *50* (21), 11815–11824. https://doi.org/10.1021/acs.est.6b03024.

(59) Di Lorenzo, R. A.; Young, C. J. Size Separation Method for Absorption Characterization in Brown Carbon: Application to an Aged Biomass Burning Sample. *Geophys. Res. Lett.* **2016**, *43* (1), 458–465. https://doi.org/10.1002/2015GL066954.

(60)   Di Lorenzo, R. A.; Washenfelder, R. A.; Attwood, A. R.; Guo, H.; Xu, L.; Ng, N. L.; Weber, R. J.; Baumann, K.; Edgerton, E.; Young, C. J. Molecular-Size-Separated Brown Carbon Absorption for Biomass-Burning Aerosol at Multiple Field Sites. *Environ. Sci. Technol.* **2017**, *51* (6), 3128–3137. https://doi.org/10.1021/acs.est.6b06160.

(61)   Wong, J. P. S.; Tsagkaraki, M.; Tsiodra, I.; Mihalopoulos, N.; Violaki, K.; Kanakidou, M.; Sciare, J.; Nenes, A.; Weber, R. J. Atmospheric Evolution of Molecular-Weight-Separated Brown Carbon from Biomass Burning. *Atmospheric Chem. Phys.* **2019**, *19* (11), 7319–7334. https://doi.org/10.5194/acp-19-7319-2019.

(62)   Ward, D. E.; Radke, L. F. Emissions Measurements from Vegetation Fires: A Comparative Evaluation of Methods and Results. *Fire Environ. Ecol. Atmospheric Clim. Importance Veg. Fires* **1993**, 53–76.

(63)   Ward, D. E.; Hardy, C. C. Smoke Emissions from Wildland Fires. *Environ. Int.* **1991**, *17* (2), 117–134. https://doi.org/10.1016/0160-4120(91)90095-8.

(64)   Grosjean, D. Atmospheric Fate of Toxic Aromatic Compounds. *Sci. Total Environ.* **1991**, *100*, 367–414. https://doi.org/10.1016/0048-9697(91)90386-S.

(65)   Nakayama, T.; Sato, K.; Matsumi, Y.; Imamura, T.; Yamazaki, A.; Uchiyama, A. Wavelength and NOx Dependent Complex Refractive Index of SOAs Generated from the Photooxidation of Toluene. *Atmospheric Chem. Phys.* **2013**, *13* (2), 531. https://doi.org/10.5194/acp-13-531-2013.

(66)   Liu, P. F.; Abdelmalki, N.; Hung, H.-M.; Wang, Y.; Brune, W. H.; Martin, S. T. Ultraviolet and Visible Complex Refractive Indices of Secondary Organic Material Produced by Photooxidation of the Aromatic Compounds Toluene and *m*-Xylene. *Atmospheric Chem. Phys.* **2015**, *15* (3), 1435–1446. https://doi.org/10.5194/acp-15-1435-2015.

(67)   Lin, P.; Liu, J.; Shilling, J. E.; Kathmann, S. M.; Laskin, J.; Laskin, A. Molecular Characterization of Brown Carbon (BrC) Chromophores in Secondary Organic Aerosol Generated from Photo-Oxidation of Toluene. *Phys. Chem. Chem. Phys.* **2015**, *17* (36), 23312–23325. https://doi.org/10.1039/C5CP02563J.

(68)   Borrás, E.; Tortajada-Genaro, L. A. Secondary Organic Aerosol Formation from the Photo-Oxidation of Benzene. *Atmos. Environ.* **2012**, *47*, 154–163. https://doi.org/10.1016/j.atmosenv.2011.11.020.

(69)   Wang, Y.; Hu, M.; Wang, Y.; Zheng, J.; Shang, D.; Yang, Y.; Liu, Y.; Li, X.; Tang, R.; Zhu, W.; Du, Z.; Wu, Y.; Guo, S.; Wu, Z.; Lou, S.; Hallquist, M.; Yu, J. Z. The Formation of Nitro-Aromatic Compounds under High NO$_x$ and Anthropogenic VOC Conditions in Urban Beijing, China. *Atmospheric Chem. Phys.* **2019**, *19* (11), 7649–7665. https://doi.org/10.5194/acp-19-7649-2019.

(70)   Palm, B. B.; Peng, Q.; Fredrickson, C. D.; Lee, B. H.; Garofalo, L. A.; Pothier, M. A.; Kreidenweis, S. M.; Farmer, D. K.; Pokhrel, R. P.; Shen, Y.; Murphy, S. M.; Permar, W.; Hu, L.; Campos, T. L.; Hall, S. R.; Ullmann, K.; Zhang, X.; Flocke, F.; Fischer, E. V.;

Thornton, J. A. Quantification of Organic Aerosol and Brown Carbon Evolution in Fresh Wildfire Plumes. *Proc. Natl. Acad. Sci.* **2020**, *117* (47), 29469–29477. https://doi.org/10.1073/pnas.2012218117.

(71)   Sun, Y. L.; Zhang, Q.; Anastasio, C.; Sun, J. Insights into Secondary Organic Aerosol Formed via Aqueous-Phase Reactions of Phenolic Compounds Based on High Resolution Mass Spectrometry. *Atmospheric Chem. Phys.* **2010**, *10* (10), 4809–4822. https://doi.org/10.5194/acp-10-4809-2010.

(72)   Yu, L.; Smith, J.; Laskin, A.; Anastasio, C.; Laskin, J.; Zhang, Q. Chemical Characterization of SOA Formed from Aqueous-Phase Reactions of Phenols with the Triplet Excited State of Carbonyl and Hydroxyl Radical. *Atmospheric Chem. Phys.* **2014**, *14* (24), 13801–13816. https://doi.org/10.5194/acp-14-13801-2014.

(73)   Yu, L.; Smith, J.; Laskin, A.; George, K. M.; Anastasio, C.; Laskin, J.; Dillner, A. M.; Zhang, Q. Molecular Transformations of Phenolic SOA during Photochemical Aging in the Aqueous Phase: Competition among Oligomerization, Functionalization, and Fragmentation. *Atmospheric Chem. Phys.* **2016**, *16* (7), 4511–4527. http://dx.doi.org.proxy.lib.umich.edu/10.5194/acp-16-4511-2016.

(74)   Smith, J. D.; Kinney, H.; Anastasio, C. Phenolic Carbonyls Undergo Rapid Aqueous Photodegradation to Form Low-Volatility, Light-Absorbing Products. *Atmos. Environ.* **2016**, *126*, 36–44. https://doi.org/10.1016/j.atmosenv.2015.11.035.

(75)   Moosmüller, H.; Chakrabarty, R. K.; Arnott, W. P. Aerosol Light Absorption and Its Measurement: A Review. *J. Quant. Spectrosc. Radiat. Transf.* **2009**, *110* (11), 844–878. https://doi.org/10.1016/j.jqsrt.2009.02.035.

(76)   Forestieri, S. D.; Helgestad, T. M.; Lambe, A. T.; Renbaum-Wolff, L.; Lack, D. A.; Massoli, P.; Cross, E. S.; Dubey, M. K.; Mazzoleni, C.; Olfert, J. S.; Sedlacek III, A. J.; Freedman, A.; Davidovits, P.; Onasch, T. B.; Cappa, C. D. Measurement and Modeling of the Multiwavelength Optical Properties of Uncoated Flame-Generated Soot. *Atmospheric Chem. Phys.* **2018**, *18* (16), 12141–12159. https://doi.org/10.5194/acp-18-12141-2018.

(77)   Flores, J. M.; Zhao, D. F.; Segev, L.; Schlag, P.; Kiendler-Scharr, A.; Fuchs, H.; Watne, Å. K.; Bluvshtein, N.; Mentel, T. F.; Hallquist, M.; Rudich, Y. Evolution of the Complex Refractive Index in the UV Spectral Region in Ageing Secondary Organic Aerosol. *Atmospheric Chem. Phys.* **2014**, *14* (11), 5793–5806. https://doi.org/10.5194/acp-14-5793-2014.

(78)   Kim, H.; Paulson, S. E. Real Refractive Indices and Volatility of Secondary Organic Aerosol Generated from Photooxidation and Ozonolysis of Limonene, α-Pinene and Toluene. *Atmospheric Chem. Phys.* **2013**, *13* (15), 7711–7723. https://doi.org/10.5194/acp-13-7711-2013.

(79)   Zarzana, K. J.; Cappa, C. D.; Tolbert, M. A. Sensitivity of Aerosol Refractive Index Retrievals Using Optical Spectroscopy. *Aerosol Sci. Technol.* **2014**, *48* (11), 1133–1144. https://doi.org/10.1080/02786826.2014.963498.

(80) Zhang, X.; Kim, H.; Parworth, C. L.; Young, D. E.; Zhang, Q.; Metcalf, A. R.; Cappa, C. D. Optical Properties of Wintertime Aerosols from Residential Wood Burning in Fresno, CA: Results from DISCOVER-AQ 2013. *Environ. Sci. Technol.* **2016**, *50* (4), 1681–1690. https://doi.org/10.1021/acs.est.5b04134.

(81) Jennings, S. G.; Pinnick, R. G.; Gillespie, J. B. Relation between Absorption Coefficient and Imaginary Index of Atmospheric Aerosol Constituents. *Appl. Opt.* **1979**, *18* (9), 1368–1371. https://doi.org/10.1364/AO.18.001368.

(82) Zangmeister, C. D.; You, R.; Lunny, E. M.; Jacobson, A. E.; Okumura, M.; Zachariah, M. R.; Radney, J. G. Measured In-Situ Mass Absorption Spectra for Nine Forms of Highly-Absorbing Carbonaceous Aerosol. *Carbon* **2018**, *136*, 85–93. https://doi.org/10.1016/j.carbon.2018.04.057.

(83) Mishchenko, M. I.; Travis, L. D.; Lacis, A. A.; Mishchenko, M. I.; Travis, L. D.; Lacis, A. A. *Scattering, Absorption, and Emission of Light by Small Particles*; Cambridge University Press: Cambridge ; New York, 2002.

(84) Liu, J.; Bergin, M.; Guo, H.; King, L.; Kotra, N.; Edgerton, E.; Weber, R. J. Size-Resolved Measurements of Brown Carbon in Water and Methanol Extracts and Estimates of Their Contribution to Ambient Fine-Particle Light Absorption. *Atmospheric Chem. Phys.* **2013**, *13* (24), 12389–12404. https://doi.org/10.5194/acp-13-12389-2013.

(85) Liu, C.; Chung, C. E.; Yin, Y.; Schnaiter, M. The Absorption Ångström Exponent of Black Carbon: From Numerical Aspects. *Atmospheric Chem. Phys.* **2018**, *18* (9), 6259–6273. https://doi.org/10.5194/acp-18-6259-2018.

(86) Rudich, Y.; Donahue, N. M.; Mentel, T. F. Aging of Organic Aerosol: Bridging the Gap Between Laboratory and Field Studies. *Annu. Rev. Phys. Chem.* **2007**, *58* (1), 321–352. https://doi.org/10.1146/annurev.physchem.58.032806.104432.

(87) Jimenez, J. L.; Canagaratna, M. R.; Donahue, N. M.; Prevot, A. S. H.; Zhang, Q.; Kroll, J. H.; DeCarlo, P. F.; Allan, J. D.; Coe, H.; Ng, N. L.; Aiken, A. C.; Docherty, K. S.; Ulbrich, I. M.; Grieshop, A. P.; Robinson, A. L.; Duplissy, J.; Smith, J. D.; Wilson, K. R.; Lanz, V. A.; Hueglin, C.; Sun, Y. L.; Tian, J.; Laaksonen, A.; Raatikainen, T.; Rautiainen, J.; Vaattovaara, P.; Ehn, M.; Kulmala, M.; Tomlinson, J. M.; Collins, D. R.; Cubison, M. J.; E; Dunlea, J.; Huffman, J. A.; Onasch, T. B.; Alfarra, M. R.; Williams, P. I.; Bower, K.; Kondo, Y.; Schneider, J.; Drewnick, F.; Borrmann, S.; Weimer, S.; Demerjian, K.; Salcedo, D.; Cottrell, L.; Griffin, R.; Takami, A.; Miyoshi, T.; Hatakeyama, S.; Shimono, A.; Sun, J. Y.; Zhang, Y. M.; Dzepina, K.; Kimmel, J. R.; Sueper, D.; Jayne, J. T.; Herndon, S. C.; Trimborn, A. M.; Williams, L. R.; Wood, E. C.; Middlebrook, A. M.; Kolb, C. E.; Baltensperger, U.; Worsnop, D. R. Evolution of Organic Aerosols in the Atmosphere. *Science* **2009**, *326* (5959), 1525–1529. https://doi.org/10.1126/science.1180353.

(88) George, I. J.; Abbatt, J. P. D. Heterogeneous Oxidation of Atmospheric Aerosol Particles by Gas-Phase Radicals. *Nat. Chem.* **2010**, *2* (9), 713–722. https://doi.org/10.1038/nchem.806.

(89) Shrivastava, M.; Cappa, C. D.; Fan, J.; Goldstein, A. H.; Guenther, A. B.; Jimenez, J. L.; Kuang, C.; Laskin, A.; Martin, S. T.; Ng, N. L.; Petaja, T.; Pierce, J. R.; Rasch, P. J.; Roldin, P.; Seinfeld, J. H.; Shilling, J.; Smith, J. N.; Thornton, J. A.; Volkamer, R.; Wang, J.; Worsnop, D. R.; Zaveri, R. A.; Zelenyuk, A.; Zhang, Q. Recent Advances in Understanding Secondary Organic Aerosol: Implications for Global Climate Forcing. *Rev. Geophys.* **2017**, *55* (2), 509–559. https://doi.org/10.1002/2016RG000540.

(90) McNeill, V. F. Aqueous Organic Chemistry in the Atmosphere: Sources and Chemical Processing of Organic Aerosols. *Environ. Sci. Technol.* **2015**, *49* (3), 1237–1244. https://doi.org/10.1021/es5043707.

(91) Kroll, J. H.; Smith, J. D.; Che, D. L.; Kessler, S. H.; Worsnop, D. R.; Wilson, K. R. Measurement of Fragmentation and Functionalization Pathways in the Heterogeneous Oxidation of Oxidized Organic Aerosol. *Phys. Chem. Chem. Phys.* **2009**, *11* (36), 8005–8014. https://doi.org/10.1039/B905289E.

(92) Jang, M.; Czoschke, N. M.; Lee, S.; Kamens, R. M. Heterogeneous Atmospheric Aerosol Production by Acid-Catalyzed Particle-Phase Reactions. *Science* **2002**, *298* (5594), 814–817. https://doi.org/10.1126/science.1075798.

(93) Moise, T.; Flores, J. M.; Rudich, Y. Optical Properties of Secondary Organic Aerosols and Their Changes by Chemical Processes. *Chem. Rev.* **2015**, *115* (10), 4400–4439. https://doi.org/10.1021/cr5005259.

(94) Saleh, R. From Measurements to Models: Toward Accurate Representation of Brown Carbon in Climate Calculations. *Curr. Pollut. Rep.* **2020**, *6* (2), 90–104. https://doi.org/10.1007/s40726-020-00139-3.

(95) Hodshire, A. L.; Akherati, A.; Alvarado, M. J.; Brown-Steiner, B.; Jathar, S. H.; Jimenez, J. L.; Kreidenweis, S. M.; Lonsdale, C. R.; Onasch, T. B.; Ortega, A. M.; Pierce, J. R. Aging Effects on Biomass Burning Aerosol Mass and Composition: A Critical Review of Field and Laboratory Studies. *Environ. Sci. Technol.* **2019**, *53* (17), 10007–10022. https://doi.org/10.1021/acs.est.9b02588.

(96) Liu, D.; He, C.; Schwarz, J. P.; Wang, X. Lifecycle of Light-Absorbing Carbonaceous Aerosols in the Atmosphere. *Npj Clim. Atmospheric Sci.* **2020**, *3* (1), 1–18. https://doi.org/10.1038/s41612-020-00145-8.

(97) Soleimanian, E.; Mousavi, A.; Taghvaee, S.; Shafer, M. M.; Sioutas, C. Impact of Secondary and Primary Particulate Matter (PM) Sources on the Enhanced Light Absorption by Brown Carbon (BrC) Particles in Central Los Angeles. *Sci. Total Environ.* **2020**, *705*, 135902. https://doi.org/10.1016/j.scitotenv.2019.135902.

(98) Wang, Q.; Han, Y.; Ye, J.; Liu, S.; Pongpiachan, S.; Zhang, N.; Han, Y.; Tian, J.; Wu, C.; Long, X.; Zhang, Q.; Zhang, W.; Zhao, Z.; Cao, J. High Contribution of Secondary Brown Carbon to Aerosol Light Absorption in the Southeastern Margin of Tibetan Plateau. *Geophys. Res. Lett.* **2019**, *46* (9), 4962–4970. https://doi.org/10.1029/2019GL082731.

(99)    Cappa, C. D.; Zhang, X.; Russell, L. M.; Collier, S.; Lee, A. K. Y.; Chen, C.-L.; Betha, R.; Chen, S.; Liu, J.; Price, D. J.; Sanchez, K. J.; McMeeking, G. R.; Williams, L. R.; Onasch, T. B.; Worsnop, D. R.; Abbatt, J.; Zhang, Q. Light Absorption by Ambient Black and Brown Carbon and Its Dependence on Black Carbon Coating State for Two California, USA, Cities in Winter and Summer. *J. Geophys. Res. Atmospheres* **2019**, *124* (3), 1550–1577. https://doi.org/10.1029/2018JD029501.

(100)   Liu, J.; Lin, P.; Laskin, A.; Laskin, J.; Kathmann, S. M.; Wise, M.; Caylor, R.; Imholt, F.; Selimovic, V.; Shilling, J. E. Optical Properties and Aging of Light-Absorbing Secondary Organic Aerosol. *Atmospheric Chem. Phys.* **2016**, *16* (19), 12815–12827. https://doi.org/10.5194/acp-16-12815-2016.

(101)   Saleh, R.; Robinson, E. S.; Tkacik, D. S.; Ahern, A. T.; Liu, S.; Aiken, A. C.; Sullivan, R. C.; Presto, A. A.; Dubey, M. K.; Yokelson, R. J.; Donahue, N. M.; Robinson, A. L. Brownness of Organics in Aerosols from Biomass Burning Linked to Their Black Carbon Content. *Nat. Geosci.* **2014**, *7* (9), 647–650. https://doi.org/10.1038/ngeo2220.

(102)   Saleh, R.; Cheng, Z.; Atwi, K. The Brown–Black Continuum of Light-Absorbing Combustion Aerosols. *Environ. Sci. Technol. Lett.* **2018**, *5* (8), 508–513. https://doi.org/10.1021/acs.estlett.8b00305.

(103)   Hettiyadura, A. P. S.; Garcia, V.; Li, C.; West, C. P.; Tomlin, J.; He, Q.; Rudich, Y.; Laskin, A. Chemical Composition and Molecular-Specific Optical Properties of Atmospheric Brown Carbon Associated with Biomass Burning. *Environ. Sci. Technol.* **2021**, *55* (4), 2511–2521. https://doi.org/10.1021/acs.est.0c05883.

(104)   Jiang, H.; Frie, A. L.; Lavi, A.; Chen, J. Y.; Zhang, H.; Bahreini, R.; Lin, Y.-H. Brown Carbon Formation from Nighttime Chemistry of Unsaturated Heterocyclic Volatile Organic Compounds. *Environ. Sci. Technol. Lett.* **2019**, *6* (3), 184–190. https://doi.org/10.1021/acs.estlett.9b00017.

(105)   Song, C.; Gyawali, M.; Zaveri, R. A.; Shilling, J. E.; Arnott, W. P. Light Absorption by Secondary Organic Aerosol from α-Pinene: Effects of Oxidants, Seed Aerosol Acidity, and Relative Humidity. *J. Geophys. Res. Atmospheres* **2013**, *118* (20), 11,741-11,749. https://doi.org/10.1002/jgrd.50767.

(106)   Atkinson, R. Gas-Phase Tropospheric Chemistry of Organic Compounds: A Review. *Atmos. Environ.* **2007**, *41*, 200–240. https://doi.org/10.1016/j.atmosenv.2007.10.068.

(107)   Decker, Z. C. J.; Zarzana, K. J.; Coggon, M.; Min, K.-E.; Pollack, I.; Ryerson, T. B.; Peischl, J.; Edwards, P.; Dubé, W. P.; Markovic, M. Z.; Roberts, J. M.; Veres, P. R.; Graus, M.; Warneke, C.; de Gouw, J.; Hatch, L. E.; Barsanti, K. C.; Brown, S. S. Nighttime Chemical Transformation in Biomass Burning Plumes: A Box Model Analysis Initialized with Aircraft Observations. *Environ. Sci. Technol.* **2019**, *53* (5), 2529–2538. https://doi.org/10.1021/acs.est.8b05359.

(108)   Finewax, Z.; de Gouw, J. A.; Ziemann, P. J. Products and Secondary Organic Aerosol Yields from the OH and NO $_3$ Radical-Initiated Oxidation of Resorcinol. *ACS Earth Space Chem.* **2019**, *3* (7), 1248–1259. https://doi.org/10.1021/acsearthspacechem.9b00112.

(109) Liu, C.; Liu, Y.; Chen, T.; Liu, J.; He, H. Rate Constant and Secondary Organic Aerosol Formation from the Gas-Phase Reaction of Eugenol with Hydroxyl Radicals. *Atmospheric Chem. Phys.* **2019**, *19* (3), 2001–2013. https://doi.org/10.5194/acp-19-2001-2019.

(110) Ahmad, W.; Coeur, C.; Tomas, A.; Fagniez, T.; Brubach, J.-B.; Cuisset, A. Infrared Spectroscopy of Secondary Organic Aerosol Precursors and Investigation of the Hygroscopicity of SOA Formed from the OH Reaction with Guaiacol and Syringol. *Appl. Opt.* **2017**, *56* (11), E116–E122. https://doi.org/10.1364/AO.56.00E116.

(111) Xu, C.; Wang, L. Atmospheric Oxidation Mechanism of Phenol Initiated by OH Radical. *J. Phys. Chem. A* **2013**, *117* (11), 2358–2364. https://doi.org/10.1021/jp308856b.

(112) Kim, H.; Barkey, B.; Paulson, S. E. Real Refractive Indices and Formation Yields of Secondary Organic Aerosol Generated from Photooxidation of Limonene and α-Pinene: The Effect of the HC/NOx Ratio. *J. Phys. Chem. A* **2012**, *116* (24), 6059–6067. https://doi.org/10.1021/jp301302z.

(113) Zhang, X.; Lin, Y.-H.; Surratt, J. D.; Zotter, P.; Prévôt, A. S. H.; Weber, R. J. Light-Absorbing Soluble Organic Aerosol in Los Angeles and Atlanta: A Contrast in Secondary Organic Aerosol. *Geophys. Res. Lett.* **2011**, *38* (21). https://doi.org/10.1029/2011GL049385.

(114) Lambe, A. T.; Cappa, C. D.; Massoli, P.; Onasch, T. B.; Forestieri, S. D.; Martin, A. T.; Cummings, M. J.; Croasdale, D. R.; Brune, W. H.; Worsnop, D. R.; Davidovits, P. Relationship between Oxidation Level and Optical Properties of Secondary Organic Aerosol. *Environ. Sci. Technol.* **2013**, *47* (12), 6349–6357. https://doi.org/10.1021/es401043j.

(115) Romonosky, D. E.; Ali, N. N.; Saiduddin, M. N.; Wu, M.; Lee, H. J. (Julie); Aiona, P. K.; Nizkorodov, S. A. Effective Absorption Cross Sections and Photolysis Rates of Anthropogenic and Biogenic Secondary Organic Aerosols. *Atmos. Environ.* **2016**, *130*, 172–179. https://doi.org/10.1016/j.atmosenv.2015.10.019.

(116) Bhattarai, C.; Samburova, V.; Sengupta, D.; Iaukea-Lum, M.; Watts, A. C.; Moosmüller, H.; Khlystov, A. Y. Physical and Chemical Characterization of Aerosol in Fresh and Aged Emissions from Open Combustion of Biomass Fuels. *Aerosol Sci. Technol.* **2018**, *52* (11), 1266–1282. https://doi.org/10.1080/02786826.2018.1498585.

(117) Watson, J. G.; Cao, J.; Chen, L.-W. A.; Wang, Q.; Tian, J.; Wang, X.; Gronstal, S.; Ho, S. S. H.; Watts, A. C.; Chow, J. C. Gaseous, $PM_{2.5}$ Mass, and Speciated Emission Factors from Laboratory Chamber Peat Combustion. *Atmospheric Chem. Phys.* **2019**, *19* (22), 14173–14193. https://doi.org/10.5194/acp-19-14173-2019.

(118) Martinsson, J.; Eriksson, A. C.; Nielsen, I. E.; Malmborg, V. B.; Ahlberg, E.; Andersen, C.; Lindgren, R.; Nyström, R.; Nordin, E. Z.; Brune, W. H.; Svenningsson, B.; Swietlicki, E.; Boman, C.; Pagels, J. H. Impacts of Combustion Conditions and Photochemical Processing on the Light Absorption of Biomass Combustion Aerosol. *Environ. Sci. Technol.* **2015**, *49* (24), 14663–14671. https://doi.org/10.1021/acs.est.5b03205.

(119) Chow, J. C.; Cao, J.; Antony Chen, L.-W.; Wang, X.; Wang, Q.; Tian, J.; Ho, S. S. H.; Watts, A. C.; Carlson, T. B.; Kohl, S. D.; Watson, J. G. Changes in $PM_{2.5}$ Peat Combustion Source Profiles with Atmospheric Aging in an Oxidation Flow Reactor. *Atmospheric Meas. Tech.* **2019**, *12* (10), 5475–5501. https://doi.org/10.5194/amt-12-5475-2019.

(120) Kumar, N. K.; Corbin, J. C.; Bruns, E. A.; Massabó, D.; Slowik, J. G.; Drinovec, L.; Močnik, G.; Prati, P.; Vlachou, A.; Baltensperger, U.; Gysel, M.; El-Haddad, I.; Prévôt, A. S. H. Production of Particulate Brown Carbon during Atmospheric Aging of Residential Wood-Burning Emissions. *Atmospheric Chem. Phys.* **2018**, *18* (24), 17843–17861. https://doi.org/10.5194/acp-18-17843-2018.

(121) Saleh, R.; Hennigan, C. J.; McMeeking, G. R.; Chuang, W. K.; Robinson, E. S.; Coe, H.; Donahue, N. M.; Robinson, A. L. Absorptivity of Brown Carbon in Fresh and Photo-Chemically Aged Biomass-Burning Emissions. *Atmospheric Chem. Phys.* **2013**, *13* (15), 7683–7693. https://doi.org/10.5194/acp-13-7683-2013.

(122) Tasoglou, A.; Saliba, G.; Subramanian, R.; Pandis, S. N. Absorption of Chemically Aged Biomass Burning Carbonaceous Aerosol. *J. Aerosol Sci.* **2017**, *113*, 141–152. https://doi.org/10.1016/j.jaerosci.2017.07.011.

(123) Cappa, C. D.; Lim, C. Y.; Hagan, D. H.; Coggon, M.; Koss, A.; Sekimoto, K.; Gouw, J. de; Onasch, T. B.; Warneke, C.; Kroll, J. H. Biomass-Burning-Derived Particles from a Wide Variety of Fuels – Part 2: Effects of Photochemical Aging on Particle Optical and Chemical Properties. *Atmospheric Chem. Phys.* **2020**, *20* (14), 8511–8532. https://doi.org/10.5194/acp-20-8511-2020.

(124) Smith, D. M.; Fiddler, M. N.; Pokhrel, R. P.; Bililign, S. Laboratory Studies of Fresh and Aged Biomass Burning Aerosol Emitted from East African Biomass Fuels – Part 1: Optical Properties. *Atmospheric Chem. Phys.* **2020**, *20* (17), 10149–10168. https://doi.org/10.5194/acp-20-10149-2020.

(125) Hodshire, A. L.; Ramnarine, E.; Akherati, A.; Alvarado, M. L.; Farmer, D. K.; Jathar, S. H.; Kreidenweis, S. M.; Lonsdale, C. R.; Onasch, T. B.; Springston, S. R.; Wang, J.; Wang, Y.; Kleinman, L. I.; Sedlacek III, A. J.; Pierce, J. R. Dilution Impacts on Smoke Aging: Evidence in BBOP Data. *Atmospheric Chem. Phys. Discuss.* **2020**, 1–21. https://doi.org/10.5194/acp-2020-300.

(126) Ahern, A. T.; Robinson, E. S.; Tkacik, D. S.; Saleh, R.; Hatch, L. E.; Barsanti, K. C.; Stockwell, C. E.; Yokelson, R. J.; Presto, A. A.; Robinson, A. L.; Sullivan, R. C.; Donahue, N. M. Production of Secondary Organic Aerosol During Aging of Biomass Burning Smoke From Fresh Fuels and Its Relationship to VOC Precursors. *J. Geophys. Res. Atmospheres* **2019**, *124* (6), 3583–3606. https://doi.org/10.1029/2018JD029068.

(127) Kumar, N. K.; Corbin, J. C.; Bruns, E. A.; Massabó, D.; Slowik, J. G.; Drinovec, L.; Močnik, G.; Prati, P.; Vlachou, A.; Baltensperger, U.; Gysel, M.; El-Haddad, I.; Prévôt, A. S. H. Production of Particulate Brown Carbon during Atmospheric Aging of Residential Wood-Burning Emissions. *Atmospheric Chem. Phys.* **2018**, *18* (24), 17843–17861. https://doi.org/10.5194/acp-18-17843-2018.

(128) Gilman, J. B.; Lerner, B. M.; Kuster, W. C.; Goldan, P. D.; Warneke, C.; Veres, P. R.; Roberts, J. M.; de Gouw, J. A.; Burling, I. R.; Yokelson, R. J. Biomass Burning Emissions and Potential Air Quality Impacts of Volatile Organic Compounds and Other Trace Gases from Fuels Common in the US. *Atmospheric Chem. Phys.* **2015**, *15* (24), 13915–13938. https://doi.org/10.5194/acp-15-13915-2015.

(129) Sekimoto, K.; Koss, A. R.; Gilman, J. B.; Selimovic, V.; Coggon, M. M.; Zarzana, K. J.; Yuan, B.; Lerner, B. M.; Brown, S. S.; Warneke, C.; Yokelson, R. J.; Roberts, J. M.; de Gouw, J. High- and Low-Temperature Pyrolysis Profiles Describe Volatile Organic Compound Emissions from Western US Wildfire Fuels. *Atmospheric Chem. Phys.* **2018**, *18* (13), 9263–9281. https://doi.org/10.5194/acp-18-9263-2018.

(130) Koss, A. R.; Sekimoto, K.; Gilman, J. B.; Selimovic, V.; Coggon, M. M.; Zarzana, K. J.; Yuan, B.; Lerner, B. M.; Brown, S. S.; Jimenez, J. L.; Krechmer, J.; Roberts, J. M.; Warneke, C.; Yokelson, R. J.; de Gouw, J. Non-Methane Organic Gas Emissions from Biomass Burning: Identification, Quantification, and Emission Factors from PTR-ToF during the FIREX 2016 Laboratory Experiment. *Atmospheric Chem. Phys.* **2018**, *18* (5), 3299–3319. https://doi.org/10.5194/acp-18-3299-2018.

(131) Lim, C. Y.; Hagan, D. H.; Coggon, M. M.; Koss, A. R.; Sekimoto, K.; Gouw, J. de; Warneke, C.; Cappa, C. D.; Kroll, J. H. Secondary Organic Aerosol Formation from the Laboratory Oxidation of Biomass Burning Emissions. *Atmospheric Chem. Phys.* **2019**, *19* (19), 12797–12809. https://doi.org/10.5194/acp-19-12797-2019.

(132) Bruns, E. A.; El Haddad, I.; Slowik, J. G.; Kilic, D.; Klein, F.; Baltensperger, U.; Prévôt, A. S. H. Identification of Significant Precursor Gases of Secondary Organic Aerosols from Residential Wood Combustion. *Sci. Rep.* **2016**, *6* (1), 27881. https://doi.org/10.1038/srep27881.

(133) Seinfeld, J. H.; Pandis, S. N. *Atmospheric Chemistry and Physics From Air Pollution to Climate Change*, Second Edition.; John Wiley & Sons Inc.: New Jersey, USA, 2006.

(134) Lohmann, U.; Lüönd, F.; Mahrt, F. *An Introduction to Clouds: From the Microscale to Climate*; Cambridge University Press, 2016.

(135) Arakaki, T.; Anastasio, C.; Kuroki, Y.; Nakajima, H.; Okada, K.; Kotani, Y.; Handa, D.; Azechi, S.; Kimura, T.; Tsuhako, A.; Miyagi, Y. A General Scavenging Rate Constant for Reaction of Hydroxyl Radical with Organic Carbon in Atmospheric Waters. *Environ. Sci. Technol.* **2013**, *47* (15), 8196–8203. https://doi.org/10.1021/es401927b.

(136) Ervens, B.; George, C.; Williams, J. E.; Buxton, G. V.; Salmon, G. A.; Bydder, M.; Wilkinson, F.; Dentener, F.; Mirabel, P.; Wolke, R.; Herrmann, H. CAPRAM 2.4 (MODAC Mechanism): An Extended and Condensed Tropospheric Aqueous Phase Mechanism and Its Application. *J. Geophys. Res. Atmospheres* **2003**, *108* (D14). https://doi.org/10.1029/2002JD002202.

(137) Ervens, B.; Sorooshian, A.; Lim, Y. B.; Turpin, B. J. Key Parameters Controlling OH-Initiated Formation of Secondary Organic Aerosol in the Aqueous Phase (AqSOA). *J.*

*Geophys. Res. Atmospheres* **2014**, *119* (7), 3997–4016.
https://doi.org/10.1002/2013JD021021.

(138) Herrmann, H.; Hoffmann, D.; Schaefer, T.; Bräuer, P.; Tilgner, A. Tropospheric Aqueous-Phase Free-Radical Chemistry: Radical Sources, Spectra, Reaction Kinetics and Prediction Tools. *ChemPhysChem* **2010**, *11* (18), 3796–3822.
https://doi.org/10.1002/cphc.201000533.

(139) Hoffmann, E. H.; Tilgner, A.; Wolke, R.; Böge, O.; Walter, A.; Herrmann, H. Oxidation of Substituted Aromatic Hydrocarbons in the Tropospheric Aqueous Phase: Kinetic Mechanism Development and Modelling. *Phys. Chem. Chem. Phys.* **2018**, *20* (16), 10960–10977. https://doi.org/10.1039/C7CP08576A.

(140) Deguillaume, L.; Leriche, M.; Desboeufs, K.; Mailhot, G.; George, C.; Chaumerliac, N. Transition Metals in Atmospheric Liquid Phases:  Sources, Reactivity, and Sensitive Parameters. *Chem. Rev.* **2005**, *105* (9), 3388–3431. https://doi.org/10.1021/cr040649c.

(141) Slade, J. H.; Knopf, D. A. Multiphase OH Oxidation Kinetics of Organic Aerosol: The Role of Particle Phase State and Relative Humidity. *Geophys. Res. Lett.* **2014**, *41* (14), 5297–5306. https://doi.org/10.1002/2014GL060582.

(142) Vione, D.; Minella, M.; Maurino, V.; Minero, C. Indirect Photochemistry in Sunlit Surface Waters: Photoinduced Production of Reactive Transient Species. *Chem. – Eur. J.* **2014**, *20* (34), 10590–10606. https://doi.org/10.1002/chem.201400413.

(143) McNeill, K.; Canonica, S. Triplet State Dissolved Organic Matter in Aquatic Photochemistry: Reaction Mechanisms, Substrate Scope, and Photophysical Properties. *Environ. Sci. Process. Impacts* **2016**, *18* (11), 1381–1399.
https://doi.org/10.1039/C6EM00408C.

(144) Corral Arroyo, P.; Bartels-Rausch, T.; Alpert, P. A.; Dumas, S.; Perrier, S.; George, C.; Ammann, M. Particle-Phase Photosensitized Radical Production and Aerosol Aging. *Environ. Sci. Technol.* **2018**, *52* (14), 7680–7688. https://doi.org/10.1021/acs.est.8b00329.

(145) Sumner, A. J.; Woo, J. L.; McNeill, V. F. Model Analysis of Secondary Organic Aerosol Formation by Glyoxal in Laboratory Studies: The Case for Photoenhanced Chemistry. *Environ. Sci. Technol.* **2014**, *48* (20), 11919–11925. https://doi.org/10.1021/es502020j.

(146) Monge, M. E.; Rosenørn, T.; Favez, O.; Müller, M.; Adler, G.; Abo Riziq, A.; Rudich, Y.; Herrmann, H.; George, C.; D'Anna, B. Alternative Pathway for Atmospheric Particles Growth. *Proc. Natl. Acad. Sci. U. S. A.* **2012**, *109* (18), 6840–6844.
https://doi.org/10.1073/pnas.1120593109.

(147) Aregahegn, K. Z.; Nozière, B.; George, C. Organic Aerosol Formation Photo-Enhanced by the Formation of Secondary Photosensitizers in Aerosols. *Faraday Discuss.* **2013**, *165* (0), 123–134. https://doi.org/10.1039/C3FD00044C.

(148) Rossignol, S.; Aregahegn, K. Z.; Tinel, L.; Fine, L.; Nozière, B.; George, C. Glyoxal Induced Atmospheric Photosensitized Chemistry Leading to Organic Aerosol Growth. *Environ. Sci. Technol.* **2014**, *48* (6), 3218–3227. https://doi.org/10.1021/es405581g.

(149) Kaur, R.; Anastasio, C. First Measurements of Organic Triplet Excited States in Atmospheric Waters. *Environ. Sci. Technol.* **2018**, *52* (9), 5218–5226. https://doi.org/10.1021/acs.est.7b06699.

(150) Kaur, R.; Labins, J. R.; Helbock, S. S.; Jiang, W.; Bein, K. J.; Zhang, Q.; Anastasio, C. Photooxidants from Brown Carbon and Other Chromophores in Illuminated Particle Extracts. *Atmospheric Chem. Phys.* **2019**, *19* (9), 6579–6594. https://doi.org/10.5194/acp-19-6579-2019.

(151) Corral Arroyo, P.; Aellig, R.; Alpert, P. A.; Volkamer, R.; Ammann, M. Halogen Activation and Radical Cycling Initiated by Imidazole-2-Carboxaldehyde Photochemistry. *Atmospheric Chem. Phys.* **2019**, *19* (16), 10817–10828. https://doi.org/10.5194/acp-19-10817-2019.

(152) Tsui, W. G.; McNeill, V. F. Modeling Secondary Organic Aerosol Production from Photosensitized Humic-like Substances (HULIS). *Environ. Sci. Technol. Lett.* **2018**, *5* (5), 255–259. https://doi.org/10.1021/acs.estlett.8b00101.

(153) Kitanovski, Z.; Čusak, A.; Grgić, I.; Claeys, M. Chemical Characterization of the Main Products Formed through Aqueous-Phase Photonitration of Guaiacol. *Atmospheric Meas. Tech.* **2014**, *7* (8), 2457–2470. https://doi.org/10.5194/amt-7-2457-2014.

(154) Vione, D.; Maurino, V.; Minero, C.; Pelizzetti, E. Phenol Photonitration upon UV Irradiation of Nitrite in Aqueous Solution I: Effects of Oxygen and 2-Propanol. *Chemosphere* **2001**, *45* (6), 893–902. https://doi.org/10.1016/S0045-6535(01)00035-2.

(155) Pang, H.; Zhang, Q.; Lu, X.; Li, K.; Chen, H.; Chen, J.; Yang, X.; Ma, Y.; Ma, J.; Huang, C. Nitrite-Mediated Photooxidation of Vanillin in the Atmospheric Aqueous Phase. *Environ. Sci. Technol.* **2019**, *53* (24), 14253–14263. https://doi.org/10.1021/acs.est.9b03649.

(156) Vidović, K.; Kroflič, A.; Šala, M.; Grgić, I. Aqueous-Phase Brown Carbon Formation from Aromatic Precursors under Sunlight Conditions. *Atmosphere* **2020**, *11* (2), 131. https://doi.org/10.3390/atmos11020131.

(157) Kroflič, A.; Huš, M.; Grilc, M.; Grgić, I. Underappreciated and Complex Role of Nitrous Acid in Aromatic Nitration under Mild Environmental Conditions: The Case of Activated Methoxyphenols. *Environ. Sci. Technol.* **2018**, *52* (23), 13756–13765. https://doi.org/10.1021/acs.est.8b01903.

(158) Vidović, K.; Lašič Jurković, D.; Šala, M.; Kroflič, A.; Grgić, I. Nighttime Aqueous-Phase Formation of Nitrocatechols in the Atmospheric Condensed Phase. *Environ. Sci. Technol.* **2018**, *52* (17), 9722–9730. https://doi.org/10.1021/acs.est.8b01161.

(159) Wong, J. P. S.; Nenes, A.; Weber, R. J. Changes in Light Absorptivity of Molecular Weight Separated Brown Carbon Due to Photolytic Aging. *Environ. Sci. Technol.* **2017**, *51* (15), 8414–8421. https://doi.org/10.1021/acs.est.7b01739.

(160) Zhao, R.; Lee, A. K. Y.; Huang, L.; Li, X.; Yang, F.; Abbatt, J. P. D. Photochemical Processing of Aqueous Atmospheric Brown Carbon. *Atmospheric Chem. Phys.* **2015**, *15* (11), 6087–6100. https://doi.org/10.5194/acp-15-6087-2015.

(161) Hems, R. F.; Abbatt, J. P. D. Aqueous Phase Photo-Oxidation of Brown Carbon Nitrophenols: Reaction Kinetics, Mechanism, and Evolution of Light Absorption. *ACS Earth Space Chem.* **2018**, *2* (3), 225–234. https://doi.org/10.1021/acsearthspacechem.7b00123.

(162) Fan, X.; Yu, X.; Wang, Y.; Xiao, X.; Li, F.; Xie, Y.; Wei, S.; Song, J.; Peng, P. The Aging Behaviors of Chromophoric Biomass Burning Brown Carbon during Dark Aqueous Hydroxyl Radical Oxidation Processes in Laboratory Studies. *Atmos. Environ.* **2019**, *205*, 9–18. https://doi.org/10.1016/j.atmosenv.2019.02.039.

(163) Hems, R. F.; Schnitzler, E. G.; Bastawrous, M.; Soong, R.; Simpson, A. J.; Abbatt, J. P. D. Aqueous Photoreactions of Wood Smoke Brown Carbon. *ACS Earth Space Chem.* **2020**, *4* (7), 1149–1160. https://doi.org/10.1021/acsearthspacechem.0c00117.

(164) Fleming, L. T.; Lin, P.; Roberts, J. M.; Selimovic, V.; Yokelson, R.; Laskin, J.; Laskin, A.; Nizkorodov, S. A. Molecular Composition and Photochemical Lifetimes of Brown Carbon Chromophores in Biomass Burning Organic Aerosol. *Atmospheric Chem. Phys.* **2020**, *20* (2), 1105–1129. https://doi.org/10.5194/acp-20-1105-2020.

(165) Magalhães, A. C. O.; Esteves da Silva, J. C. G.; Pinto da Silva, L. Density Functional Theory Calculation of the Absorption Properties of Brown Carbon Chromophores Generated by Catechol Heterogeneous Ozonolysis. *ACS Earth Space Chem.* **2017**, *1* (6), 353–360. https://doi.org/10.1021/acsearthspacechem.7b00061.

(166) Lavi, A.; Lin, P.; Bhaduri, B.; Carmieli, R.; Laskin, A.; Rudich, Y. Characterization of Light-Absorbing Oligomers from Reactions of Phenolic Compounds and Fe(III). *ACS Earth Space Chem.* **2017**, *1* (10), 637–646. https://doi.org/10.1021/acsearthspacechem.7b00099.

(167) Al Nimer, A.; Rocha, L.; Rahman, M. A.; Nizkorodov, S. A.; Al-Abadleh, H. A. Effect of Oxalate and Sulfate on Iron-Catalyzed Secondary Brown Carbon Formation. *Environ. Sci. Technol.* **2019**, *53* (12), 6708–6717. https://doi.org/10.1021/acs.est.9b00237.

(168) Rahman, M. A.; Al-Abadleh, H. A. Surface Water Structure and Hygroscopic Properties of Light Absorbing Secondary Organic Polymers of Atmospheric Relevance. *ACS Omega* **2018**, *3* (11), 15519–15529. https://doi.org/10.1021/acsomega.8b02066.

(169) Tran, A.; Williams, G.; Younus, S.; Ali, N. N.; Blair, S. L.; Nizkorodov, S. A.; Al-Abadleh, H. A. Efficient Formation of Light-Absorbing Polymeric Nanoparticles from the Reaction of Soluble Fe(III) with C4 and C6 Dicarboxylic Acids. *Environ. Sci. Technol.* **2017**, *51* (17), 9700–9708. https://doi.org/10.1021/acs.est.7b01826.

(170) Chen, H.; Laskin, A.; Baltrusaitis, J.; Gorski, C. A.; Scherer, M. M.; Grassian, V. H. Coal Fly Ash as a Source of Iron in Atmospheric Dust. *Environ. Sci. Technol.* **2012**, *46* (4), 2112–2120. https://doi.org/10.1021/es204102f.

(171) Xu, J.; Cui, T.; Fowler, B.; Fankhauser, A.; Yang, K.; Surratt, J. D.; McNeill, V. F. Aerosol Brown Carbon from Dark Reactions of Syringol in Aqueous Aerosol Mimics. *ACS Earth Space Chem.* **2018**, *2* (6), 608–617. https://doi.org/10.1021/acsearthspacechem.8b00010.

(172) Bones, D. L.; Henricksen, D. K.; Mang, S. A.; Gonsior, M.; Bateman, A. P.; Nguyen, T. B.; Cooper, W. J.; Nizkorodov, S. A. Appearance of Strong Absorbers and Fluorophores in Limonene-O3 Secondary Organic Aerosol Due to NH4+-Mediated Chemical Aging over Long Time Scales. *J. Geophys. Res. Atmospheres* **2010**, *115* (D5). https://doi.org/10.1029/2009JD012864.

(173) Nguyen, T. B.; Laskin, A.; Laskin, J.; Nizkorodov, S. A. Brown Carbon Formation from Ketoaldehydes of Biogenic Monoterpenes. *Faraday Discuss.* **2013**, *165* (0), 473–494. https://doi.org/10.1039/C3FD00036B.

(174) Laskin, J.; Laskin, A.; Nizkorodov, S. A.; Roach, P.; Eckert, P.; Gilles, M. K.; Wang, B.; Lee, H. J. (Julie); Hu, Q. Molecular Selectivity of Brown Carbon Chromophores. *Environ. Sci. Technol.* **2014**, *48* (20), 12047–12055. https://doi.org/10.1021/es503432r.

(175) Lee, H. J. (Julie); Laskin, A.; Laskin, J.; Nizkorodov, S. A. Excitation–Emission Spectra and Fluorescence Quantum Yields for Fresh and Aged Biogenic Secondary Organic Aerosols. *Environ. Sci. Technol.* **2013**, *47* (11), 5763–5770. https://doi.org/10.1021/es400644c.

(176) Shapiro, E. L.; Szprengiel, J.; Sareen, N.; Jen, C. N.; Giordano, M. R.; McNeill, V. F. Light-Absorbing Secondary Organic Material Formed by Glyoxal in Aqueous Aerosol Mimics. *Atmospheric Chem. Phys.* **2009**, *9* (7), 2289–2300. https://doi.org/10.5194/acp-9-2289-2009.

(177) Powelson, M. H.; Espelien, B. M.; Hawkins, L. N.; Galloway, M. M.; De Haan, D. O. Brown Carbon Formation by Aqueous-Phase Carbonyl Compound Reactions with Amines and Ammonium Sulfate. *Environ. Sci. Technol.* **2014**, *48* (2), 985–993. https://doi.org/10.1021/es4038325.

(178) Sareen, N.; Schwier, A. N.; Shapiro, E. L.; Mitroo, D.; McNeill, V. F. Secondary Organic Material Formed by Methylglyoxal in Aqueous Aerosol Mimics. *Atmospheric Chem. Phys.* **2010**, *10* (3), 997–1016. https://doi.org/10.5194/acp-10-997-2010.

(179) Yu, G.; Bayer, A. R.; Galloway, M. M.; Korshavn, K. J.; Fry, C. G.; Keutsch, F. N. Glyoxal in Aqueous Ammonium Sulfate Solutions: Products, Kinetics and Hydration Effects. *Environ. Sci. Technol.* **2011**, *45* (15), 6336–6342. https://doi.org/10.1021/es200989n.

(180) Kampf, C. J.; Jakob, R.; Hoffmann, T. Identification and Characterization of Aging Products in the Glyoxal/Ammonium Sulfate System - Implications for Light-Absorbing Material in Atmospheric Aerosols. *Atmospheric Chem. Phys.* **2012**, *12* (14), 6323.

(181) Drozd, G. T.; McNeill, V. F. Organic Matrix Effects on the Formation of Light-Absorbing Compounds from α-Dicarbonyls in Aqueous Salt Solution. *Environ. Sci. Process. Impacts* **2014**, *16* (4), 741–747. https://doi.org/10.1039/C3EM00579H.

(182) Kampf, C. J.; Filippi, A.; Zuth, C.; Hoffmann, T.; Opatz, T. Secondary Brown Carbon Formation via the Dicarbonyl Imine Pathway: Nitrogen Heterocycle Formation and Synergistic Effects. *Phys. Chem. Chem. Phys.* **2016**, *18* (27), 18353–18364. https://doi.org/10.1039/C6CP03029G.

(183) Nozière, B.; Dziedzic, P.; Córdova, A. Products and Kinetics of the Liquid-Phase Reaction of Glyoxal Catalyzed by Ammonium Ions (NH4+). *J. Phys. Chem. A* **2009**, *113* (1), 231–237. https://doi.org/10.1021/jp8078293.

(184) Galloway, M. M.; Chhabra, P. S.; Chan, A. W. H.; Surratt, J. D.; Flagan, R. C.; Seinfeld, J. H.; Keutsch, F. N. Glyoxal Uptake on Ammonium Sulphate Seed Aerosol: Reaction Products and Reversibility of Uptake under Dark and Irradiated Conditions. *Atmospheric Chem. Phys.* **2009**, *9* (10), 3331–3345. https://doi.org/10.5194/acp-9-3331-2009.

(185) Hawkins, L. N.; Welsh, H. G.; Alexander, M. V. Evidence for Pyrazine-Based Chromophores in Cloud Water Mimics Containing Methylglyoxal and Ammonium Sulfate. *Atmospheric Chem. Phys.* **2018**, *18* (16), 12413–12431. https://doi.org/10.5194/acp-18-12413-2018.

(186) Stangl, C. M.; Johnston, M. V. Aqueous Reaction of Dicarbonyls with Ammonia as a Potential Source of Organic Nitrogen in Airborne Nanoparticles. *J. Phys. Chem. A* **2017**, *121* (19), 3720–3727. https://doi.org/10.1021/acs.jpca.7b02464.

(187) Marrero-Ortiz, W.; Hu, M.; Du, Z.; Ji, Y.; Wang, Y.; Guo, S.; Lin, Y.; Gomez-Hermandez, M.; Peng, J.; Li, Y.; Secrest, J.; Zamora, M. L.; Wang, Y.; An, T.; Zhang, R. Formation and Optical Properties of Brown Carbon from Small α-Dicarbonyls and Amines. *Environ. Sci. Technol.* **2019**, *53* (1), 117–126. https://doi.org/10.1021/acs.est.8b03995.

(188) Gao, Y.; Zhang, Y. Formation and Photochemical Investigation of Brown Carbon by Hydroxyacetone Reactions with Glycine and Ammonium Sulfate. *RSC Adv.* **2018**, *8* (37), 20719–20725. https://doi.org/10.1039/C8RA02019A.

(189) Maxut, A.; Nozière, B.; Fenet, B.; Mechakra, H. Formation Mechanisms and Yields of Small Imidazoles from Reactions of Glyoxal with NH4+ in Water at Neutral PH. *Phys. Chem. Chem. Phys.* **2015**, *17* (31), 20416–20424. https://doi.org/10.1039/C5CP03113C.

(190) Hawkins, L. N.; Lemire, A. N.; Galloway, M. M.; Corrigan, A. L.; Turley, J. J.; Espelien, B. M.; De Haan, D. O. Maillard Chemistry in Clouds and Aqueous Aerosol As a Source of Atmospheric Humic-Like Substances. *Environ. Sci. Technol.* **2016**, *50* (14), 7443–7452. https://doi.org/10.1021/acs.est.6b00909.

(191) Haan, D. O. D.; Corrigan, A. L.; Smith, K. W.; Stroik, D. R.; Turley, J. J.; Lee, F. E.; Tolbert, M. A.; Jimenez, J. L.; Cordova, K. E.; Ferrell, G. R. Secondary Organic Aerosol-Forming Reactions of Glyoxal with Amino Acids. *Environ. Sci. Technol.* **2009**, *43* (8), 2818–2824. https://doi.org/10.1021/es803534f.

(192) Gao, Y.; Zhang, Y. Optical Properties Investigation of the Reactions between Methylglyoxal and Glycine/Ammonium Sulfate. *Spectrochim. Acta. A. Mol. Biomol. Spectrosc.* **2019**, *215*, 112–121. https://doi.org/10.1016/j.saa.2019.02.087.

(193) Gao, Y.; Zhang, Y. Formation and Photochemical Properties of Aqueous Brown Carbon through Glyoxal Reactions with Glycine. *RSC Adv.* **2018**, *8* (67), 38566–38573. https://doi.org/10.1039/C8RA06913A.

(194) Harrison, A. W.; Waterson, A. M.; De Bruyn, W. J. Spectroscopic and Photochemical Properties of Secondary Brown Carbon from Aqueous Reactions of Methylglyoxal. *ACS Earth Space Chem.* **2020**. https://doi.org/10.1021/acsearthspacechem.0c00061.

(195) Grace, D. N.; Lugos, E. N.; Ma, S.; Griffith, D. R.; Hendrickson, H. P.; Woo, J. L.; Galloway, M. M. Brown Carbon Formation Potential of the Biacetyl–Ammonium Sulfate Reaction System. *ACS Earth Space Chem.* **2020**, *4* (7), 1104–1113. https://doi.org/10.1021/acsearthspacechem.0c00096.

(196) Grace, D. N.; Sharp, J. R.; Holappa, R. E.; Lugos, E. N.; Sebold, M. B.; Griffith, D. R.; Hendrickson, H. P.; Galloway, M. M. Heterocyclic Product Formation in Aqueous Brown Carbon Systems. *ACS Earth Space Chem.* **2019**, *3* (11), 2472–2481. https://doi.org/10.1021/acsearthspacechem.9b00235.

(197) Lee, A. K. Y.; Zhao, R.; Li, R.; Liggio, J.; Li, S.-M.; Abbatt, Jonathan. P. D. Formation of Light Absorbing Organo-Nitrogen Species from Evaporation of Droplets Containing Glyoxal and Ammonium Sulfate. *Environ. Sci. Technol.* **2013**, *47* (22), 12819–12826. https://doi.org/10.1021/es402687w.

(198) De Haan, D. O.; Hawkins, L. N.; Kononenko, J. A.; Turley, J. J.; Corrigan, A. L.; Tolbert, M. A.; Jimenez, J. L. Formation of Nitrogen-Containing Oligomers by Methylglyoxal and Amines in Simulated Evaporating Cloud Droplets. *Environ. Sci. Technol.* **2011**, *45* (3), 984–991. https://doi.org/10.1021/es102933x.

(199) Nguyen, T. B.; Lee, P. B.; Updyke, K. M.; Bones, D. L.; Laskin, J.; Laskin, A.; Nizkorodov, S. A. Formation of Nitrogen- and Sulfur-Containing Light-Absorbing Compounds Accelerated by Evaporation of Water from Secondary Organic Aerosols. *J. Geophys. Res. Atmospheres* **2012**, *117* (D1). https://doi.org/10.1029/2011JD016944.

(200) De Haan, D. O.; Hawkins, L. N.; Welsh, H. G.; Pednekar, R.; Casar, J. R.; Pennington, E. A.; de Loera, A.; Jimenez, N. G.; Symons, M. A.; Zauscher, M.; Pajunoja, A.; Caponi, L.; Cazaunau, M.; Formenti, P.; Gratien, A.; Pangui, E.; Doussin, J.-F. Brown Carbon Production in Ammonium- or Amine-Containing Aerosol Particles by Reactive Uptake of Methylglyoxal and Photolytic Cloud Cycling. *Environ. Sci. Technol.* **2017**, *51* (13), 7458–7466. https://doi.org/10.1021/acs.est.7b00159.

(201) Ackendorf, J. M.; Ippolito, M. G.; Galloway, M. M. PH Dependence of the Imidazole-2-Carboxaldehyde Hydration Equilibrium: Implications for Atmospheric Light Absorbance. *Environ. Sci. Technol. Lett.* **2017**, *4* (12), 551–555. https://doi.org/10.1021/acs.estlett.7b00486.

(202) Sareen, N.; Moussa, S. G.; McNeill, V. F. Photochemical Aging of Light-Absorbing Secondary Organic Aerosol Material. *J. Phys. Chem. A* **2013**, *117* (14), 2987–2996. https://doi.org/10.1021/jp309413j.

(203) Felber, T.; Schaefer, T.; Herrmann, H. OH-Initiated Oxidation of Imidazoles in Tropospheric Aqueous-Phase Chemistry. *J. Phys. Chem. A* **2019**, *123* (8), 1505–1513. https://doi.org/10.1021/acs.jpca.8b11636.

(204) Beier, T.; Cotter, E. R.; Galloway, M. M.; Woo, J. L. *In Situ* Surface Tension Measurements of Hanging Droplet Methylglyoxal/Ammonium Sulfate Aerosol Mimics under Photooxidative Conditions. *ACS Earth Space Chem.* **2019**, acsearthspacechem.9b00123. https://doi.org/10.1021/acsearthspacechem.9b00123.

(205) You, B.; Li, S.; Tsona, N. T.; Li, J.; Xu, L.; Yang, Z.; Cheng, S.; Chen, Q.; George, C.; Ge, M.; Du, L. Environmental Processing of Short-Chain Fatty Alcohols Induced by Photosensitized Chemistry of Brown Carbons. *ACS Earth Space Chem.* **2020**, *4* (4), 631–640. https://doi.org/10.1021/acsearthspacechem.0c00023.

(206) Aiona, P. K.; Lee, H. J.; Leslie, R.; Lin, P.; Laskin, A.; Laskin, J.; Nizkorodov, S. A. Photochemistry of Products of the Aqueous Reaction of Methylglyoxal with Ammonium Sulfate. *ACS Earth Space Chem.* **2017**, *1* (8), 522–532. https://doi.org/10.1021/acsearthspacechem.7b00075.

(207) De Haan, D. O.; Pajunoja, A.; Hawkins, L. N.; Welsh, H. G.; Jimenez, N. G.; De Loera, A.; Zauscher, M.; Andretta, A. D.; Joyce, B. W.; De Haan, A. C.; Riva, M.; Cui, T.; Surratt, J. D.; Cazaunau, M.; Formenti, P.; Gratien, A.; Pangui, E.; Doussin, J.-F. Methylamine's Effects on Methylglyoxal-Containing Aerosol: Chemical, Physical, and Optical Changes. *ACS Earth Space Chem.* **2019**, *3* (9), 1706–1716. https://doi.org/10.1021/acsearthspacechem.9b00103.

(208) Kasthuriarachchi, N. Y.; Rivellini, L.-H.; Chen, X.; Li, Y. J.; Lee, A. K. Y. Effect of Relative Humidity on Secondary Brown Carbon Formation in Aqueous Droplets. *Environ. Sci. Technol.* **2020**. https://doi.org/10.1021/acs.est.0c01239.

(209) Fleming, L. T.; Ali, N. N.; Blair, S. L.; Roveretto, M.; George, C.; Nizkorodov, S. A. Formation of Light-Absorbing Organosulfates during Evaporation of Secondary Organic Material Extracts in the Presence of Sulfuric Acid. *ACS Earth Space Chem.* **2019**, *3* (6), 947–957. https://doi.org/10.1021/acsearthspacechem.9b00036.

(210) De Haan, D. O.; Jansen, K.; Rynaski, A. D.; Sueme, W. R. P.; Torkelson, A. K.; Czer, E. T.; Kim, A. K.; Rafla, M. A.; De Haan, A. C.; Tolbert, M. A. Brown Carbon Production by Aqueous-Phase Interactions of Glyoxal and SO2. *Environ. Sci. Technol.* **2020**, *54* (8), 4781–4789. https://doi.org/10.1021/acs.est.9b07852.

(211) Pratap, V.; Battaglia, M. A.; Carlton, A. G.; Hennigan, C. J. No Evidence for Brown Carbon Formation in Ambient Particles Undergoing Atmospherically Relevant Drying. *Environ. Sci. Process. Impacts* **2020**, *22* (2), 442–450. https://doi.org/10.1039/C9EM00457B.

(212) Hinks, M. L.; Brady, M. V.; Lignell, H.; Song, M.; Grayson, J. W.; Bertram, A. K.; Lin, P.; Laskin, A.; Laskin, J.; Nizkorodov, S. A. Effect of Viscosity on Photodegradation Rates in Complex Secondary Organic Aerosol Materials. *Phys. Chem. Chem. Phys.* **2016**, *18* (13), 8785–8793. https://doi.org/10.1039/C5CP05226B.

(213) M. Bell, D.; Imre, D.; Martin, S. T.; Zelenyuk, A. The Properties and Behavior of α-Pinene Secondary Organic Aerosol Particles Exposed to Ammonia under Dry Conditions. *Phys. Chem. Chem. Phys.* **2017**, *19* (9), 6497–6507. https://doi.org/10.1039/C6CP08839B.

(214) Li, C.; He, Q.; Schade, J.; Passig, J.; Zimmermann, R.; Meidan, D.; Laskin, A.; Rudich, Y. Dynamic Changes in Optical and Chemical Properties of Tar Ball Aerosols by Atmospheric Photochemical Aging. *Atmospheric Chem. Phys.* **2019**, *19* (1), 139–163. https://doi.org/10.5194/acp-19-139-2019.

(215) Fankhauser, A. M.; Bourque, M.; Almazan, J.; Marin, D.; Fernandez, L.; Hutheesing, R.; Ferdousi, N.; Tsui, W. G.; McNeill, V. F. Impact of Environmental Conditions on Secondary Organic Aerosol Production from Photosensitized Humic Acid. *Environ. Sci. Technol.* **2020**, *54* (9), 5385–5390. https://doi.org/10.1021/acs.est.9b07485.

(216) Liu, Y.; Liggio, J.; Staebler, R.; Li, S.-M. Reactive Uptake of Ammonia to Secondary Organic Aerosols: Kinetics of Organonitrogen Formation. *Atmospheric Chem. Phys.* **2015**, *15* (23), 13569–13584. https://doi.org/10.5194/acp-15-13569-2015.

(217) Gen, M.; Huang, D. D.; Chan, C. K. Reactive Uptake of Glyoxal by Ammonium-Containing Salt Particles as a Function of Relative Humidity. *Environ. Sci. Technol.* **2018**, *52* (12), 6903–6911. https://doi.org/10.1021/acs.est.8b00606.

(218) Mabato, B. R. G.; Gen, M.; Chu, Y.; Chan, C. K. Reactive Uptake of Glyoxal by Methylaminium-Containing Salts as a Function of Relative Humidity. *ACS Earth Space Chem.* **2019**, *3* (2), 150–157. https://doi.org/10.1021/acsearthspacechem.8b00154.

(219) Pillar, E. A.; Camm, R. C.; Guzman, M. I. Catechol Oxidation by Ozone and Hydroxyl Radicals at the Air–Water Interface. *Environ. Sci. Technol.* **2014**, *48* (24), 14352–14360. https://doi.org/10.1021/es504094x.

(220) Schnitzler, E. G.; Liu, T.; Hems, R. F.; Abbatt, J. P. D. Heterogeneous OH Oxidation of Primary Brown Carbon Aerosol: Effects of Relative Humidity and Volatility. *Environ. Sci. Process. Impacts* **2020**, *22* (11), 2162–2171. https://doi.org/10.1039/D0EM00311E.

(221) Reid, J. P.; Bertram, A. K.; Topping, D. O.; Laskin, A.; Martin, S. T.; Petters, M. D.; Pope, F. D.; Rovelli, G. The Viscosity of Atmospherically Relevant Organic Particles. *Nat. Commun.* **2018**, *9* (1), 956. https://doi.org/10.1038/s41467-018-03027-z.

(222) Song, M.; Liu, P. F.; Hanna, S. J.; Li, Y. J.; Martin, S. T.; Bertram, A. K. Relative Humidity-Dependent Viscosities of Isoprene-Derived Secondary Organic Material and Atmospheric Implications for Isoprene-Dominant Forests. *Atmospheric Chem. Phys.* **2015**, *15* (9), 5145–5159. https://doi.org/10.5194/acp-15-5145-2015.

(223) Renbaum-Wolff, L.; Grayson, J. W.; Bateman, A. P.; Kuwata, M.; Sellier, M.; Murray, B. J.; Shilling, J. E.; Martin, S. T.; Bertram, A. K. Viscosity of α-Pinene Secondary Organic Material and Implications for Particle Growth and Reactivity. *Proc. Natl. Acad. Sci.* **2013**, *110* (20), 8014–8019. https://doi.org/10.1073/pnas.1219548110.

(224) Song, M.; Liu, P. F.; Hanna, S. J.; Zaveri, R. A.; Potter, K.; You, Y.; Martin, S. T.; Bertram, A. K. Relative Humidity-Dependent Viscosity of Secondary Organic Material from Toluene Photo-Oxidation and Possible Implications for Organic Particulate Matter over Megacities. *Atmospheric Chem. Phys.* **2016**, *16* (14), 8817–8830. https://doi.org/10.5194/acp-16-8817-2016.

(225) Zhou, S.; Shiraiwa, M.; McWhinney, R. D.; Pöschl, U.; Abbatt, J. P. D. Kinetic Limitations in Gas-Particle Reactions Arising from Slow Diffusion in Secondary Organic Aerosol. *Faraday Discuss.* **2013**, *165* (0), 391–406. https://doi.org/10.1039/C3FD00030C.

(226) Zhou, S.; Lee, A. K. Y.; McWhinney, R. D.; Abbatt, J. P. D. Burial Effects of Organic Coatings on the Heterogeneous Reactivity of Particle-Borne Benzo[a]Pyrene (BaP) toward Ozone. *J. Phys. Chem. A* **2012**, *116* (26), 7050–7056. https://doi.org/10.1021/jp3030705.

(227) Chen, C.; Enekwizu, O. Y.; Ma, X.; Jiang, Y.; Khalizov, A. F.; Zheng, J.; Ma, Y. Effect of Organic Coatings Derived from the OH-Initiated Oxidation of Amines on Soot Morphology and Cloud Activation. *Atmospheric Res.* **2020**, *239*, 104905. https://doi.org/10.1016/j.atmosres.2020.104905.

(228) Pagels, J.; Khalizov, A. F.; McMurry, P. H.; Zhang, R. Y. Processing of Soot by Controlled Sulphuric Acid and Water Condensation—Mass and Mobility Relationship. *Aerosol Sci. Technol.* **2009**, *43* (7), 629–640. https://doi.org/10.1080/02786820902810685.

(229) Zhang, R.; Khalizov, A. F.; Pagels, J.; Zhang, D.; Xue, H.; McMurry, P. H. Variability in Morphology, Hygroscopicity, and Optical Properties of Soot Aerosols during Atmospheric Processing. *Proc. Natl. Acad. Sci.* **2008**, *105* (30), 10291–10296. https://doi.org/10.1073/pnas.0804860105.

(230) Khalizov, A. F.; Xue, H.; Wang, L.; Zheng, J.; Zhang, R. Enhanced Light Absorption and Scattering by Carbon Soot Aerosol Internally Mixed with Sulfuric Acid. *J. Phys. Chem. A* **2009**, *113* (6), 1066–1074. https://doi.org/10.1021/jp807531n.

(231) Moosmüller, H.; Chakrabarty, R. K.; Arnott, W. P. Aerosol Light Absorption and Its Measurement: A Review. *J. Quant. Spectrosc. Radiat. Transf.* **2009**, *110* (11), 844–878. https://doi.org/10.1016/j.jqsrt.2009.02.035.

(232) Sumlin, B. J.; Heinson, W. R.; Chakrabarty, R. K. Retrieving the Aerosol Complex Refractive Index Using PyMieScatt: A Mie Computational Package with Visualization

Capabilities. *J. Quant. Spectrosc. Radiat. Transf.* **2018**, *205*, 127–134.
https://doi.org/10.1016/j.jqsrt.2017.10.012.

(233) Zhang, X.; Lin, Y.-H.; Surratt, J. D.; Weber, R. J. Sources, Composition and Absorption
Ångström Exponent of Light-Absorbing Organic Components in Aerosol Extracts from
the Los Angeles Basin. *Environ. Sci. Technol.* **2013**, *47* (8), 3685–3693.
https://doi.org/10.1021/es305047b.

(234) Li, C.; He, Q.; Hettiyadura, A. P. S.; Käfer, U.; Shmul, G.; Meidan, D.; Zimmermann, R.;
Brown, S. S.; George, C.; Laskin, A.; Rudich, Y. Formation of Secondary Brown Carbon
in Biomass Burning Aerosol Proxies through NO3 Radical Reactions. *Environ. Sci.
Technol.* **2020**, *54* (3), 1395–1405. https://doi.org/10.1021/acs.est.9b05641.

(235) Laskin, A.; Laskin, J.; Nizkorodov, S. A. Chemistry of Atmospheric Brown Carbon.
*Chem. Rev.* **2015**, *115* (10), 4335–4382. https://doi.org/10.1021/cr5006167.

(236) Chen, Y.; Bond, T. C. Light Absorption by Organic Carbon from Wood Combustion.
*Atmospheric Chem. Phys.* **2010**, *10* (4), 1773–1787. https://doi.org/10.5194/acp-10-1773-
2010.

(237) Cremer, J. W.; Thaler, K. M.; Haisch, C.; Signorell, R. Photoacoustics of Single Laser-
Trapped Nanodroplets for the Direct Observation of Nanofocusing in Aerosol
Photokinetics. *Nat. Commun.* **2016**, *7*, 10941. https://doi.org/10.1038/ncomms10941.

(238) Arangio, A. M.; Slade, J. H.; Berkemeier, T.; Pöschl, U.; Knopf, D. A.; Shiraiwa, M.
Multiphase Chemical Kinetics of OH Radical Uptake by Molecular Organic Markers of
Biomass Burning Aerosols: Humidity and Temperature Dependence, Surface Reaction,
and Bulk Diffusion. *J. Phys. Chem. A* **2015**, *119* (19), 4533–4544.
https://doi.org/10.1021/jp510489z.

(239) Slade, J. H.; Knopf, D. A. Heterogeneous OH Oxidation of Biomass Burning Organic
Aerosol Surrogate Compounds: Assessment of Volatilisation Products and the Role of OH
Concentration on the Reactive Uptake Kinetics. *Phys. Chem. Chem. Phys.* **2013**, *15* (16),
5898–5915. https://doi.org/10.1039/C3CP44695F.

(240) Liu, P.; Li, Y. J.; Wang, Y.; Bateman, A. P.; Zhang, Y.; Gong, Z.; Bertram, A. K.; Martin,
S. T. Highly Viscous States Affect the Browning of Atmospheric Organic Particulate
Matter. *ACS Cent. Sci.* **2018**, *4* (2), 207–215. https://doi.org/10.1021/acscentsci.7b00452.

(241) Wang, Y.; Liu, P.; Li, Y. J.; Bateman, A. P.; Martin, S. T.; Hung, H.-M. The Reactivity of
Toluene-Derived Secondary Organic Material with Ammonia and the Influence of Water
Vapor. *J. Phys. Chem. A* **2018**, *122* (38), 7739–7747.
https://doi.org/10.1021/acs.jpca.8b06685.

(242) Ullmann, D. A.; Hinks, M. L.; Maclean, A. M.; Butenhoff, C. L.; Grayson, J. W.;
Barsanti, K.; Jimenez, J. L.; Nizkorodov, S. A.; Kamal, S.; Bertram, A. K. Viscosities,
Diffusion Coefficients, and Mixing Times of Intrinsic Fluorescent Organic Molecules in
Brown Limonene Secondary Organic Aerosol and Tests of the Stokes–Einstein Equation.

*Atmospheric Chem. Phys.* **2019**, *19* (3), 1491–1503. https://doi.org/10.5194/acp-19-1491-2019.

(243) DeRieux, W.-S. W.; Li, Y.; Lin, P.; Laskin, J.; Laskin, A.; Bertram, A. K.; Nizkorodov, S. A.; Shiraiwa, M. Predicting the Glass Transition Temperature and Viscosity of Secondary Organic Material Using Molecular Composition. *Atmospheric Chem. Phys.* **2018**, *18* (9), 6331–6351. https://doi.org/10.5194/acp-18-6331-2018.

(244) Henry, K. M.; Donahue, N. M. Photochemical Aging of α-Pinene Secondary Organic Aerosol: Effects of OH Radical Sources and Photolysis. *J. Phys. Chem. A* **2012**, *116* (24), 5932–5940. https://doi.org/10.1021/jp210288s.

(245) Wong, J. P. S.; Zhou, S.; Abbatt, J. P. D. Changes in Secondary Organic Aerosol Composition and Mass Due to Photolysis: Relative Humidity Dependence. *J. Phys. Chem. A* **2015**, *119* (19), 4309–4316. https://doi.org/10.1021/jp506898c.

(246) Mang, S. A.; Henricksen, D. K.; Bateman, A. P.; Andersen, M. P. S.; Blake, D. R.; Nizkorodov, S. A. Contribution of Carbonyl Photochemistry to Aging of Atmospheric Secondary Organic Aerosol. *J. Phys. Chem. A* **2008**, *112* (36), 8337–8344. https://doi.org/10.1021/jp804376c.

(247) Malecha, K. T.; Cai, Z.; Nizkorodov, S. A. Photodegradation of Secondary Organic Aerosol Material Quantified with a Quartz Crystal Microbalance. *Environ. Sci. Technol. Lett.* **2018**, *5* (6), 366–371. https://doi.org/10.1021/acs.estlett.8b00231.

(248) Baboomian, V. J.; Gu, Y.; Nizkorodov, S. A. Photodegradation of Secondary Organic Aerosols by Long-Term Exposure to Solar Actinic Radiation. *ACS Earth Space Chem.* **2020**, *4* (7), 1078–1089. https://doi.org/10.1021/acsearthspacechem.0c00088.

(249) Malecha, K. T.; Nizkorodov, S. A. Feasibility of Photosensitized Reactions with Secondary Organic Aerosol Particles in the Presence of Volatile Organic Compounds. *J. Phys. Chem. A* **2017**, *121* (26), 4961–4967. https://doi.org/10.1021/acs.jpca.7b04066.

(250) Monge, M. E.; Rosenørn, T.; Favez, O.; Müller, M.; Adler, G.; Riziq, A. A.; Rudich, Y.; Herrmann, H.; George, C.; D'Anna, B. Alternative Pathway for Atmospheric Particles Growth. *Proc. Natl. Acad. Sci.* **2012**, *109* (18), 6840–6844. https://doi.org/10.1073/pnas.1120593109.

(251) Corral Arroyo, P.; Bartels-Rausch, T.; Alpert, P. A.; Dumas, S.; Perrier, S.; George, C.; Ammann, M. Particle-Phase Photosensitized Radical Production and Aerosol Aging. *Environ. Sci. Technol.* **2018**, *52* (14), 7680–7688. https://doi.org/10.1021/acs.est.8b00329.

(252) De Haan, D. O.; Hawkins, L. N.; Welsh, H. G.; Pednekar, R.; Casar, J. R.; Pennington, E. A.; de Loera, A.; Jimenez, N. G.; Symons, M. A.; Zauscher, M.; Pajunoja, A.; Caponi, L.; Cazaunau, M.; Formenti, P.; Gratien, A.; Pangui, E.; Doussin, J.-F. Brown Carbon Production in Ammonium- or Amine-Containing Aerosol Particles by Reactive Uptake of Methylglyoxal and Photolytic Cloud Cycling. *Environ. Sci. Technol.* **2017**, *51* (13), 7458–7466. https://doi.org/10.1021/acs.est.7b00159.

(253) Zhu, S.; Horne, J. R.; Montoya-Aguilera, J.; Hinks, M. L.; Nizkorodov, S. A.; Dabdub, D. Modeling Reactive Ammonia Uptake by Secondary Organic Aerosol in CMAQ: Application to the Continental US. *Atmospheric Chem. Phys.* **2018**, *18* (5), 3641–3657. https://doi.org/10.5194/acp-18-3641-2018.

(254) Horne, J. R.; Zhu, S.; Montoya-Aguilera, J.; Hinks, M. L.; Wingen, L. M.; Nizkorodov, S. A.; Dabdub, D. Reactive Uptake of Ammonia by Secondary Organic Aerosols: Implications for Air Quality. *Atmos. Environ.* **2018**, *189*, 1–8. https://doi.org/10.1016/j.atmosenv.2018.06.021.

(255) Montoya-Aguilera, J.; Hinks, M. L.; Aiona, P. K.; Wingen, L. M.; Horne, J. R.; Zhu, S.; Dabdub, D.; Laskin, A.; Laskin, J.; Lin, P.; Nizkorodov, S. A. Reactive Uptake of Ammonia by Biogenic and Anthropogenic Organic Aerosols. In *Multiphase Environmental Chemistry in the Atmosphere*; ACS Symposium Series; American Chemical Society, 2018; Vol. 1299, pp 127–147. https://doi.org/10.1021/bk-2018-1299.ch007.

(256) Babar, Z. B.; Park, J.-H.; Lim, H.-J. Influence of NH3 on Secondary Organic Aerosols from the Ozonolysis and Photooxidation of α-Pinene in a Flow Reactor. *Atmos. Environ.* **2017**, *164*, 71–84. https://doi.org/10.1016/j.atmosenv.2017.05.034.

(257) Huang, M.; Xu, J.; Cai, S.; Liu, X.; Zhao, W.; Hu, C.; Gu, X.; Fang, L.; Zhang, W. Characterization of Brown Carbon Constituents of Benzene Secondary Organic Aerosol Aged with Ammonia. *J. Atmospheric Chem.* **2018**, *75* (2), 205–218. https://doi.org/10.1007/s10874-017-9372-x.

(258) Chu, B.; Zhang, X.; Liu, Y.; He, H.; Sun, Y.; Jiang, J.; Li, J.; Hao, J. Synergetic Formation of Secondary Inorganic and Organic Aerosol: Effect of SO2 and NH3 on Particle Formation and Growth. *Atmospheric Chem. Phys.* **2016**, *16* (22), 14219–14230. https://doi.org/10.5194/acp-16-14219-2016.

(259) Xu, J.; Huang, M.-Q.; Cai, S.-Y.; Liao, Y.-M.; Hu, C.-J.; Zhao, W.-X.; Gu, X.-J.; Zhang, W.-J. Chemical Composition and Reaction Mechanisms for Aged P-Xylene Secondary Organic Aerosol in the Presence of Ammonia. *J. Chin. Chem. Soc.* **2018**, *65* (5), 578–590. https://doi.org/10.1002/jccs.201700249.

(260) Huang, M.; Xu, J.; Cai, S.; Liu, X.; Hu, C.; Gu, X.; Zhao, W.; Fang, L.; Zhang, W. Chemical Analysis of Particulate Products of Aged 1,3,5-Trimethylbenzene Secondary Organic Aerosol in the Presence of Ammonia. *Atmospheric Pollut. Res.* **2018**, *9* (1), 146–155. https://doi.org/10.1016/j.apr.2017.08.003.

(261) Fairhurst, M. C.; Ezell, M. J.; Finlayson-Pitts, B. J. Knudsen Cell Studies of the Uptake of Gaseous Ammonia and Amines onto C3–C7 Solid Dicarboxylic Acids. *Phys. Chem. Chem. Phys.* **2017**, *19* (38), 26296–26309. https://doi.org/10.1039/C7CP05252A.

(262) Liggio, J.; Li, S.-M.; McLaren, R. Reactive Uptake of Glyoxal by Particulate Matter. *J. Geophys. Res. Atmospheres* **2005**, *110* (D10). https://doi.org/10.1029/2004JD005113.

(263) Trainic, M.; Abo Riziq, A.; Lavi, A.; Flores, J. M.; Rudich, Y. The Optical, Physical and Chemical Properties of the Products of Glyoxal Uptake on Ammonium Sulfate Seed Aerosols. *Atmospheric Chem. Phys.* **2011**, *11* (18), 9697–9707. https://doi.org/10.5194/acp-11-9697-2011.

(264) Li, Z.; Nizkorodov, S. A.; Chen, H.; Lu, X.; Yang, X.; Chen, J. Nitrogen-Containing Secondary Organic Aerosol Formation by Acrolein Reaction with Ammonia/Ammonium. *Atmospheric Chem. Phys.* **2019**, *19* (2), 1343–1356. https://doi.org/10.5194/acp-19-1343-2019.

(265) Abbatt, J. P. D.; Lee, A. K. Y.; Thornton, J. A. Quantifying Trace Gas Uptake to Tropospheric Aerosol: Recent Advances and Remaining Challenges. *Chem. Soc. Rev.* **2012**, *41* (19), 6555–6581. https://doi.org/10.1039/C2CS35052A.

(266) Pillar, E. A.; Zhou, R.; Guzman, M. I. Heterogeneous Oxidation of Catechol. *J. Phys. Chem. A* **2015**, *119* (41), 10349–10359. https://doi.org/10.1021/acs.jpca.5b07914.

(267) Pillar, E. A.; Guzman, M. I. Oxidation of Substituted Catechols at the Air–Water Interface: Production of Carboxylic Acids, Quinones, and Polyphenols. *Environ. Sci. Technol.* **2017**, *51* (9), 4951–4959. https://doi.org/10.1021/acs.est.7b00232.

(268) Ge, Y.; Liu, Y.; Chu, B.; He, H.; Chen, T.; Wang, S.; Wei, W.; Cheng, S. Ozonolysis of Trimethylamine Exchanged with Typical Ammonium Salts in the Particle Phase. *Environ. Sci. Technol.* **2016**, *50* (20), 11076–11084. https://doi.org/10.1021/acs.est.6b04375.

(269) Magalhães, A. C. O.; Esteves da Silva, J. C. G.; Pinto da Silva, L. Density Functional Theory Calculation of the Absorption Properties of Brown Carbon Chromophores Generated by Catechol Heterogeneous Ozonolysis. *ACS Earth Space Chem.* **2017**, *1* (6), 353–360. https://doi.org/10.1021/acsearthspacechem.7b00061.

(270) Rahman, M. A.; Al-Abadleh, H. A. Surface Water Structure and Hygroscopic Properties of Light Absorbing Secondary Organic Polymers of Atmospheric Relevance. *ACS Omega* **2018**, *3* (11), 15519–15529. https://doi.org/10.1021/acsomega.8b02066.

(271) Sumlin, B. J.; Pandey, A.; Walker, M. J.; Pattison, R. S.; Williams, B. J.; Chakrabarty, R. K. Atmospheric Photooxidation Diminishes Light Absorption by Primary Brown Carbon Aerosol from Biomass Burning. *Environ. Sci. Technol. Lett.* **2017**, *4* (12), 540–545. https://doi.org/10.1021/acs.estlett.7b00393.

(272) Sengupta, D.; Samburova, V.; Bhattarai, C.; Kirillova, E.; Mazzoleni, L.; Iaukea-Lum, M.; Watts, A.; Moosmüller, H.; Khlystov, A. Light Absorption by Polar and Non-Polar Aerosol Compounds from Laboratory Biomass Combustion. *Atmospheric Chem. Phys.* **2018**, *18* (15), 10849–10867. https://doi.org/10.5194/acp-18-10849-2018.

(273) Browne, E. C.; Zhang, X.; Franklin, J. P.; Ridley, K. J.; Kirchstetter, T. W.; Wilson, K. R.; Cappa, C. D.; Kroll, J. H. Effect of Heterogeneous Oxidative Aging on Light Absorption by Biomass Burning Organic Aerosol. *Aerosol Sci. Technol.* **2019**, *53* (6), 663–674. https://doi.org/10.1080/02786826.2019.1599321.

(274) Kuang, Y.; Shang, J. Changes in Light Absorption by Brown Carbon in Soot Particles Due to Heterogeneous Ozone Aging in a Smog Chamber. *Environ. Pollut.* **2020**, *266*, 115273. https://doi.org/10.1016/j.envpol.2020.115273.

(275) George, I. J.; Abbatt, J. P. D. Heterogeneous Oxidation of Atmospheric Aerosol Particles by Gas-Phase Radicals. *Nat. Chem.* **2010**, *2* (9), 713–722. https://doi.org/10.1038/nchem.806.

(276) Pöschl, U.; Letzel, T.; Schauer, C.; Niessner, R. Interaction of Ozone and Water Vapor with Spark Discharge Soot Aerosol Particles Coated with Benzo[a]Pyrene: O3 and H2O Adsorption, Benzo[a]Pyrene Degradation, and Atmospheric Implications. *J. Phys. Chem. A* **2001**, *105* (16), 4029–4041. https://doi.org/10.1021/jp004137n.

(277) Schauer, J. J.; Kleeman, M. J.; Cass, G. R.; Simoneit, B. R. T. Measurement of Emissions from Air Pollution Sources. 3. C $_1$ −C $_{29}$ Organic Compounds from Fireplace Combustion of Wood. *Environ. Sci. Technol.* **2001**, *35* (9), 1716–1728. https://doi.org/10.1021/es001331e.

(278) Schnitzler, E. G.; Abbatt, J. P. D. Heterogeneous OH Oxidation of Secondary Brown Carbon Aerosol. *Atmospheric Chem. Phys.* **2018**, *18* (19), 14539–14553. https://doi.org/10.5194/acp-18-14539-2018.

(279) Adachi, K.; Sedlacek, A. J.; Kleinman, L.; Springston, S. R.; Wang, J.; Chand, D.; Hubbe, J. M.; Shilling, J. E.; Onasch, T. B.; Kinase, T.; Sakata, K.; Takahashi, Y.; Buseck, P. R. Spherical Tarball Particles Form through Rapid Chemical and Physical Changes of Organic Matter in Biomass-Burning Smoke. *Proc. Natl. Acad. Sci.* **2019**, *116* (39), 19336–19341. https://doi.org/10.1073/pnas.1900129116.

(280) Adler, G.; Wagner, N. L.; Lamb, K. D.; Manfred, K. M.; Schwarz, J. P.; Franchin, A.; Middlebrook, A. M.; Washenfelder, R. A.; Womack, C. C.; Yokelson, R. J.; Murphy, D. M. Evidence in Biomass Burning Smoke for a Light-Absorbing Aerosol with Properties Intermediate between Brown and Black Carbon. *Aerosol Sci. Technol.* **2019**, *53* (9), 976–989. https://doi.org/10.1080/02786826.2019.1617832.

(281) Teich, M.; Pinxteren, D. van; Wang, M.; Kecorius, S.; Wang, Z.; Müller, T.; Močnik, G.; Herrmann, H. Contributions of Nitrated Aromatic Compounds to the Light Absorption of Water-Soluble and Particulate Brown Carbon in Different Atmospheric Environments in Germany and China. *Atmospheric Chem. Phys.* **2017**, *17* (3), 1653–1672. https://doi.org/10.5194/acp-17-1653-2017.

(282) Li, C.; He, Q.; Fang, Z.; Brown, S. S.; Laskin, A.; Cohen, S. R.; Rudich, Y. Laboratory Insights into the Diel Cycle of Optical and Chemical Transformations of Biomass Burning Brown Carbon Aerosols. *Environ. Sci. Technol.* **2020**. https://doi.org/10.1021/acs.est.0c04310.

(283) Li, C.; He, Q.; Hettiyadura, A. P. S.; Käfer, U.; Shmul, G.; Meidan, D.; Zimmermann, R.; Brown, S. S.; George, C.; Laskin, A.; Rudich, Y. Formation of Secondary Brown Carbon in Biomass Burning Aerosol Proxies through NO3 Radical Reactions. *Environ. Sci. Technol.* **2020**, *54* (3), 1395–1405. https://doi.org/10.1021/acs.est.9b05641.

(284) Zhong, M.; Jang, M. Dynamic Light Absorption of Biomass-Burning Organic Carbon Photochemically Aged under Natural Sunlight. *Atmospheric Chem. Phys.* **2014**, *14* (3), 1517–1525. https://doi.org/10.5194/acp-14-1517-2014.

(285) Lin, P.; Bluvshtein, N.; Rudich, Y.; Nizkorodov, S. A.; Laskin, J.; Laskin, A. Molecular Chemistry of Atmospheric Brown Carbon Inferred from a Nationwide Biomass Burning Event. *Environ. Sci. Technol.* **2017**, *51* (20), 11561–11570. https://doi.org/10.1021/acs.est.7b02276.

(286) Wang, X.; Heald, C. L.; Sedlacek, A. J.; Sá, S. S. de; Martin, S. T.; Alexander, M. L.; Watson, T. B.; Aiken, A. C.; Springston, S. R.; Artaxo, P. Deriving Brown Carbon from Multiwavelength Absorption Measurements: Method and Application to AERONET and Aethalometer Observations. *Atmospheric Chem. Phys.* **2016**, *16* (19), 12733–12752. https://doi.org/10.5194/acp-16-12733-2016.

(287) Wang, X.; Heald, C. L.; Liu, J.; Weber, R. J.; Campuzano-Jost, P.; Jimenez, J. L.; Schwarz, J. P.; Perring, A. E. Exploring the Observational Constraints on the Simulation of Brown Carbon. *Atmospheric Chem. Phys.* **2018**, *18* (2), 635–653. https://doi.org/10.5194/acp-18-635-2018.

(288) June, N. A.; Wang, X.; Chen, L.-W. A.; Chow, J. C.; Watson, J. G.; Wang, X.; Henderson, B. H.; Zheng, Y.; Mao, J. Spatial and Temporal Variability of Brown Carbon in the United States: Implications for Direct Radiative Effects. *Geophys. Res. Lett.* **2020**, *47* (23), e2020GL090332. https://doi.org/10.1029/2020GL090332.

(289) Koop, T.; Bookhold, J.; Shiraiwa, M.; Pöschl, U. Glass Transition and Phase State of Organic Compounds: Dependency on Molecular Properties and Implications for Secondary Organic Aerosols in the Atmosphere. *Phys. Chem. Chem. Phys.* **2011**, *13* (43), 19238–19255. https://doi.org/10.1039/C1CP22617G.

(290) Gilardoni, S.; Massoli, P.; Paglione, M.; Giulianelli, L.; Carbone, C.; Rinaldi, M.; Decesari, S.; Sandrini, S.; Costabile, F.; Gobbi, G. P.; Pietrogrande, M. C.; Visentin, M.; Scotto, F.; Fuzzi, S.; Facchini, M. C. Direct Observation of Aqueous Secondary Organic Aerosol from Biomass-Burning Emissions. *Proc. Natl. Acad. Sci.* **2016**, *113* (36), 10013–10018. https://doi.org/10.1073/pnas.1602212113.

(291) Choudhary, V.; Rajput, P.; Singh, D. K.; Singh, A. K.; Gupta, T. Light Absorption Characteristics of Brown Carbon during Foggy and Non-Foggy Episodes over the Indo-Gangetic Plain. *Atmospheric Pollut. Res.* **2018**, *9* (3), 494–501. https://doi.org/10.1016/j.apr.2017.11.012.

(292) Wang, Q.; Ye, J.; Wang, Y.; Zhang, T.; Ran, W.; Wu, Y.; Tian, J.; Li, L.; Zhou, Y.; Hang Ho, S. S.; Dang, B.; Zhang, Q.; Zhang, R.; Chen, Y.; Zhu, C.; Cao, J. Wintertime Optical Properties of Primary and Secondary Brown Carbon at a Regional Site in the North China Plain. *Environ. Sci. Technol.* **2019**, *53* (21), 12389–12397. https://doi.org/10.1021/acs.est.9b03406.

(293) Jo, D. S.; Park, R. J.; Lee, S.; Kim, S.-W.; Zhang, X. A Global Simulation of Brown Carbon: Implications for Photochemistry and Direct Radiative Effect. *Atmospheric Chem. Phys.* **2016**, *16* (5), 3413–3432. https://doi.org/10.5194/acp-16-3413-2016.

(294) Phillips, S. M.; Smith, G. D. Light Absorption by Charge Transfer Complexes in Brown Carbon Aerosols. *Environ. Sci. Technol. Lett.* **2014**, *1* (10), 382–386. https://doi.org/10.1021/ez500263j.

(295) Phillips, S. M.; Smith, G. D. Further Evidence for Charge Transfer Complexes in Brown Carbon Aerosols from Excitation–Emission Matrix Fluorescence Spectroscopy. *J. Phys. Chem. A* **2015**, *119* (19), 4545–4551. https://doi.org/10.1021/jp510709e.

(296) Trofimova, A.; Hems, R. F.; Liu, T.; Abbatt, J. P. D.; Schnitzler, E. G. Contribution of Charge-Transfer Complexes to Absorptivity of Primary Brown Carbon Aerosol. *ACS Earth Space Chem.* **2019**. https://doi.org/10.1021/acsearthspacechem.9b00116.

(297) Crounse, J. D.; Nielsen, L. B.; Jørgensen, S.; Kjaergaard, H. G.; Wennberg, P. O. Autoxidation of Organic Compounds in the Atmosphere. *J. Phys. Chem. Lett.* **2013**, *4* (20), 3513–3520. https://doi.org/10.1021/jz4019207.

(298) Gallimore, P. J.; Kalberer, M. Characterizing an Extractive Electrospray Ionization (EESI) Source for the Online Mass Spectrometry Analysis of Organic Aerosols. *Environ. Sci. Technol.* **2013**, *47* (13), 7324–7331. https://doi.org/10.1021/es305199h.

(299) Lopez-Hilfiker, F. D.; Pospisilova, V.; Huang, W.; Kalberer, M.; Mohr, C.; Stefenelli, G.; Thornton, J. A.; Baltensperger, U.; Prevot, A. S. H.; Slowik, J. G. An Extractive Electrospray Ionization Time-of-Flight Mass Spectrometer (EESI-TOF) for Online Measurement of Atmospheric Aerosol Particles. *Atmospheric Meas. Tech.* **2019**, *12* (9), 4867–4886. https://doi.org/10.5194/amt-12-4867-2019.

(300) Fleming, L. T.; Lin, P.; Roberts, J. M.; Selimovic, V.; Yokelson, R.; Laskin, J.; Laskin, A.; Nizkorodov, S. A. Molecular Composition and Photochemical Lifetimes of Brown Carbon Chromophores in Biomass Burning Organic Aerosol. *Atmospheric Chem. Phys.* **2020**, *20* (2), 1105–1129. https://doi.org/10.5194/acp-20-1105-2020.

(301) Lin, P.; Fleming, L. T.; Nizkorodov, S. A.; Laskin, J.; Laskin, A. Comprehensive Molecular Characterization of Atmospheric Brown Carbon by High Resolution Mass Spectrometry with Electrospray and Atmospheric Pressure Photoionization. *Anal. Chem.* **2018**, *90* (21), 12493–12502. https://doi.org/10.1021/acs.analchem.8b02177.

TOC Graphic: